5 Photovoltaics

Introduction

Photovoltaics consists of the two words *photo* and *volta*. Photo (Greek phõs, photós) means 'light', while volta (Count Volta, 1745-1827, Italian physicist) is a unit for electrical voltage. In other words, photovoltaics takes sunlight and converts it directly into electricity.

The **history of photovoltaics** started in 1839, when Becquerel discovered the photoelectric effect. But it took another hundred years for the age of semiconductors to start. In 1949, Shockley developed a model for p-n transitions, and in 1954 the first silicon solar cell literally saw the light of day at Bell Labs in the US. At the time, the first cell had an efficiency of around 5 %. Costs were not an issue; after all, the cell was to provide electricity to vessels and satellites in space.

Since then, the efficiency of solar cells has continued to rise. In the lab, silicon cells easily have efficiencies above 20 % these days. New materials have also been tested, and some of them are now used. The cost of solar cells has been brought down considerably. In off-grid applications, photovoltaics is already competitive. But even on the grid, the cost of power from photovoltaics is already equal to or below power from the grid (grid parity) in a number of countries – and counting. As more and more PV is installed, costs will come down even further. In a few years, photovoltaics will be competitive with power from the grid worldwide.

Of all sources of renewable electricity, photovoltaics has the widest range of applications. It is especially **modular**. In other words, the power generator can come in almost any size – from a few milliwatts for pocket calculators and watches to multi-megawatts for utility-scale power plants.

For a long time, photovoltaics was mainly used in consumer applications, toys, and off-grid applications, such as telecommunications facilities. Germany's **1,000 Roofs Program** launched at the beginning of the 1990s led to the construction of 2,250 PV systems connected to the grid, demonstrating for the first time that photovoltaics was a good source of power on a significant scale. In central Europe, photovoltaics poses tremendous potential. It can be installed on roofs and façades without taking up any space. Building-integrated PV has the potential to cover a third of power demand in Germany in the midterm.

Figure 4.1 shows a roof-integrated photovoltaic system built in the United States back in the 1980s. At the time, capacities exceeding 100 kW_p broke records, but today the largest PV power plants have more than 100 megawatts. Thanks to the priority that renewable power has

Copyright © 2016. Taylor & Francis Group. All rights reserved.

Quaschning, Volker. Understanding Renewable Energy Systems, Taylor & Francis Group, 2016. ProQuest Ebook Central, http://ebookcentral.proquest.com/lib/byu/detail.action?docID=4470609.
Created from byu on 2021-11-05 15:55:38.

on the grid and to feed-in tariffs specified in the German **Renewable Energy Act**, Germany became a leader in photovoltaics at the end of the 1990s. Until then, Japan had dominated the market.

Figure 5.1 Roof-integrated photovoltaic system (Georgetown University in Washington, DC, built in 1984, 4,464 solar modules, 337 kW_p total capacity)

Table 5.1 Overview of key electrotechnical parameters

Name	*Symbol*	*Unit*	*Name*	*Symbol*	*Unit*
Electrical energy	W, E	W s, J	Specific resistance	ρ	Ω m
Electrical output	$P = U \cdot I$	W	Electrical field strength	$E = -dU/ds$	V / m
Electrical voltage	U	V	Inductance (coil)	L	H = V s/ A
Electrical current	I	A	Capacity	C	F = A s/ V
Electrical resistance	$R = U / I$		Electrical charge	$Q = \int I dt$	C = A s
Electric conductance	$G = 1 / R$	S	Force in electrical field	$F = E \cdot Q$	N

In Germany, installation figures have skyrocketed in recent years. Since 2011, Germany has had more installed PV capacity than nuclear capacity. Photovoltaics now plays a crucial role in German power supply.

This chapter presents the basics, such as how photovoltaics works, how to calculate a photovoltaic system, and what its applications are. Table 5.1 shows an overview of the key electrotechnical parameters used in such descriptions.

How solar cells work

Bohr's atomic model

Copyright © 2016. Taylor & Francis Group. All rights reserved.

Quaschning, Volker. Understanding Renewable Energy Systems, Taylor & Francis Group, 2016. ProQuest Ebook Central, http://ebookcentral.proquest.com/lib/byu/detail.action?docID=4470609.
Created from byu on 2021-11-05 15:55:38.

Starting with the Bohr model of individual atoms, the energy band model for solids will be discussed to describe how semiconducting solar cells work. In Bohr's atomic model, electron mass orbits the nucleus

$$m_e = 9{,}1093897 \cdot 10^{-31}\ \text{kg} \quad (5.1)$$

with a radius of r_n at orbital frequency ω_n . The result is the **centrifugal force**:

$$F_Z = m_e \cdot r_n \cdot \omega_n^2 \quad (5.2)$$

Between the nucleus, which consists of Z positively charged protons and additional neutrons without a charge, and the electron with the **elementary charge**

$$e = 1{,}60217733 \cdot 10^{-19}\ \text{A s} \quad (5.3)$$

the **coulomb charge** holds things together:

$$F_C = \frac{1}{4\neq \cdot \varepsilon_0} \cdot \frac{Z \cdot e^2}{r_n^2}, \text{ with} \quad (5.4)$$

$$\varepsilon_0 = 8{,}85418781762 \cdot 10^{-12} \frac{\text{A s}}{\text{V m}} \quad (5.5)$$

being the **electric force constant** or the dielectric constant. The coulomb force and the centrifugal force must balance each other out for the electron to stay within its orbital. Here, orbits must have an angular momentum that is an integer multiple of

$$\hbar = \frac{h}{2 \cdot \neq} \quad (5.6)$$

with $\hbar$ calculated from **Planck's constant**

$$h = 6{,}6260755 \cdot 10^{-34}\ \text{Js} \quad (5.7)$$

Quantization of the angular momentum produces:

$$n \cdot \hbar = m_e \cdot r_n^2 \cdot \omega_n \quad (5.8)$$

With that and the equilibrium $F_Z = F_C$, we get the following equation for the orbital's radius

$$r_n = \frac{n^2 \cdot \hbar^2 \cdot 4 \cdot \neq \cdot \varepsilon_0}{Z \cdot e^2 \cdot m_e} \quad (5.9)$$

and for the **orbital frequency**:

Copyright © 2016. Taylor & Francis Group. All rights reserved.

Quaschning, Volker. Understanding Renewable Energy Systems, Taylor & Francis Group, 2016. ProQuest Ebook Central, http://ebookcentral.proquest.com/lib/byu/detail.action?docID=4470609.
Created from byu on 2021-11-05 15:55:38.

$$\omega_n = \frac{1}{(4 \cdot \neq \cdot \varepsilon_0)^2} \cdot \frac{Z^2 \cdot e^4 \cdot m_e}{\hbar^3 \cdot n^3} \tag{5.10}$$

The integral index n indicates the number of each orbital. The energy that an electron carries along with it on its orbital is:

$$E_n = \tfrac{1}{2} \cdot m_e \cdot v_e^2 = \tfrac{1}{2} \cdot m_e \cdot r_n^2 \cdot \omega_n^2 = \frac{1}{n^2} \cdot \frac{Z^2 \cdot e^4 \cdot m_e}{32 \cdot \neq^2 \cdot \varepsilon_0^2 \cdot \hbar^2} \tag{5.11}$$

The energy of a hydrogen atom with atomic number $Z = 1$ on the first orbital ($n = 1$) is $E_{1,Z=1} = 13.59$ eV.

If an electron is to be lifted to the next orbital up, the amount of external energy required is $\Delta E = E_n - E_{n+1}$. Keep in mind here that the number of electrons that can be within a single orbital is limited. The first orbital ($n = 1$) can have two electrons; the second, 8, then 18, 32, 50, etc. As n increases, the orbital's energy decreases, eventually reaching $E_\infty = 0$ at $n = \infty$. In addition to the Bohr model, there are other models describing the atom not discussed here (see [Her12]).

Photoelectric effect

The energy of photons in the light provides the energy to move an electron into a higher orbital. The **photon's energy** at wavelengths λ is calculated as

$$E = \frac{h \cdot c}{\lambda} \tag{5.12}$$

with the speed of light $c = 2.99792458 \cdot 10^8$ m/s. If a photon with 13.59 eV of energy impacts an electron in the first orbital of a hydrogen atom, the energy suffices to lift the electron on to orbital E_∞, thereby completely separating it from the nucleus. This energy is also called ionization energy, while the process of photons completely removing electrons from the nucleus is called the external **photoelectric effect**. In the example of hydrogen, the photon has to have a wavelength λ smaller than 90 nm, which only x-rays have.

In photovoltaics, visible, ultraviolet, and infrared radiation is used, and the protons here have far less energy; therefore, the external photoelectric effect does not apply as it requires radiation with high energy. Instead, the internal photoelectric effect applies, as explained below.

Copyright © 2016. Taylor & Francis Group. All rights reserved.

Quaschning, Volker. Understanding Renewable Energy Systems, Taylor & Francis Group, 2016. ProQuest Ebook Central, http://ebookcentral.proquest.com/lib/byu/detail.action?docID=4470609.
Created from byu on 2021-11-05 15:55:38.

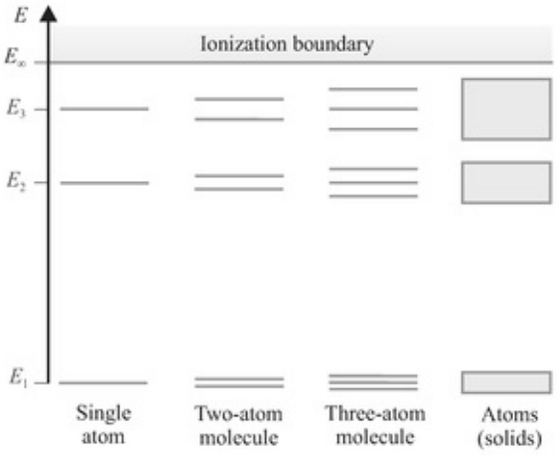

Figure 5.2 Energy states of electrons in an atom, in molecules, and in solids

In individual atoms, electrons have precisely defined energy states, but in the molecules consisting of multiple atoms electrons interact and break up identical energy levels into closely related neighbouring levels. In a solid with k atoms, the individual levels are so close that they cannot be separated. Energy bands are created in the process for the individual energy levels in the electron orbitals (Figure 5.2). As explained above, only a limited number of electrons can inhabit these energy bands.

In the band model, the bands are filled up with electrons from the first one to the last in order. The first completely filled band is called the **valence band** VB. The next band up is the **conduction band** CB, which can be either partly filled or completely empty. The space between the valence band and the conduction band cannot contain energy states; this area is called the band gap E_g.

Depending on how the bands are arranged and how many electrons they contained, solids are divided into the categories of electric conductors, semiconductors, and nonconducting isolators (Figure 5.3). Conductors either have a conduction band only partly filled with electrons or overlapping conduction and valence bands. If the conduction band partly contains electrons, the electrons can move within the solid, therefore allowing electrons to be conducted. The specific electrical resistance of conductors is very low at $\rho < 10^{-5}$ Ω m. Conductors are generally metallic materials.

Isolators have a large specific electrical resistance at $\rho > 10^{7}$ Ω m. Their conduction band has no electrons, and the great band gap ($E_g \geq 5$ eV) means that electrons have a hard time moving from the valence band into the conduction band.

Copyright © 2016. Taylor & Francis Group. All rights reserved.

Quaschning, Volker. Understanding Renewable Energy Systems, Taylor & Francis Group, 2016. ProQuest Ebook Central, http://ebookcentral.proquest.com/lib/byu/detail.action?docID=4470609.
Created from byu on 2021-11-05 15:55:38.

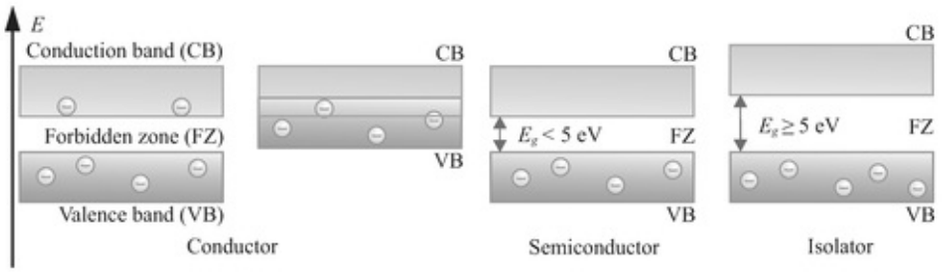

Figure 5.3 Energy bands for conductors, semiconductors, and isolators

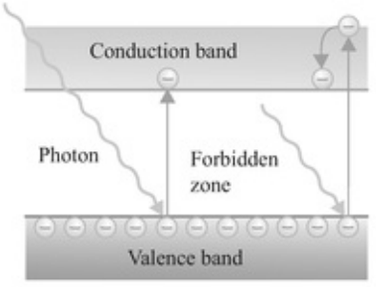

Figure 5.4 Photons moving electrons from the valence band into the conduction band (internal photoelectric effect)

For photovoltaics, **semiconductors** are crucial. Their conductivity ranges from 10^{-5} Ω m to 10^{7} Ω m. Like isolators, their conductance band has no electrons, but the relatively small band gap (E_g < 5 eV) means that solar energy can move electrons into the conduction band (Figure 5.4). When photons move electrons into the conduction band, we speak of the **internal photoelectric effect**.

If the photon's energy is smaller than the band gap, the electron cannot get through to the conduction band. If the photon's energy is too great, the electron does enter the conduction band, but part of the energy is lost because the electron falls back to the edge of the conduction band.

Technically, the internal photoelectric effect can be used for photoelectric resistance, which changes relative to irradiance, or to generate electricity – as in photovoltaics.

How a solar cell works

Table 5.2 Band gaps of various semiconductors at 300 K

Copyright © 2016. Taylor & Francis Group. All rights reserved.

Quaschning, Volker. Understanding Renewable Energy Systems, Taylor & Francis Group, 2016. ProQuest Ebook Central, http://ebookcentral.proquest.com/lib/byu/detail.action?docID=4470609.
Created from byu on 2021-11-05 15:55:38.

IV semiconductors		*III-V semiconductors*		*II-VI semiconductors*	
Material	E_g	*Material*	E_g	*Material*	E_g
Si	1.107 eV	GaAs	1.35 eV	CdTe	1.44 eV
Ge	0.67 eV	InSb	0.165 eV	ZnSe	2.58 eV
Sn	0.08 eV	InP	1.27 eV	ZnTe	2.26 eV
		GaP	2.24 eV	HgSe	0.30 eV

(Data: [Lec92])

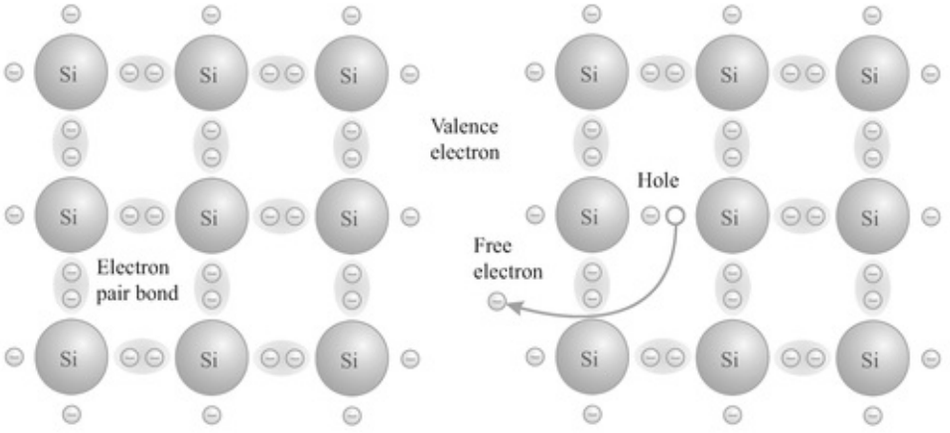

Figure 5.5 The crystal structure of silicon (left); intrinsic conductivity of electron holes in the crystal lattice (right)

Photovoltaics also uses semiconductors. They generally have four electrons – called valence electrons – in the outermost electron shell. Elements from Group IV of the periodic table are the main semiconductors; examples include silicon (Si), germanium (Ge), and tin (Sn). Compounds of two elements from Group III and V (called III-V compounds) also have four valence electrons, as do II-VI compounds and combinations of various elements. An example of a III-V semiconductor is gallium arsenide (GaAs); a II-VI semiconductor is cadmium telluride (CdTe). Table 5.2 shows the various band gaps of a few semiconductors.

Silicon is commonly used in photovoltaics. It is the second most common element in the earth's crust after oxygen, but is usually only found in chemical bonds.

Silicon (Si) is a semiconductor from Group IV of the periodic table of elements; it has four valence electrons in the outermost shell. Tw o electrons from neighbouring atoms form a covalent bond in the silicon crystal lattice to form a stable electron configuration. In a way, the two atoms now share the electrons. The covalent bond with four neighbours gives silicon the stable electron configuration of the noble gas argon (Ar). In the band model, the valence band is full and the conduction band empty. Light and heat can lift an electron from the valence band into the conduction band. The electron is then free to move around in the crystal lattice. An electron hole is left behind in the valence band, as shown in Figure 5.5. These electron holes produce the semiconductor's **intrinsic conductivity**.

For each electron, there is an electron hole. In other words, there are always the same number of electrons as electron holes. We then speak of **electron density** n and **hole density**

Copyright © 2016. Taylor & Francis Group. All rights reserved.

Quaschning, Volker. Understanding Renewable Energy Systems, Taylor & Francis Group, 2016. ProQuest Ebook Central, http://ebookcentral.proquest.com/lib/byu/detail.action?docID=4470609.
Created from byu on 2021-11-05 15:55:38.

p:

$$n = p \quad (5.13)$$

The product of electron density and electron hole density is called the **intrinsic carrier density** n_i, and it is relative to absolute temperature T and band gap E_g:

$$n \cdot p = n_i^2 = n_{i0}^2 \cdot T^3 \cdot \exp\left(-\frac{E_g}{k \cdot T}\right) \quad (5.14)$$

The **Boltzmann constant** applies:

$$k = 1.380658 \cdot 10^{-23}\ \mathrm{J/K} \quad (5.15)$$

For silicon, $n_{i0} = 4.62 \cdot 10^{15}\ \mathrm{cm^{-3}\ K^{-3/2}}$. At absolute zero ($T = 0$ K), there are therefore no free electrons or holes, but their number increases quickly as temperatures rise.

If electric voltage is connected to the silicon lattice, negatively charged electrons flow towards the anode. Bound electrons next to a hole can switch places and enter the hole, which then moves in the opposite direction – when voltage is connected, it moves towards the cathode. The **mobility** μ_n and μ_p of the electrons and holes in the semiconductor also depends on the temperature. For silicon, μ_n and μ_p can be calculated with $\mu_{0n} = 1350\ \mathrm{cm^2/(V\ s)}$ and $\mu_{0p} = 480\ \mathrm{cm^2/(V\ s)}$ at $T_0 = 300$ K via:

$$\mu_n = \mu_{0n} \cdot \left(\frac{T}{T_0}\right)^{-3/2} \quad (5.16) \text{ and } \mu_p = \mu_{0p} \cdot \left(\frac{T}{T_0}\right)^{-3/2} \quad (5.17)$$

The **electric conductivity**

$$\kappa = \frac{1}{\rho} = e \cdot (n \cdot \mu_n + p \cdot \mu_p) = e \cdot n_i \cdot (\mu_n + \mu_p) \quad (5.18)$$

of the semiconductor is the sum of the electron and hole current. At low temperatures, conductivity drops considerably. This effect is used to make temperature sensors for low temperatures.

Copyright © 2016. Taylor & Francis Group. All rights reserved.

Quaschning, Volker. Understanding Renewable Energy Systems, Taylor & Francis Group, 2016. ProQuest Ebook Central, http://ebookcentral.proquest.com/lib/byu/detail.action?docID=4470609.
Created from byu on 2021-11-05 15:55:38.

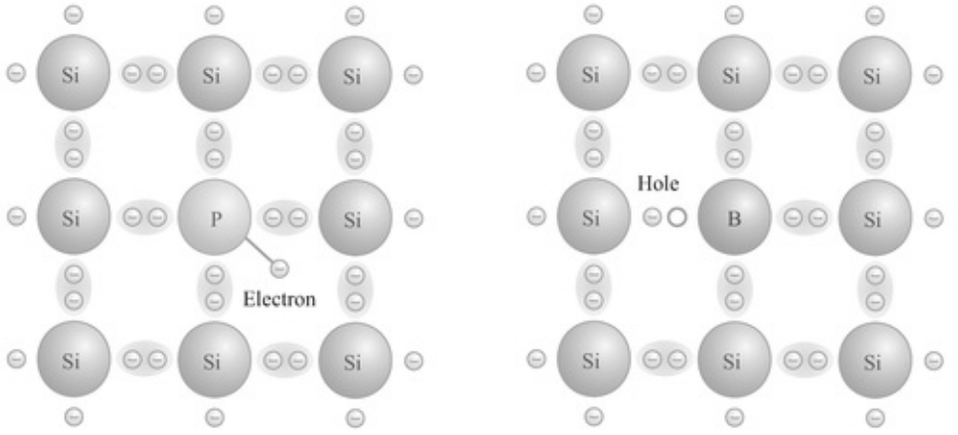

Figure 5.6 n- and p-doped silicon

Light also affects electrical conductivity. It is used to make light-sensitive photoelectric resistors. However, external electric voltage has to be applied in the process. Intrinsic conductivity cannot be used to generate electrical current. Here, another effect is used: **doping**.

Atoms from Group V, such as phosphorus (P) and antimony (Sb) have five valence electrons, unlike silicon. If these atoms are put into the silicon lattice, the fifth electron cannot bind with a neighbouring electron. Because that electron is only loosely bound, it takes very little energy to separate it from the atom compared with a properly bound electron. It is then available as a free electron. The addition of atoms from Group V is called n-doping. The foreign atoms are called **donors**.

In **n-doping, the density of free electrons is calculated**

$$n = \sqrt{\frac{n_D \cdot N_L}{2}} \cdot \exp\left(-\frac{E_D}{2 \cdot k \cdot T}\right) \tag{5.19}$$

from the density n_D of donor atoms, the effective density state N_L in the conduction band, and the donors' ionization energy E_D which is the energy needed to separate the electrons. In silicon at a temperature of T = 300 K, N_L = 3.22·10 19 cm^{-3}, and with phosphorus atoms as donors E_D = 0.044 eV.

With n-doping, there are far more free electrons than electron holes, so the electrons are called the majority carriers. Electric conductivity is mainly based on the transport of electrons, and the semiconductor is n-conductive.

If atoms from Group III are used instead of from Group V – such as boron (B) and aluminium (Al) – with three valence electrons, a valence electron is then missing in the silicon lattice, so there is an extra electron hole. It then takes little energy E_A relative to an n-type conductor to separate the whole so it can 'move freely'. Electric conductivity is mainly based on the transport of positive charge carriers – the electron holes. By means of p-doping, the

Copyright © 2016. Taylor & Francis Group. All rights reserved.

Quaschning, Volker. Understanding Renewable Energy Systems, Taylor & Francis Group, 2016. ProQuest Ebook Central, http://ebookcentral.proquest.com/lib/byu/detail.action?docID=4470609.
Created from byu on 2021-11-05 15:55:38.

semiconductor becomes p-conductive. The foreign atoms are called **acceptors**.

The acceptor density n_A, the effective density state N_V in the valence band, and the ionization energy E_A ($N_V = 1.83 \cdot 10^{19}$ cm^{-3} for silicon at $T = 300$ K and $E_A = 0{,}045$ eV for boron) produces the following **density of extra holes** for a **p-type semiconductor**:

$$p = \sqrt{\frac{n_A \cdot N_V}{2}} \cdot \exp\left(-\frac{E_A}{2 \cdot k \cdot T}\right) \tag{5.20}$$

If a p-type and an n-type semiconductor come into contact, a p–n **junction** is created. As explained above, the n-type semiconductor has excess free electrons; the p-type semiconductor, excess free electron holes. The electrons then move from the n-type semiconductor to the p-type semiconductor, whereas the holes move in the opposite direction (Figure 5.7).

An area with few free charge carriers results at the transitional zone. Where electrons have moved into the p-zone, they leave behind positively ionized doping atoms. The depletion region then has a positive charge. Where holes have diffused into the n-zone, they leave behind negatively iodized doping atoms, resulting in a negatively charged depletion region.

An electric field is thus created between the n-side and the p-side, and it opposes the motion of the charge carriers so that diffusion does not continue infinitely. The result is a **differential potential** .

$$U_d = \frac{k \cdot T}{e} \cdot \ln \frac{n_A \cdot n_D}{n_i^2} \tag{5.21}$$

Because of the charge neutrality, the widths d_n and d_p of the depletion regions in each semiconductor zone are:

$$d_n \cdot n_D = d_p \cdot n_A \tag{5.22}$$

The following applies for the **total width of the depletion zone**:

$$d = d_n + d_p = \sqrt{\frac{2 \cdot \varepsilon_r \cdot \varepsilon_0 \cdot U_d}{e} \cdot \frac{n_A + n_D}{n_A \cdot n_D}} \tag{5.23}$$

Copyright © 2016. Taylor & Francis Group. All rights reserved.

Quaschning, Volker. Understanding Renewable Energy Systems, Taylor & Francis Group, 2016. ProQuest Ebook Central, http://ebookcentral.proquest.com/lib/byu/detail.action?docID=4470609.
Created from byu on 2021-11-05 15:55:38.

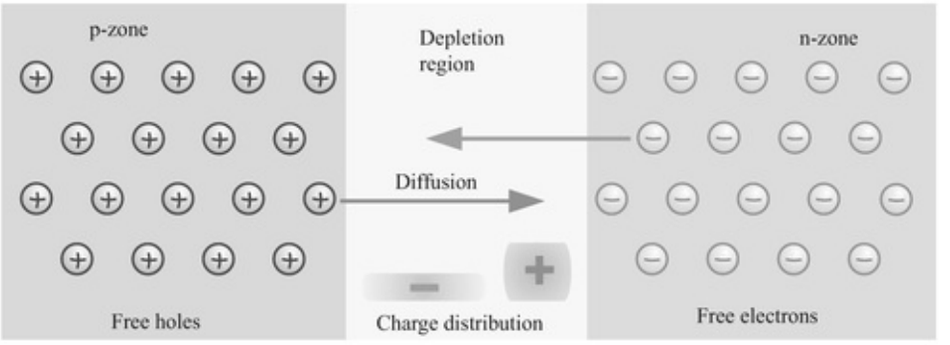

Figure 5.7 Depletion region at the p–n junction caused by the diffusion of electrons and electron holes

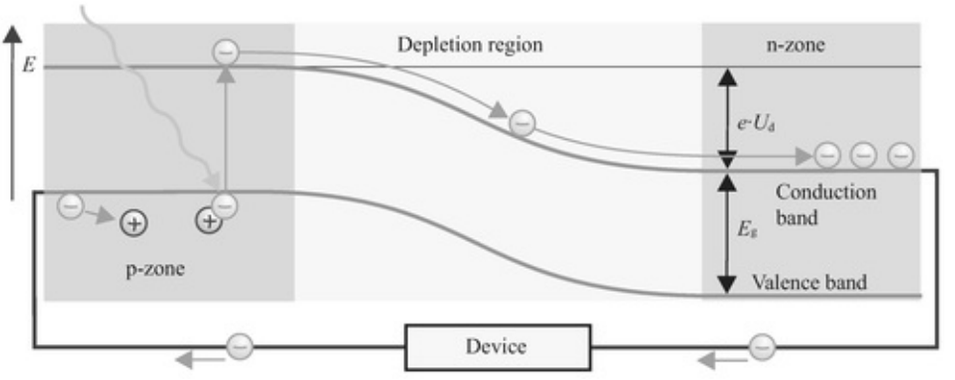

Figure 5.8 How a solar cell works in the energy band model

For silicon with a hole concentration of $n_D = 2 \cdot 10^{16}$ cm^{-3} and $n_A = 1 \cdot 10^{16}$ cm^{-3} at a temperature of $T = 300$ K, the differential potential is $U_d = 0.73$ V. At $\varepsilon_r = 11.8$, $d_n = 0.13$ µm and $d_p = 0.25$ µm.

If photons then move electrons from the valence band into the conduction band within the depletion zone, thereby separating them from the atom, they then move through the electric field into the n-side, and the holes created in the process move into the p-side. In the energy band model, the process can be illustrated by bending the bands into the depletion zone. The current is closed if connected to a device that consumes electricity (Figure 5.8).

As explained above, a solar cell only uses part of the energy from the photons. If the energy from the photons is less than the band gap, their energy will not suffice to move an electron from the valence band into the conduction band. This is the case at wavelengths greater than:

$$\lambda_{max} = \frac{h \cdot c}{E_g} = \frac{1{,}24 \ \mu m \ eV}{E_g} \tag{5.24}$$

But at wavelengths near the band gap, not all of the incident irradiance is converted into electric energy. Part of the solar radiation is reflected, while another part passes through the semiconductor unused. In addition, electrons can be recombined with electron holes within the semiconductor, meaning that they fall back into the valence band before they reach the point

Copyright © 2016. Taylor & Francis Group. All rights reserved.

Quaschning, Volker. Understanding Renewable Energy Systems, Taylor & Francis Group, 2016. ProQuest Ebook Central, http://ebookcentral.proquest.com/lib/byu/detail.action?docID=4470609.
Created from byu on 2021-11-05 15:55:38.

of power consumption. Figure 5.9 shows these events.

Likewise, only part of the energy from radiation at short wavelengths with high energy is used because the energy that exceeds the band gap is lost when electrons fall back into the edge of the conduction band. The amount of energy that can be used therefore greatly depends upon the wavelength of incident light. The part that can be used is expressed as the external quantum efficiency $\eta_{ext}(\lambda)$ relative to the wavelength. This efficiency indicates how many of the incident photons within a given wavelength actually produce current.

As explained above, solar cells are only able to optically absorb part of the photons. Because of reflection and transmission, some of the photons remain unused. The degree of absorption $\alpha(\lambda)$, reflection $\rho(\lambda)$, and transmission $\tau(\lambda)$ can be used along with the external quantum efficiency η_{ext} to calculate the internal quantum efficiency.

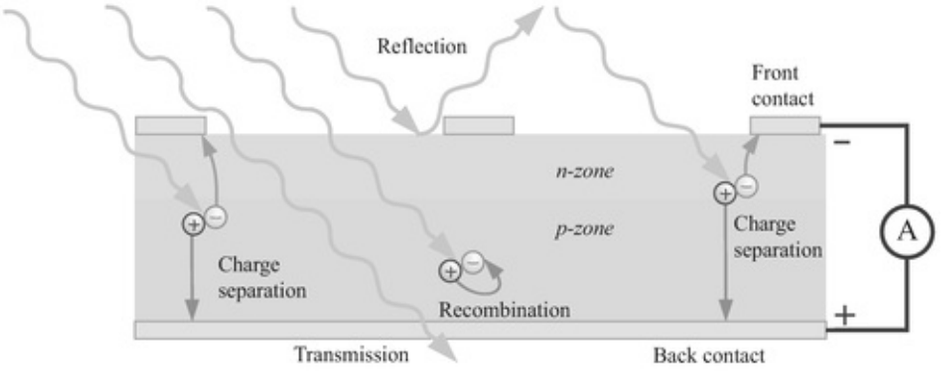

Figure 5.9 Events within a solar cell exposed to sunlight

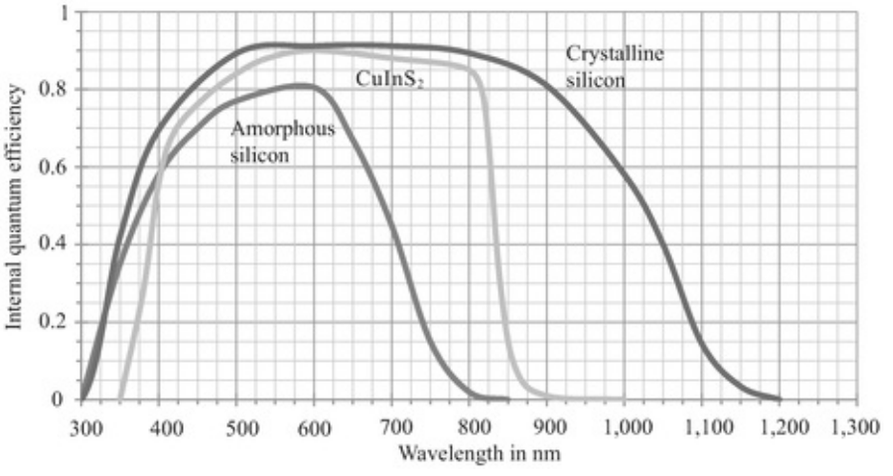

Figure 5.10 Typical curve for the internal quantum efficiency of various solar cell types

$$\eta_{int}(\lambda) = \frac{\eta_{ext}(\lambda)}{\alpha(\lambda)} = \frac{\eta_{ext}(\lambda)}{1-\rho(\lambda)-\tau(\lambda)} \tag{5.25}$$

Figure 5.10 shows the typical **internal quantum efficiency** for various solar cells.

Copyright © 2016. Taylor & Francis Group. All rights reserved.

Quaschning, Volker. Understanding Renewable Energy Systems, Taylor & Francis Group, 2016. ProQuest Ebook Central, http://ebookcentral.proquest.com/lib/byu/detail.action?docID=4470609.
Created from byu on 2021-11-05 15:55:38.

Depending on the solar cell's specific design and quality, its characteristics may differ within the same type. The higher and wider the curve of quantum efficiency is, the greater the solar cell's efficiency.

Spectral sensitivity is another major parameter:

$$S(\lambda) = \frac{e \cdot \lambda}{h \cdot c} \cdot \eta_{\text{ext}}(\lambda) = \frac{\lambda}{1{,}24\ \mu\,\text{m}} \cdot \frac{\text{A}}{\text{W}} \cdot \eta_{\text{ext}}(\lambda) \tag{5.26}$$

It is calculated from external quantum efficiency η_{ext} and wavelength λ. Figure 5.11 shows spectral sensitivity S relative to wavelength λ. It is relatively easy to measure spectral sensitivity. A solar cell with area A is exposed to a known monochromatic irradiance $E(\lambda)$, and the short circuit current $I_{\text{K}}(\lambda)$ is measured:

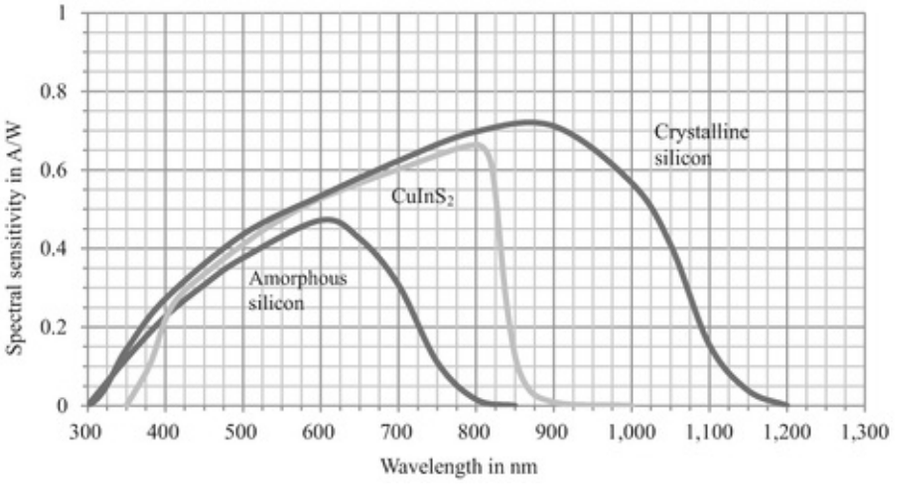

Figure 5.11 Typical curve of a solar cell's spectral sensitivity for various solar cell types

$$S(\lambda) = \frac{I_{\text{K}}(\lambda)}{A \cdot E(\lambda)} \tag{5.27}$$

Often, relative spectral sensitivity

$$S_{\text{rel}}(\lambda) = \frac{S(\lambda)}{S_{\text{max}}} \tag{5.28}$$

is indicated at a value between 0 and 1. It is based on spectral sensitivity $S(\lambda)$ and maximum spectral sensitivity S_{max}.

If both ends of the solar cell are short-circuited, the short circuit current or, approximately, the **photoelectric current** I_{Ph} starts flowing. This current can be calculated based on the solar cell's area A, spectral sensitivity S, and the spectrum of sunlight (such as the AM1.5g spectrum mentioned in Chapter 2):

Copyright © 2016. Taylor & Francis Group. All rights reserved.

Quaschning, Volker. Understanding Renewable Energy Systems, Taylor & Francis Group, 2016. ProQuest Ebook Central, http://ebookcentral.proquest.com/lib/byu/detail.action?docID=4470609.
Created from byu on 2021-11-05 15:55:38.

$$I_{Ph} = \int S(\lambda) \cdot E(\lambda) \cdot A \cdot d\lambda \quad (5.29)$$

The share of irradiance E in incident irradiance E_0, absorbed by the semiconductor depends on semiconductor's thickness d and the material's **absorption coefficient** α:

$$E = E_0 \cdot (1 - \exp(-\alpha \cdot d)) \quad (5.30)$$

A distinction is made between direct and indirect semiconductors. The absorption coefficient of indirect semiconductors, such as silicon, is much lower. In indirect semiconductors, the photons also need to transmit crystal momentum to the electron in addition to the energy required. The electrons thus have a harder time crossing the band gap in indirect semiconductors.

For the direct semiconductor GaAs, the absorption coefficient α(GaAs) ≈ 630 mm^{-1}, but the value drops for silicon to α(Si) ≈ 7.2 mm− 1 for radiation at a wavelength of around 1 µm. If both semiconductors are to absorb the same share of sunlight, the silicon semiconductor has to be 87.5 times thicker than the GaAs. For more exact calculations, the absorption coefficient has to be calculated relative to wavelengths. For crystalline silicon solar cells to have high absorption, the crystal has to be at least 200 µm thick. Light trapping – when the light reflects inside the material – extends the path of light, so the material can be thinner.

There are also other effects in photovoltaics and other cell technologies, such as MIS cells, not discussed here; see the bibliography ([Wag07, Goe05, Lew01]).

Manufacturing solar cells and solar modules

Solar cells made of crystalline silicon

Various semiconductor materials can be used to make solar cells. The most common one is silicon. Below, we therefore only discuss how to make solar cells from silicon.

Silicon is the second most common element on earth after oxygen; it occurs, for instance, in silicon dioxide (SiO_2), commonly known as sand. To get silicon out of silicon dioxide, temperatures of around 1800 °C are needed for the following reduction process:

$$SiO_2 + 2C \xrightarrow{1800\,^\circ C} Si + 2CO \quad (5.31)$$

The product is called **metallurgical silicon** (MG-Si), which is still has a lot of impurities at a purity of 98%. In an aluminothermic reduction, silicon can also be produced:

$$3SiO_2 + 4Al \xrightarrow{1100\,^\circ C \ldots 1200\,^\circ C} 2Al_2O_3 + 3Si \quad (5.32)$$

Copyright © 2016. Taylor & Francis Group. All rights reserved.

Quaschning, Volker. Understanding Renewable Energy Systems, Taylor & Francis Group, 2016. ProQuest Ebook Central, http://ebookcentral.proquest.com/lib/byu/detail.action?docID=4470609.
Created from byu on 2021-11-05 15:55:38.

But this process also produces silicon with great impurities. To make semiconductors for the computer industry, electronic-grade silicon (EG-Si) with impurities of only 10^{-10}% is required. The requirements are not quite so high for solar-grade silicon (SOG-Si), though purification processes are also needed.

In the Siemens process, hydrogen chloride (HCl) is added to silicon. In an exothermic reaction, trichlorosilane ($SiHCl_3$) and hydrogen (H_2) are created:

$$Si + 3\ HC1 \longrightarrow SiHCl_3, + H_2 \quad (5.33)$$

Triclorosilane is fluid at 30 °C, and distillation systems remove impurities from it. The silicon is then recovered by means of **chemical vapour deposition** (CVD). At temperatures exceeding 1,000 °C, silicon is deposited on a thin silicon ingot inside the reactor when the trichlorosilane is put into the reactor along with highly pure hydrogen:

$$4\,SiHCl_3 + 2H_2 \xrightarrow{1200\,^\circ C} 3\,Si + SiCl_4 + 8\,HCl \quad (5.34)$$

The result is highly pure silicon ingots up to 30 cm thick and 2 m long. These ingots can then be used to make **polycrystalline solar cells**. A lot of manufacturers melt down the silicon once again and pour it into square blocks. The crystals of polycrystalline silicon are irregularly arranged. These crystals meet at 'grain boundaries', where losses occur within the solar cell.

One recent poll appointed research has been on directly cleaning metallurgical silicon during manufacture without the relatively complex silane process. Called 'upgraded metallurgical silicon' (UMG-Si), this product does not have the purity of electronics-grade silicon from the silane process. It is therefore also called 'dirty silicon'. Nonetheless, UMG silicon can be used to make solar cells with quite good efficiencies.

Table 5.3 provides an overview of the abbreviations already used and a few others to come so you can keep an overview.

To increase the efficiency of solar cells, **monocrystalline material** can be made from polycrystalline silicon. Two methods are used: seed crystal is pulled out of molten silicon in the Czochralski process; the other process is called zone melting. The seed crystal is dipped into molten polycrystalline silicon to produce the desired monocrystalline precursor material. The grain boundaries disappear, thereby reducing losses within the cell.

The pure polycrystalline and monocrystalline rods and blocks are called 'ingots'. The crystalline silicon ingots are then cut, usually by wire saws, into wafers some 150 µm to 250 µm thick. Some 30 to 50 % of the material is lost as waste in the process. Further technical developments have managed to reduce the thickness of the wafers over the past few years, thereby reducing the amount of material needed – and lowering costs. The silicon waste produced during the sawing of wafers combines with grains of silicon carbide and oil or glycol (which are used in the sawing process) to produce **slurry**. Until recently, the recovery of pure

Copyright © 2016. Taylor & Francis Group. All rights reserved.

Quaschning, Volker. Understanding Renewable Energy Systems, Taylor & Francis Group, 2016. ProQuest Ebook Central, http://ebookcentral.proquest.com/lib/byu/detail.action?docID=4470609.
Created from byu on 2021-11-05 15:55:38.

silicon from this slurry was prohibitively expensive. Now, recycling processes are affordable.

The alternative to a wire saw is zone melting, which used to be used commercially but is now rare. In the **string ribbon process** (SR process) silicon is first melted. In this process, two thin ribbons are pulled through the molten silicon. The molten silicon forms a thin film between the two ribbons similar to bubbles of soap and hardens.

The **EFG process** (edge-defined film-fed growth) also starts with molten silicon. But here, an octagonal mold with a thin gap inside it is dipped into the molten silicon. Capillary forces pushed the silicon into the gap. A foil is lowered onto this silicon, which then forms

Table 5.3 Overview of common abbreviations related to silicon

Abbreviation	*Full name*	*Note*
Si	Silicon	General term
a-Si, α-Si	Amorphous silicon	Used in thin-film photovoltaics
Cz-Si	Czochralski silicon	Mono-Si from the Czochralski process
EG-Si	Electronic-grade silicon	For computer processors > 99.999999999 %
FZ-Si	Float-zone silicon	Mono-Si
EFG-Si	Edge-defined film-fedgrowth Si	Octagonal silicon
MG-Si	Metallurgical-grade silicon	Purity > 98 %
Mono-Si	Monocrystalline silicon	Generally black in appearance
Poly-Si	Polycrystalline silicon	The most common type on the market
μc-Si	Microcrystalline silicon	Niche product
PVG-Si	Photovoltaic-grade silicon	Essentially the same as solar silicon
SOG-Si	Solar-grade silicon	Solar silicon, purity > 99.99 %
SR-Si	String ribbon silicon	Created by growth along a ribbon
UMG-Si	Upgraded MG-Si	Purity > 99.99 %

Copyright © 2016. Taylor & Francis Group. All rights reserved.

Quaschning, Volker. Understanding Renewable Energy Systems, Taylor & Francis Group, 2016. ProQuest Ebook Central, http://ebookcentral.proquest.com/lib/byu/detail.action?docID=4470609.
Created from byu on 2021-11-05 15:55:38.

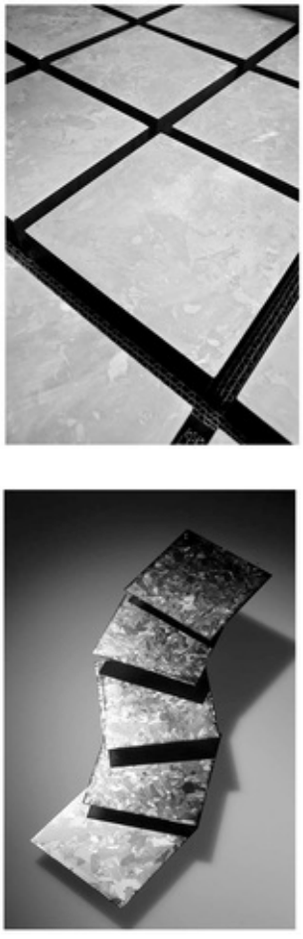

Figure 5.12 Polycrystalline silicon for solar cells. Left: raw silicon; middle: silicon ingots; right: silicon wafers (photos: PV Crystalox Solar plc.)

a fluid film on the foil. The foil is lifted, and the fluid silicon solidifies on its underside. The result is a long octagon that can be separated at the edges to make silicon wafers.

Whether the sawing or the pulling process is used, the result is always silicon **wafers**. In various stages, the wafers then have to be cleaned, doped, and have contacts added to them. Any damage caused during the sawing process is first removed with hydrofluoric acid. Otherwise, the wafers would break too easily in further processing.

Atoms of phosphorus or boron are added to dope the silicon for the p–n transition. Here, the vapour deposition process is used. At temperatures between 800 °C and 1200 °C, gaseous dopants are combined with a carrier gas, such as nitrogen (N_2) or oxygen (O_2). This gas then flows over the wafers, and the dopant atoms are deposited on the silicon semiconductor relative to the gas mixture, the temperature, and the flow rate. The doped semiconductor's surface is then cleaned by means of etching.

A screen printing process then adds contacts to the front and back of the cell. Metal and alloys based on aluminium or silver are used as material for the contacts. On the back, the contact usually covers the entire area, while the front has thin contact fingers so that as little of the solar cell as possible is shaded.

Copyright © 2016. Taylor & Francis Group. All rights reserved.

Quaschning, Volker. Understanding Renewable Energy Systems, Taylor & Francis Group, 2016. ProQuest Ebook Central, http://ebookcentral.proquest.com/lib/byu/detail.action?docID=4470609.
Created from byu on 2021-11-05 15:55:38.

Finally, an **antireflection coating** is added, giving the solar cell its characteristic blue colour. Metallic silicon reflects light well, but the coaching reduces the reflection of light dramatically. Generally, a roughly 70 nm thick layer of silicon nitride (Si_3N_4) is used. Silicon dioxide (SiO_2) and titanium dioxide (TiO_2) can also be used as antireflection layers. It is now also possible to make antireflection coatings in other colours than blue so that photovoltaic modules can be better integrated aesthetically in buildings. Figure 5.13 shows a cross-section of a crystalline solar cell.

There are various ways to increase a solar cell's efficiency further. For instance, the solar cell's surface can have microscopic pyramids added to it in order to increase the surface so that more sunlight can be absorbed. The front contacts can also be buried. Lasers were used to give BP's Saturn cell its **laser grooved buried contacts**, **LGBC**). The lasers cut small grooves into the front of the cell, into which the front contacts are chemically deposited. These 'buried' contacts are only an eighth as large, but deeper. As a result, reflection losses from the front contacts are reduced.

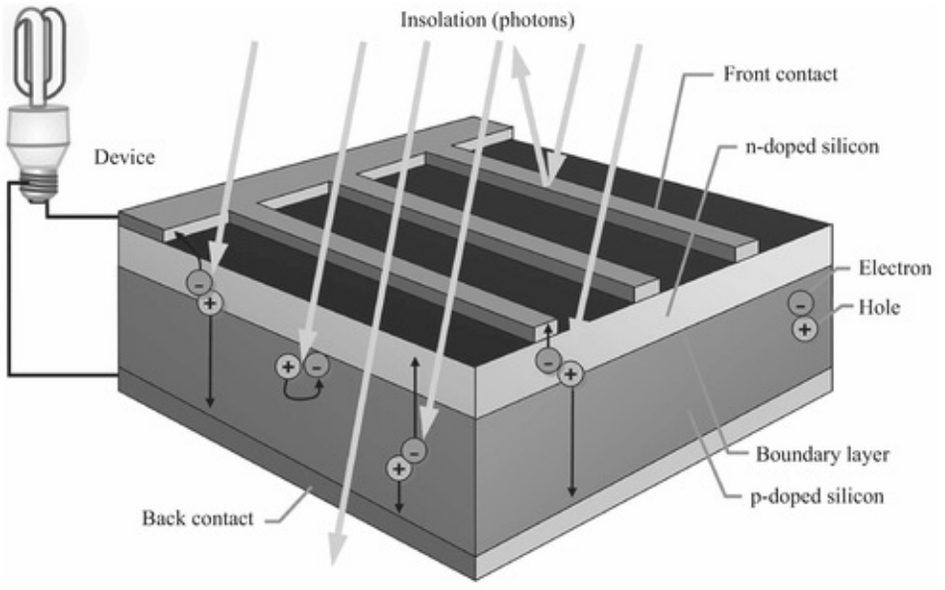

Figure 5.13 The structure of a crystalline solar cell

Reflections are reduced even further if the front contacts are moved to the back. **Back-contact solar cells** have both contacts on the back. They are electrically isolated from each other.

If monocrystalline solar cell material is combined with amorphous silicon, the results can also be very high efficiency. The **HIT cell** (HIT: heterojunction with intrinsic thin-layer) is made by Sanyo.

All of these efforts increase the solar cell's efficiency. In serial production, efficiencies can exceed 20 %. But the extra effort also makes manufacturing more complicated.

Copyright © 2016. Taylor & Francis Group. All rights reserved.

Quaschning, Volker. Understanding Renewable Energy Systems, Taylor & Francis Group, 2016. ProQuest Ebook Central, http://ebookcentral.proquest.com/lib/byu/detail.action?docID=4470609.
Created from byu on 2021-11-05 15:55:38.

Solar modules made of crystalline cells

Without protection from the elements, individual solar cells would quickly be destroyed, so they are combined in **modules**. A crystalline solar cell typically has an edge length of 10 cm to 20 cm. Solar modules used in battery systems generally contain 32 to 40 cells. There are, however, other module sizes with far fewer or far more cells for grid-connected systems.

As with solar thermal flat-plate collectors, low-iron panes of glass are used as covers. The back generally also has either a pane of glass or plastic foil (usually Tedlar). The solar cells are embedded in plastic between the cover and the rear foil or rear glass pane. Generally, EVA (ethylene vinyl acetate) hardened at temperatures up to 150 °C at low pressure for 10 to 15 minutes is used. The process is called **lamination**. To prevent the glass from breaking and facilitate installation, the modules are then put into a frame. Connections are usually made with sockets and plugs. Bypass diodes are also installed to provide protection from dangerous operating conditions. The section 'Technical data for solar modules' later in this chapter provides the technical data for a few solar modules.

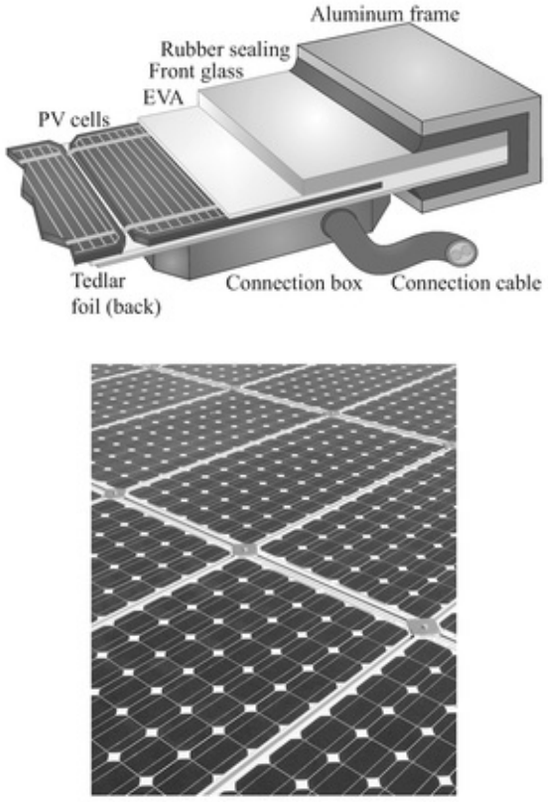

Figure 5.14 Left: the basic structure of a solar module; right: installed solar modules

Copyright © 2016. Taylor & Francis Group. All rights reserved.

Quaschning, Volker. Understanding Renewable Energy Systems, Taylor & Francis Group, 2016. ProQuest Ebook Central, http://ebookcentral.proquest.com/lib/byu/detail.action?docID=4470609.
Created from byu on 2021-11-05 15:55:38.

Solar cells made of amorphous silicon

In addition to cells made of crystalline silicon, thin-film cells are also now common. Such cells can either be made of amorphous silicon or other materials, such as cadmium telluride (CdTe) or copper-indium-diselenide (CIS). Thin-film cells have the benefit of making do with very little material, and they are expected to be very affordable. For these reasons, thin-films cells are held to have great development potential. The efficiency of thin-films cells is, however, currently far below that of crystalline silicon cells. In other words, you need more modules taking up more space and entailing greater insulation costs for the same output.

Solar cells made of amorphous silicon have a carrier substrate, which is generally glass. A transparent conducting oxide (**TCO**), such as tin oxide, is sprayed onto the glass. A laser then cuts this surface into strips for the later application of front contacts. Silicon and the dopant are then applied to the substrate by means of vapour deposition at high temperatures. First, a 10 nm p-layer is applied, followed by 10 nm of buffer layer. Then comes an intrinsic layer of 500 nm amorphous silicon, followed by a 20 nm n-layer. The rear contacts made of aluminium powder are then screen-printed on, and the cells are embedded in a polymer layer for protection. Figure 5.15 shows the basic structure of an amorphous silicon cell.

When the silicon is applied by means of vapour deposition, its crystalline structure is lost, so the atoms are amorphous. Amorphous silicon solar cells can be roughly 100 times thinner than crystalline cells because the former has a much higher absorption coefficient than the latter. The band gap of amorphous silicon is a bit greater at 1.7 eV. A lot less material is needed, and manufacturing can be streamlined. In the lab, efficiencies of up to 12 % have been reached. Nonetheless, solar cells made of amorphous silicon are mainly used for small applications, such as pocket calculators and watches, because their efficiency is far lower than that of crystalline cells at 6–7 %, compared with 20 %, respectively. In addition, amorphous solar cells undergo a degradation process that reduces efficiency by 1–2 % in the first few months of use before it finally stabilizes at a lower level.

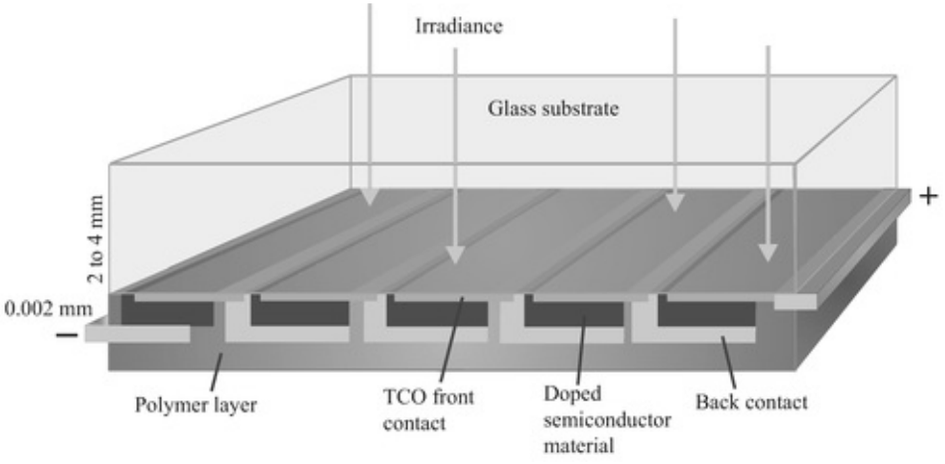

Copyright © 2016. Taylor & Francis Group. All rights reserved.

Quaschning, Volker. Understanding Renewable Energy Systems, Taylor & Francis Group, 2016. ProQuest Ebook Central, http://ebookcentral.proquest.com/lib/byu/detail.action?docID=4470609.
Created from byu on 2021-11-05 15:55:38.

Figure 5.15 The basic structure of an amorphous silicon solar cell

Solar cells made of other materials

Increasingly, other thin-film materials are used instead of amorphous silicon. A very wide range of materials and technologies are also being tested. The following materials are now used in serial production:

- cadmium telluride (CdTe)
- cadmium sulphide (CdS)
- copper-indium-sulphide (CIS)
- copper-indium-diselenide ($CuInSe_2$ or CIS)
- copper-indium-gallium-diselenide/sulphide (CIGS).

The manufacturing process is similar to the one for amorphous silicon solar cells. While global silicon reserves are practically inexhaustible, other materials, such as tellurium, are only available to a limited extent. CdTe and CIS can reach higher efficiencies than amorphous silicon can. Nonetheless, the efficiency of thin-film solar cells is noticeably lower than that of crystalline solar cells. Because more module surface is therefore needed to produce the same amount of power, installation costs are therefore higher. On the other hand, less material is required and production processes can be streamlined, so thin-film cells are less expensive than crystalline cells to manufacture. It is too soon to tell which option will prevail.

Thin-film cells can also be made of polycrystalline silicon. **Microcrystalline cells** consist of extremely small polycrystalline areas on a substrate. Microcrystalline and amorphous cell material is combined to produce micromorph solar cells.

Other promising technological developments include solar cells containing pigment based on titanium dioxide (TiO_2) and organic solar cells. Both of these technologies are, however, still in the research stage. The main progress needs to be made in efficiency and the long-term stability of the cells.

In space, other materials, such as gallium arsenide (GaAs), are used. GaAs is especially resistant to cosmic radiation and has high efficiencies exceeding 20 %. It is also too expensive to use on earth. In contrast, more expensive materials can be used in concentrating photovoltaics because these cells are so small. Tandem and triple cells combine two or three materials, respectively, of different band gaps. The uppermost layer of cell material absorbs shortwave light. Long waves pass through this layer and are absorbed by those underneath. In this way, the spectrum of light is better exploited, and efficiency levels can exceed 40 %.

Copyright © 2016. Taylor & Francis Group. All rights reserved.

Quaschning, Volker. Understanding Renewable Energy Systems, Taylor & Francis Group, 2016. ProQuest Ebook Central, http://ebookcentral.proquest.com/lib/byu/detail.action?docID=4470609.
Created from byu on 2021-11-05 15:55:38.

Module tests and quality assurance

Under real-world conditions, solar modules are designed to run for at least 20 to 30 years. Various test methods have been developed to check whether a serially manufactured solar module is likely to run properly for that long. IEC 61215 [DIN05b] and IEC 61646 [DIN08] are two standards that specify comprehensive test procedures for crystalline and thin-film solar modules. First, the manufacturer sends eight samples to a certified test lab, which conducts the following tests:

- visual inspection and output measurement
- wet insulation resistance
- long-term test under outdoor conditions (60 kWh/m²)
- long-term hotspot test with cell shading
- temperature test of bypass diodes
- UV pretreatment test (15 kWh/m²)
- damp humidity test (10 cycles from −40 °C to +85 °C at 85 % rel. humidity)
- thermal cycling (50 and 200 cycles from −40 °C to +85 °C)
- damp heat test (1000 h at 85 °C and 85 % rel. humidity)
- hail impact (25 mm balls of ice shot at a velocity of 23 m/s)
- static load test and resistance test of connections .

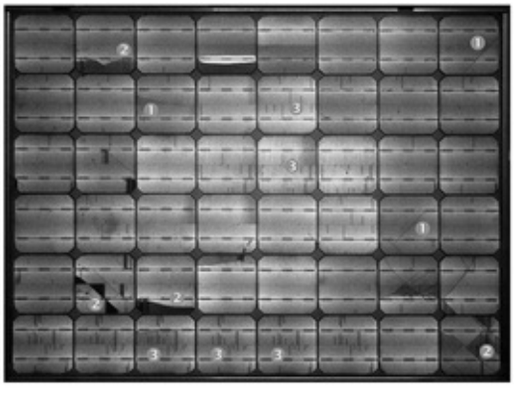

Copyright © 2016. Taylor & Francis Group. All rights reserved.

Quaschning, Volker. Understanding Renewable Energy Systems, Taylor & Francis Group, 2016. ProQuest Ebook Central, http://ebookcentral.proquest.com/lib/byu/detail.action?docID=4470609.
Created from byu on 2021-11-05 15:55:38.

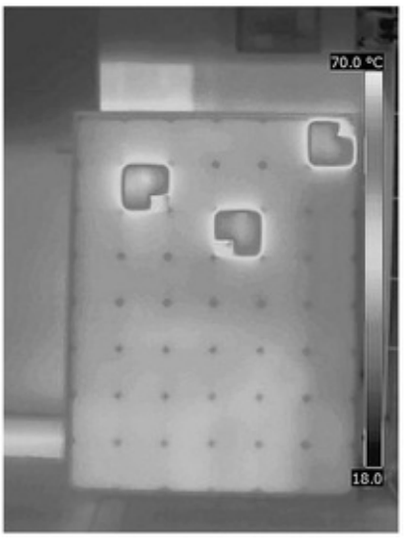

Figure 5.16 Left: an image of electroluminescence reveals damaged cells (1: micro-fissures, 2: broken cells, 3: contact degradation/flawed screen printing). Right: thermography of a module with three partly shaded solar cells. Photos: Oliver Suchaneck, HTW Berlin

If all of the tests are passed, the modules are considered reliable for the long term. Keep in mind, however, that this standard merely concerns type certification. Quality can easily fluctuate during serial production. Subsequent sample tests therefore make sense. If the modules are to be built in special locations, such as close to the sea or on farms, additional tests, such as salt mist tests and tests of ammonia resistance, can help detect whether problems might occur in advance.

Other test methods provide additional information about production quality and possible flaws. A **lamination test** can reveal whether the lamination process went optimally or whether the EVA foil can be expected to age prematurely. **Electroluminescence (EL)** can reveal cell flaws within the module. Here, the module is connected to an external power source in the dark. The solar cells then emit infrared radiation, which can be recorded with a special camera. The images show great differences in brightness that cannot be seen with the naked eye, indicating differences in cell production, poor contacts, and micro-fissures. **Thermography** is also useful. Here, an infrared camera visualizes temperature differences while a PV system is running. Shaded cells and individual cells with low outputs heat up, thereby reducing power production; in the worst case, the entire system fails. Flawed contacts and improperly connected modules can also be detected in this way.

Electrical description of solar cells

Copyright © 2016. Taylor & Francis Group. All rights reserved.

Quaschning, Volker. Understanding Renewable Energy Systems, Taylor & Francis Group, 2016. ProQuest Ebook Central, http://ebookcentral.proquest.com/lib/byu/detail.action?docID=4470609.
Created from byu on 2021-11-05 15:55:38.

Simple equivalent circuit

A solar cell has the same physical structure as a **diode**. It consists of an n-doped and a p-doped semiconductor with a depletion region, meaning that a solar cell not exposed to sunlight acts quite like a diode and can be described as one in simplified fashion.

The saturation current in reverse bias I_S and diode factor m are used in the following formula for cell current I relative to cell voltage (here $U = U_D$):

$$I = -I_D = -I_S \cdot \left(\exp\left(\frac{U_D}{m \cdot U_T} \right) - 1 \right) \tag{5.35}$$

The temperature factor U_T at a temperature of 25 °C is U_T = 25.7 mV. The saturation current I_S is roughly 10^{-10} A. The diode factor m is 1 in an ideal diode. If the diode factor is chosen between 1 and 5, we can better describe a solar cell.

When a solar cell is exposed to sunlight, a power source can be connected in parallel to the diode in the simplified equivalent circuit. The power source produces photocurrent I_{Ph}, which is relative to irradiance E via the coefficient c_0:

$$I_{ph} = c_0 \cdot E \tag{5.36}$$

Kirchhoff's first law gives us the equation for the solar cell's **current–voltage characteristic** in the simplified equivalent circuit, as shown in Figure 5.17. Figure 5.18 shows the curve at different levels of irradiance.

$$I = I_{Ph} - I_D = I_{Ph} - I_S \cdot \left(\exp\left(\frac{U}{m \cdot U_T} \right) - 1 \right) \tag{5.37}$$

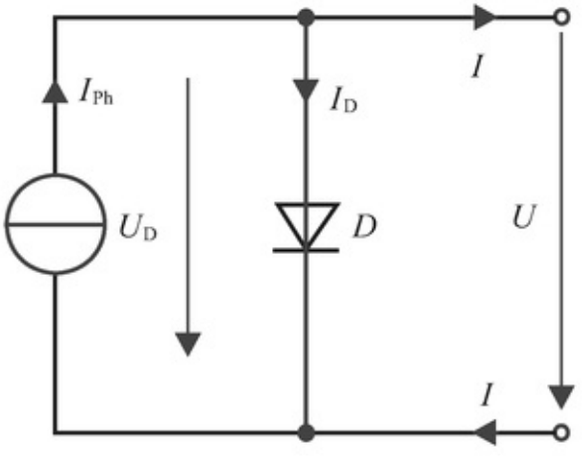

Figure 5.17 A solar cell's simplified equivalent circuit

Copyright © 2016. Taylor & Francis Group. All rights reserved.

Quaschning, Volker. Understanding Renewable Energy Systems, Taylor & Francis Group, 2016. ProQuest Ebook Central, http://ebookcentral.proquest.com/lib/byu/detail.action?docID=4470609.
Created from byu on 2021-11-05 15:55:38.

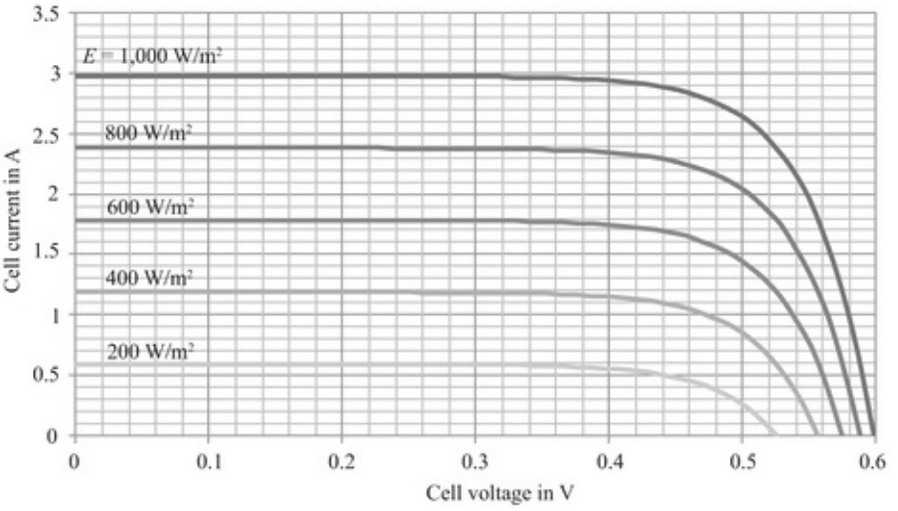

Figure 5.18 Influence of irradiance E on a solar cell's current-voltage characteristic

Expanded equivalent circuit (single-diode model)

For most applications, the simple equivalent circuit suffices to describe solar cells. The current-voltage characteristic only differs from actual values by a few percent. For a more exact description, however, the simple equivalent circuit has to become more sophisticated. In a real solar cell, voltage drops on the path that charge carriers take from the semiconductor to the external contacts. Series resistance R_S causes this reduction in voltage. Leak current along the edge of the solar cell can also be observed and described as parallel resistance R_P. Figure 5.19 shows both types of resistance in an equivalent circuit.

In real cells, series resistance R_S comes in at a few milliohms, while parallel resistance R_P is generally much greater than 10 Ω. Figures 5.20 and 5.21 show the influence of these two types of resistance on the current-voltage characteristic, also called the I–V curve.

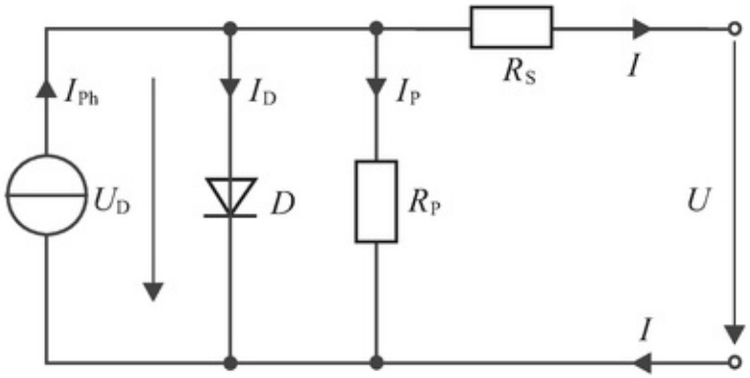

Figure 5.19 Expanded equivalent circuit for a solar cell (single-diode model)

Copyright © 2016. Taylor & Francis Group. All rights reserved.

Quaschning, Volker. Understanding Renewable Energy Systems, Taylor & Francis Group, 2016. ProQuest Ebook Central, http://ebookcentral.proquest.com/lib/byu/detail.action?docID=4470609.
Created from byu on 2021-11-05 15:55:38.

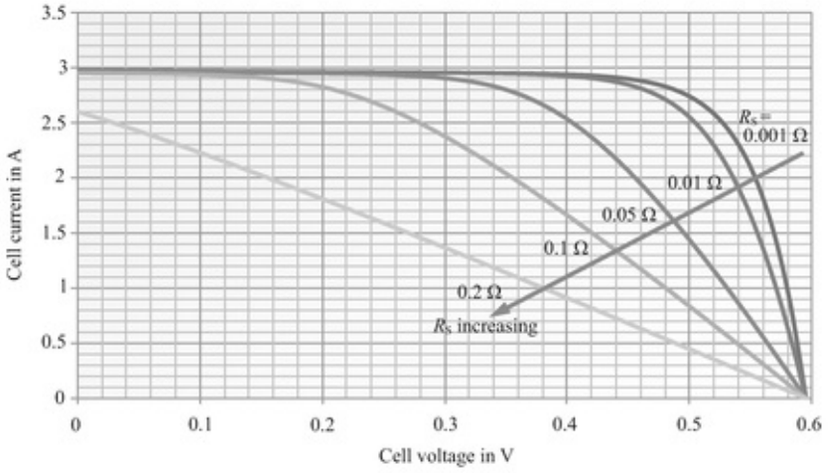

Figure 5.20 Influence of series resistance R_S on a solar cell's current–voltage characteristic

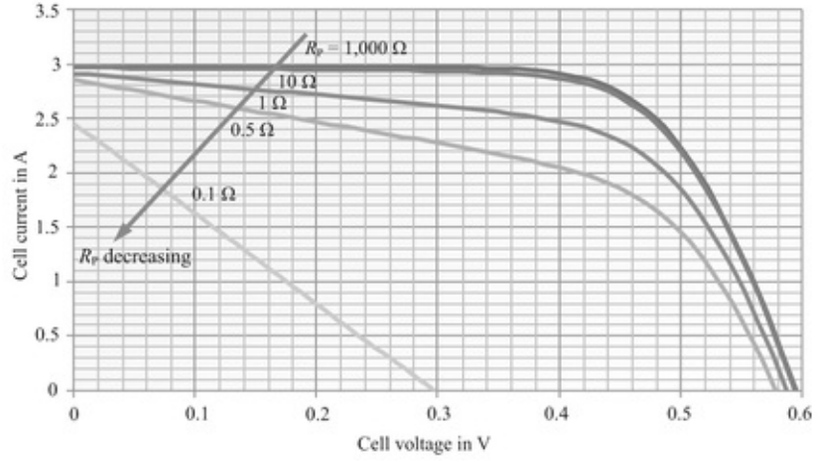

Figure 5.21 Influence of parallel resistance R_p on a solar cell's current–voltage characteristic

Kirchhoff's node law $0 = I_{ph} - I_D - I_p - I$ is vised with the formula $I_P = \frac{U_D}{R_P} = \frac{U + I \cdot R_S}{R_P}$ for the I—V curve of the solar cell's expanded equivalent circuit:

$$0 = I_{Ph} - I_S \cdot \left(\exp\left(\frac{U + I \cdot R_S}{m \cdot U_T} \right) - 1 \right) - \frac{U + I \cdot R_S}{R_P} - I \qquad (5.38)$$

However, this implicit formula cannot be broken down into I and U as easily as the formula for the simplified equivalent circuit could (5.37). Rather, we need numeric methods.

One of the most common options is the Newton Method to find the root of a function. A solar cell's I–V curve can be expressed in a closed formula:

$$f(U,I) = 0. \qquad (5.39)$$

The current I of a given voltage U_V and the voltage U of a given current I_V are to be determined. The solution is the root of the function $f(U,I)$. To reach this solution, the following

Copyright © 2016. Taylor & Francis Group. All rights reserved.

Quaschning, Volker. Understanding Renewable Energy Systems, Taylor & Francis Group, 2016. ProQuest Ebook Central, http://ebookcentral.proquest.com/lib/byu/detail.action?docID=4470609.
Created from byu on 2021-11-05 15:55:38.

formulae are calculated in an iterative process:

$$U_{i+1} = U_i - \frac{\mathrm{f}(U_i, I_\mathrm{V})}{\frac{\mathrm{d}\,\mathrm{f}(U_i, I_\mathrm{V})}{\mathrm{d}U}} \text{ and } I_{i+1} = I_i - \frac{\mathrm{f}(U_\mathrm{V}, I_i)}{\frac{\mathrm{d}\,\mathrm{f}(U_\mathrm{V}, I_i)}{\mathrm{d}I}} \tag{5.40}$$

Starting from U_0 and I_0, a solution for the implicit formula for a given current I_V or voltage U_V can be found by repeating the iteration until the difference between the iterated steps falls below a previously selected value ε. The iteration is discontinued when: $| U_i - U_{i-1} | < \varepsilon$ or $| I_i - I_{i-1} | < \varepsilon$.

The Newton Method quickly produces convergence depending on the starting values U_0 and I_0. For diode breakdowns, pre-iteration with another method can be useful.

The iteration to determine a solar cell's current I met a given voltage U_V is as follows in accordance with 5.38:

$$I_{i+1} = I_i - \frac{I_\mathrm{ph} - I_\mathrm{S} \cdot \left(\exp\left(\frac{U_\mathrm{V} + I_i \cdot R_\mathrm{S}}{m \cdot U_\mathrm{T}} \right) - 1 \right) - \frac{U_\mathrm{V} + I_i \cdot R_\mathrm{S}}{R_\mathrm{P}} - I_i}{-\frac{I_\mathrm{S} \cdot R_\mathrm{S}}{m \cdot U_\mathrm{T}} \cdot \exp\left(\frac{U_\mathrm{V} + I_i \cdot R_\mathrm{S}}{m \cdot U_\mathrm{T}} \right) - \frac{R_\mathrm{S}}{R_\mathrm{P}} - 1} \tag{5.41}$$

Two-diode model

The two-diode model is an even better way of describing a solar cell (Figure 5.22). Here, a second diode is parallel to the first. Each has a different saturation current and diode factor. For crystalline silicon solar cells, this model provides a nearly optimal description. It is, however, only of limited use for thin-film solar cells. The deviations are especially great under partial loads.

The implicit formula for the two-diode model is:

$$0 = I_\mathrm{ph} - I_{\mathrm{S}1} \cdot \left(\exp\left(\frac{U + I \cdot R_\mathrm{S}}{m_1 \cdot U_\mathrm{T}} \right) - 1 \right) - I_{\mathrm{S}2} \cdot \left(\exp\left(\frac{U + I \cdot R_\mathrm{S}}{m_2 \cdot U_\mathrm{T}} \right) - 1 \right) - \frac{U + I \cdot R_\mathrm{S}}{R_\mathrm{P}} - I \tag{5.42}$$

Copyright © 2016. Taylor & Francis Group. All rights reserved.

Quaschning, Volker. Understanding Renewable Energy Systems, Taylor & Francis Group, 2016. ProQuest Ebook Central, http://ebookcentral.proquest.com/lib/byu/detail.action?docID=4470609.
Created from byu on 2021-11-05 15:55:38.

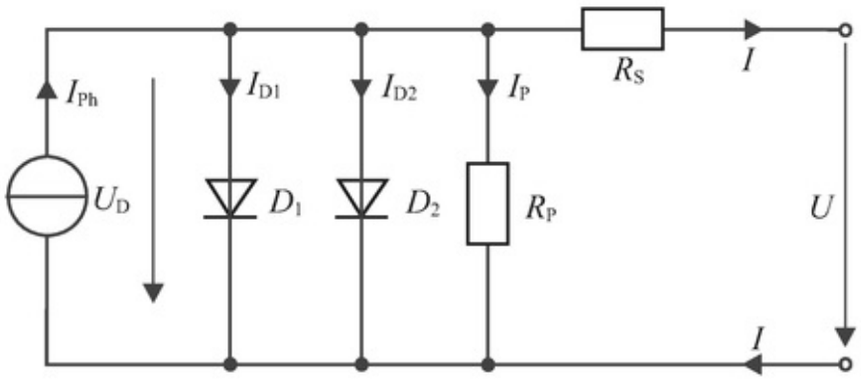

Figure 5.22 Two-diode model of a solar cell

Table 5.4 Parameters for various PV modules for the two-diode model [PRE94]

Parameter	c_0	I_{S1}	I_{S2}	m_1	m_2	R_S	R_P
Unit	m²/V	nA	µA	–	–	mΩ	Ω
AEG PQ 40/50	$2.92 \cdot 10^{-3}$	1.082	12.24	1	2	13.66	34.9
Siemens M50	$3.11 \cdot 10^{-3}$	0.878	12.71	1	2	13.81	13.0
Kyocera LA441J59	$3.09 \cdot 10^{-3}$	1.913	8.25	1	2	12.94	94.1

The first diode is generally an ideal diode ($m_1 = 1$), while the diode factor of the second diode is $m_2 = 2$. This calculation also has to be performed in a numeric method. Table 5.4 shows the parameters that can be used to simulate some PV modules well.

Two-diode model with expansion term

The solar cell's equivalent circuit has to be expanded further so we can describe the curve in the negative breakdown area, where there are great negative voltages. An expansion term, shown as an additional current source in Figure 5.23 $I(U_D)$, describes the diode breakdown in the negative voltage area. This source of current generates current relative to diode voltage U_D, thus allowing us to describe the solar cell's electrical behaviour when the voltage is considerably negative.

Breakdown voltage U_{Br}, the landslide breakdown exponent n and adjustment value for conductance b are used in the following formula for the I–V curve:

$$0 = I_{Ph} - I_{S1}\left(\exp\left(\frac{U + I \cdot R_S}{m_1 \cdot U_T}\right) - 1\right) - I_{S2}\left(\exp\left(\frac{U + I \cdot R_S}{m_2 \cdot U_T}\right) - 1\right) - \frac{U + I \cdot R_S}{R_P} - I \quad (5.43)$$

$$\underbrace{- b \cdot \left(U + I \cdot R_S\right) \cdot \left(1 - \frac{U + I \cdot R_S}{U_{Br}}\right)^{-n}}_{\text{Exparsion term}}$$

Copyright © 2016. Taylor & Francis Group. All rights reserved.

Quaschning, Volker. Understanding Renewable Energy Systems, Taylor & Francis Group, 2016. ProQuest Ebook Central, http://ebookcentral.proquest.com/lib/byu/detail.action?docID=4470609.
Created from byu on 2021-11-05 15:55:38.

Figure 5.24 shows a polycrystalline solar cell's I–V curve. The parameters $I_{S1} = 3 \cdot 10^{-10}$ A, $m_1 = 1$, $I_{S2} = 6 \cdot 10^{-6}$ A, $m_2 = 2$, $R_S = 0.13\ \Omega$, $R_P = 30\ \Omega$, $U_{Br} = -18$ v, $b = 2.33$ mS and $n = 1.9$ are used to determine the curve.

The great series resistance comes about in this case when the resistance of the connection lines is taken into account. The positive voltage and current range represents the cell's generator range. If the voltage or current is negative, the cell consumes power. An external voltage source or other solar cells must provide the electrical output for this to happen.

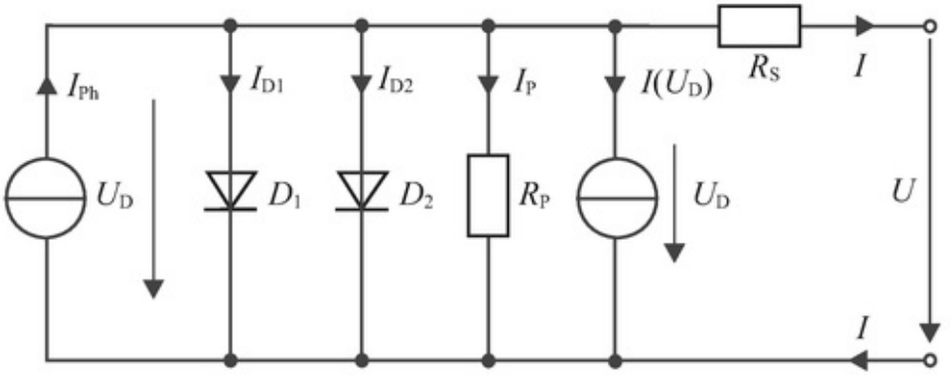

Figure 5.23 A two-diode equivalent circuit with a second source of current for a breakdown under negative voltage

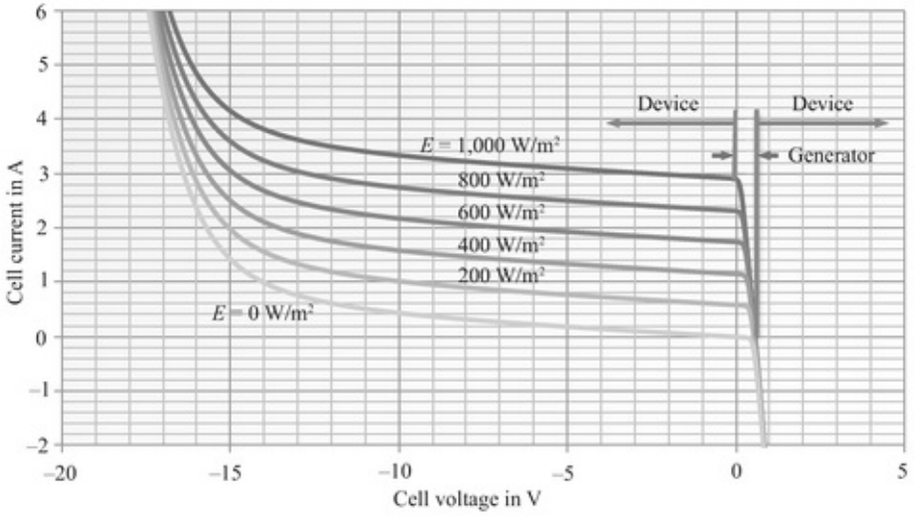

Figure 5.24 A polycrystalline cell's I–V curve over the entire voltage range

Other electrical cell parameters

Up to now, we have only spoken about the voltage and current of solar cells. Here, we discuss other electrical cell parameters. Table 5.5 provides an overview of the main solar cell parameters.

If the cell is short-circuited, the terminal voltage at the solar cell is zero. The short circuit

Copyright © 2016. Taylor & Francis Group. All rights reserved.

Quaschning, Volker. Understanding Renewable Energy Systems, Taylor & Francis Group, 2016. ProQuest Ebook Central, http://ebookcentral.proquest.com/lib/byu/detail.action?docID=4470609.
Created from byu on 2021-11-05 15:55:38.

current I_{sc}, which is roughly equivalent to the photocurrent I_{Ph}, then flows. Because the photocurrent is proportional to irradiance E, this also applies for **short circuit current**:

$$I_{SC} \approx I_{Ph} = c_0 \cdot E$$

Table 5.5 Electrical solar cell parameters

Designation	*Symbol*	*Unit*	*Note*
Open-circuit voltage	U_{SC}	V	$U_{OC} \sim \ln E$
Short-circuit voltage	I_{SC}	A	$I_{OC} \approx I_{Ph} \sim E$
MPP voltage	U_{MPP}	V	$U_{MPP} < U_{OC}$
MPP current	I_{MPP}	A	$I_{MPP} < I_{SC}$
MPP output	P_{MPP}	W or W_p	$P_{MPP} = U_{MPP}\, I_{MPP}$
Fill factor	FF		$FF = P_{MPP} / (U_{OC}\, I_{SC}) < 1$
Efficiency	η	%	$\eta = P_{MPP} / (E\, A)$

If the cell has an open circuit with current I at zero, the cell has **open-circuit voltage** U_{OC}. In the I–V curve of the simplified equivalent circuit, U_{OC} can be calculated with $I = 0$:

$$U_{OC} = m \cdot U_T \cdot \ln\left(\frac{I_{SC}}{I_S} + 1\right) \tag{5.44}$$

Because short-circuit current I_{SC} has a linear relation to irradiance E, the relation of open-circuit voltage is as follows:

$$U_{OC} \sim \ln(E) \tag{5.45}$$

A solar cell's maximum output can be determined at a specific voltage. Figure 5.25 shows the output-voltage characteristic along with the current-voltage characteristic. The output curve clearly has a maximum point. One therefore speaks of a **maximum power point** (**MPP**).

The voltage U_{MPP} at the *MPP* is less than the open-circuit voltage U_{OC}, and the current I_{MPP} is less than the short-circuit voltage I_{SC}. The current and voltage both depend upon irradiance and temperature, as with short-circuit current and open-circuit voltage. The output P_{MPP} at the *MPP* is calculated as follows:

$$P_{MPP} = U_{MPP} \cdot I_{MPP} < U_{OC} \cdot I_{SC} \tag{5.46}$$

The share of current is more important in the interdependence on irradiance, so the MPP output roughly increases proportional to irradiance E.

Copyright © 2016. Taylor & Francis Group. All rights reserved.

Quaschning, Volker. Understanding Renewable Energy Systems, Taylor & Francis Group, 2016. ProQuest Ebook Central, http://ebookcentral.proquest.com/lib/byu/detail.action?docID=4470609.
Created from byu on 2021-11-05 15:55:38.

The MPP output of solar cells and modules is usually determined under **standard test conditions** (**STC**) (E = 1000 W/m², ϑ = 25 °C, spectral AM1.5g) to facilitate comparisons. Because solar modules almost always have a lower output under natural conditions, W_p (**watts-peak**) is often the designation used for the finding from the measurement.

The parameters of solar modules are therefore also determined under **Normal Operating Test Conditions** (**NOTCs**). Here, measurements are taken at a **Normal Operating Cell Temperature** (**NOCT**) at an irradiance of 800 W/m², an ambient temperature of 20 °C, spectrum AM1.5g, and a wind velocity of 1 m/s. Generally, the NOCT is around 45 °C.

The fill factor *FF* is another parameter:

$$FF = \frac{P_{MPP}}{U_{OC} \cdot I_{SC}} = \frac{U_{MPP} \cdot I_{MPP}}{U_{OC} \cdot I_{SC}} \tag{5.47}$$

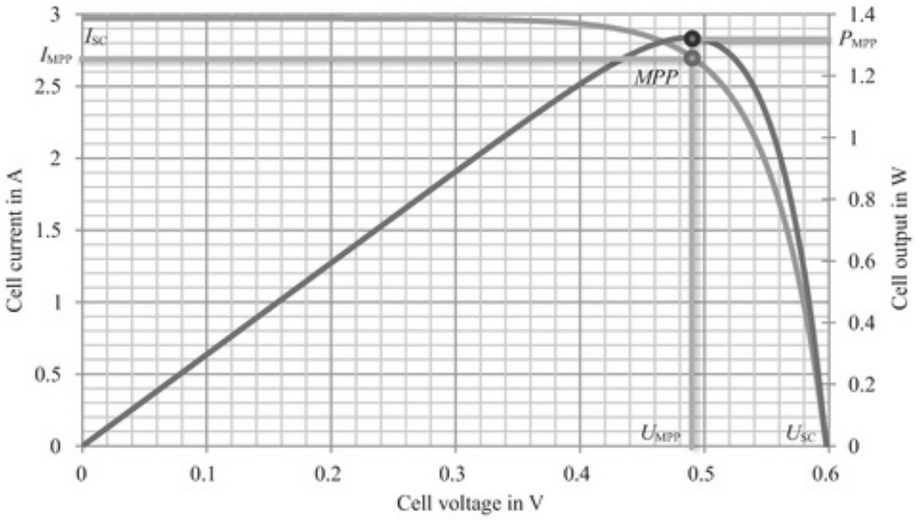

Figure 5.25 A solar cell's I–V and P–U curves with MPP

Table 5.6 Maximum efficiencies and fill factors for various cell technologies

Cell/module type	η_{max} *cell, lab*	η_{max} *cell, series*	η_{max} *module, series*	*FF module, series*
Mono-Si	25.0 %	22.9 %	20.4 %	0.80
Poly-Si	20.4 %	17.8 %	16.0 %	0.78
SR-Si	17.8 %	15.6 %	14.1 %	0.74
EFG-Si	18.2 %	14.4 %	12.8 %	0.72
HIT	23.0 %	21.6 %	19.0 %	0.78
µc-Si / a-Si	11.9 %	10.4 %	10.1 %	0.68
a-Si	12.5 %	-7.6 %	-7.4 %	0.67
CdS / CdTe	17.3 %	12.8 %	11.8 %	0.74
CIS / CIGS	20.3 %	15.1 %	14.5 %	0.73

Copyright © 2016. Taylor & Francis Group. All rights reserved.

Quaschning, Volker. Understanding Renewable Energy Systems, Taylor & Francis Group, 2016. ProQuest Ebook Central, http://ebookcentral.proquest.com/lib/byu/detail.action?docID=4470609.
Created from byu on 2021-11-05 15:55:38.

Concentrator	43.5 %	40.0 %	29.5 %	0.85
GaAs	26.4 %	- [1)]	- [1)]	- [1)]
Dye-sensitized	11.8 %	- [2)]	- [2)]	- [2)]
Organic	10.6 %	- [2)]	- [2)]	- [2)]

Note: As of 07/2012 [1)] Only special applications, such as outer space [2)] Not yet in serial production

It serves as a quality criterion for solar cells by describing how close the solar cell's I–V curve is to the rectangle of U_{OC} and I_{SC} . This value is always less than one.

A solar cell's **efficiency** η is the product of the MPP output P_{MPP}, irradiance E, and the solar cell's area A:

$$\eta = \frac{P_{MPP}}{E \cdot A} = \frac{FF \cdot U_{OC} \cdot I_{SC}}{E \cdot A} \tag{5.48}$$

Usually, efficiency is indicated under standard test conditions. Table 5.6 shows the maximum efficiencies and typical fill factors for various types of cells and modules. The module's efficiency is always less than the cell's because the module's frame and the space between the cells do not have any output.

Temperature factors

The formulae used to describe solar cell models always assume a constant temperature of 25 °C. But as described above, a solar cell's curve changes relative to temperature. Now, we discussed how the formulae used for this calculation can be changed to take account of different temperatures.

First, the temperature voltage is no longer a fixed value, but has to be calculated for each specific temperature.

The **temperature voltage** is calculated from the absolute temperature in Kelvin (T = ϑ K/°C + 273.15 K), the Boltzmann constant k = $1.380658 \cdot 10^{-23}$ J/K, and the elementary charge e = $1.60217733 \cdot 10^{-19}$ As:

$$U_T = \frac{k \cdot T}{e} \tag{5.49}$$

Copyright © 2016. Taylor & Francis Group. All rights reserved.

Quaschning, Volker. Understanding Renewable Energy Systems, Taylor & Francis Group, 2016. ProQuest Ebook Central, http://ebookcentral.proquest.com/lib/byu/detail.action?docID=4470609.
Created from byu on 2021-11-05 15:55:38.

The temperature factor of **saturation currents** I_{S1} and I_{S2} can be calculated from the coefficients c_{S1} and c_{S2} and the band gap E_g from Table 5.2 [Wol77]:

$$I_{S1} = c_{S1} \cdot T^3 \cdot \exp\left(-\frac{E_g}{k \cdot T}\right) \tag{5.50}$$

$$I_{S2} = c_{S2} \cdot T^{5/2} \cdot \exp\left(-\frac{E_g}{2 \cdot k \cdot T}\right) \tag{5.51}$$

Open-circuit voltage drops as saturation currents increase along with the temperature. To simplify further calculations, we will leave out consideration of how series resistance R_S, parallel resistance R_P, and diode factors change according to temperatures.

In formulae (5.50) and (5.51), the role of band gaps relative to temperature is left out, but it is crucial in determining **photocurrent** I_{Ph}. The band gap decreases as temperatures increase, so photons need less energy to move electrons into the valence band, thereby increasing photocurrent. The temperature dependence of photocurrent is calculated as follows using the coefficients c_1 and c_2:

$$I_{ph}(T) = -(c_1 + c_2 \bullet T) \cdot E \tag{5.52}$$

Table 5.7 Parameters for the temperature factors of various PV modules [PRE94]

Parameter	c_{S1}	c_{S2}	c_1	c_2
unit	A/K^3	$A\,K^{-5/2}$	m^2/V	$m^2/(V\,K)$
AEG PQ 40/50	210.4	$18.1 \cdot 10^{-3}$	$2.24 \cdot 10^{-3}$	$2.286 \cdot 10^{-6}$
Siemens M50	170.8	$18.8 \cdot 10^{-3}$	$3.06 \cdot 10^{-3}$	$0.179 \cdot 10^{-6}$
Kyocera LA441J59	371.9	$12.2 \cdot 10^{-3}$	$2.51 \cdot 10^{-3}$	$1.932 \cdot 10^{-6}$

Table 5.7 shows the parameters used to calculate the temperature factors of various solar modules.

A number of calculations are simplified by assuming that the current, voltage, and output of solar cells and modules change in line with voltage. We then only need three temperature coefficients for the description.

As explained above, short-circuit current increases with temperatures. Normally, short-circuit current I_{SC} is indicated under standard test conditions (ϑ = 25 °C). The temperature coefficient α_{ISC} of short-circuit current is used to calculate short-circuit current at another temperature:

Copyright © 2016. Taylor & Francis Group. All rights reserved.

Quaschning, Volker. Understanding Renewable Energy Systems, Taylor & Francis Group, 2016. ProQuest Ebook Central, http://ebookcentral.proquest.com/lib/byu/detail.action?docID=4470609.
Created from byu on 2021-11-05 15:55:38.

$$I_{SC}(\vartheta_2) = I_{SC}(\vartheta_1) \cdot (1 + \alpha_{ISC} \cdot (\vartheta_2 - \vartheta_1)) \quad (5.53)$$

The temperature coefficient of MPP current generally only slightly deviates from that of short-circuit current. If the coefficient is given as a relative parameter, the same coefficient can be used for short-circuit current and MPP current.

The temperature coefficient α_{UOC} of open-circuit voltage is calculated in the same way as short-circuit current, but in the negative. As the temperature increases, open-circuit voltage drops faster than short-circuit current increases.

Because the temperature coefficient of voltage is greater than that of current, there is also a negative temperature coefficient α_{PMPP} for MPP output. For silicon solar cells, it is generally around -4 %/°C = $-4 \cdot 10^{-3}$ /°C. In other words, when the temperature increases by 25 °C, output decreases by 10 %.

Figure 5.26 shows I–V curves relative to a changing temperature ϑ. Clearly, open-circuit voltage drops considerably as the temperature increases. In contrast, short-circuit current only increases slightly. As a result, MPP output is reduced as temperatures rise, as described above.

The temperature response of different solar cell materials varies. Above all, amorphous silicon, micromorph silicon, and cadmium-telluride have relatively constant power generation

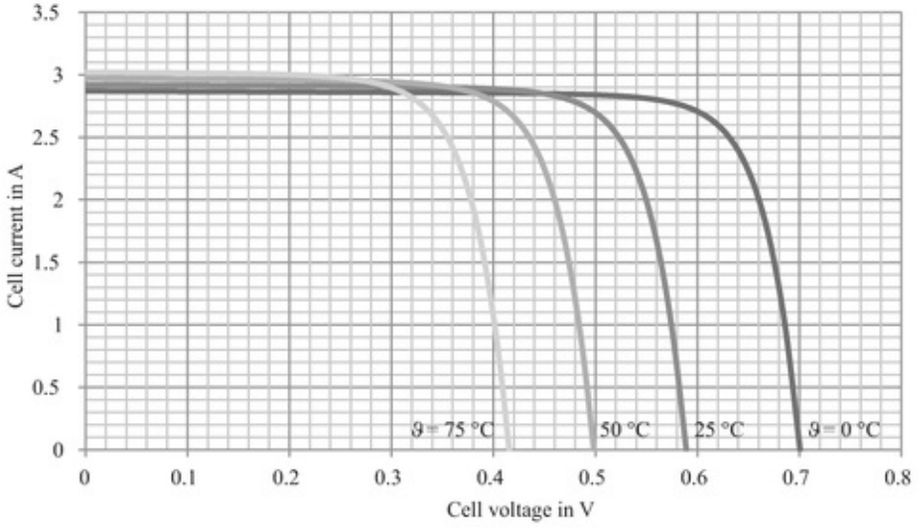

Figure 5.26 How temperatures affect a solar cell's characteristic curve

Table 5.8 Typical temperature coefficients for current, voltage, and output for some common types of solar modules

Cell/module type	α_{UOC} *in %/°C*	α_{ISC} *in %/°C*	α_P *in %/°C*
Mono-Si	−0.21 – −0.48	+0.02 – +0.08	−0.32 – −0.51
Poly-Si	−0.29 – −0.42	+0.03 – +0.07	−0.32 – −0.51
SR-Si	−0.34 – −0.41	+0.05 – +0.06	−0.42 – −0.51

Copyright © 2016. Taylor & Francis Group. All rights reserved.

Quaschning, Volker. Understanding Renewable Energy Systems, Taylor & Francis Group, 2016. ProQuest Ebook Central, http://ebookcentral.proquest.com/lib/byu/detail.action?docID=4470609.
Created from byu on 2021-11-05 15:55:38.

EFG-Si	−0.38 – −0.50	+0.1	−0.45 – −0.47
HIT	−0.25 – −0.26	+0.03	−0.3
µc-Si / a-Si	−0.30	+0.07	−0.24
a-Si	−0.27 – −0.38	+0.1	−0.18 – −0.23
CdS / CdTe	−0.25	+0.04	−0.18 – −0.25
CIS / CIGS	−0.26 – −0.29	+0.04	−0.35 – −0.5

across different temperatures. In other words, they have a relatively low temperature coefficient. In hot regions and wherever the modules are poorly ventilated, these materials ensure greater power output. Table 5.8 shows some typical temperature coefficients for various cell materials.

In practice, the cell temperature relevant for power generation is far above the ambient temperature. The part of the solar energy that the cell does not convert into electricity heats up the module. The module's temperature ϑ_M, which is roughly equivalent to the cell's temperature, can be calculated from the ambient temperature ϑ_U and the irradiance E incident on the solar module:

$$\vartheta_M = \vartheta_U + c \cdot \frac{E}{1000 \ \frac{W}{m^2}} \tag{5.54}$$

The factor c indicates the proportionality constant, which is relative to how the solar module is installed. Table 5.9 shows various values for module installation. The exact module temperature can therefore deviate considerably from the value calculated. Wind can also cool modules, thereby reducing temperatures. Cell efficiency also influences temperature. At high efficiencies, less solar energy is converted into heat. In contrast, the module's temperature can increase considerably in spots if it is shaded.

Determining parameters

To simulate a special solar cell, such as with the simplified equivalent circuit, the cell parameters (here I_{Ph} and I_S) are generally determined from measured values in the cell's characteristic curve because a theoretical calculation is extremely complex. To simplify matters, the photocurrent I_{Ph} can be assumed to be the same as the measured short-circuit current I_{SC}. For an ideal diode, the diode factor m is 1. We thus already know two parameters ($I_{Ph} = I_{SC}$ and $m = 1$). The simplified equivalent circuit also includes the diode's saturation current I_S, which can be determined by including open-circuit voltage U_{OC} to find I_S:

Copyright © 2016. Taylor & Francis Group. All rights reserved.

Quaschning, Volker. Understanding Renewable Energy Systems, Taylor & Francis Group, 2016. ProQuest Ebook Central, http://ebookcentral.proquest.com/lib/byu/detail.action?docID=4470609.
Created from byu on 2021-11-05 15:55:38.

$$I_S = \frac{I_{SC}}{\exp\left(\frac{U_{OC}}{U_T}\right) - 1} \approx I_{SC} \cdot \exp\left(-\frac{U_{OC}}{U_T}\right) \tag{5.55}$$

Table 5.9 Proportionality constant *c* for a calculation of module temperature with various types of installation [DGS08]

Type of installation	*c in °C*
Ground-mounted	22
On roof, large gap	28
On/in roof, good rear ventilation	29
On/in roof, poor rear ventilation	32
On or integrated in façade, good rear ventilation	35
On or integrated in façade, poor rear ventilation	39
Roof integration, no rear ventilation	43
Roof integration, no rear ventilation	55

Then, all of the parameters have been determined for the simplified equivalent circuit with an ideal diode ($m = 1$). However, this model only provides a rough overlapping of the calculated characteristic curve and the values measured. For a non-ideal diode, another diode factor ($m > 1$) is used. The two interrelated parameters m and I_S can be calculated in a software program such as Mathematica™ from the solar cell's characteristic curve for the power generation range in a relatively straightforward manner.

Comparing the simplified equivalent circuit and a real diode produces a very good correspondence between measurements and simulations.

But while the parameters m and I_S are not that difficult to determine, the additional parameters R_S and R_P in the expanded equivalent circuit for the single-diode model are. As the number of free parameters increases, even sophisticated mathematics programs quickly reach their limits. To ensure proper convergence in determining parameters, the starting values have to be chosen close to the final values. It is relatively easy to select the starting values for R_P and R_S.

Parallel resistance R_P can be brought closer to zero increasing the I–V curve for voltage. **Series resistance** R_S can be approximated by increasing the curve beyond open-circuit voltage:

$$R_P \approx \left.\frac{\partial U}{\partial I}\right|_{U=0} \tag{5.56}$$

$$R_S \approx \left.\frac{\partial U}{\partial I}\right|_{U>>U_L} \tag{5.57}$$

Copyright © 2016. Taylor & Francis Group. All rights reserved.

Quaschning, Volker. Understanding Renewable Energy Systems, Taylor & Francis Group, 2016. ProQuest Ebook Central, http://ebookcentral.proquest.com/lib/byu/detail.action?docID=4470609.
Created from byu on 2021-11-05 15:55:38.

For the negative diode breakdown U_{Br}, the parameters b and n can be determined like the other parameters – by using the values measured for the negative breakdown.

Electrical description of solar modules

Solar cells in series circuits

Because of the low voltage, solar cells are not used individually, but rather in a series circuit within a module. In return, the modules are either in parallel circuits, series circuits, or a combination of the two.

Because a number of modules are designed for use with 12 V lead batteries, the optimal number of cells for this purpose has become the standard: 32 to 40. There are, however, modules with far more or fewer cells in series circuits for other purposes.

When n cells are in series circuits as shown in Figure 5.27, the current I_i through all the cells i is identical, but the cell voltages U_i add up to produce the module's voltage U:

$$I = I_1 = I_2 = \ldots = I_n \quad (5.58) \qquad U = \sum_{i=1}^{n} U_i \quad (5.59)$$

If all of the cells are identical and have the same conditions (irradiance and the temperature), the following applies for the total voltage:

$$V = n \bullet U_i \quad (5.60)$$

The I–V curve for series circuits is easy to derive from an individual cell's characteristic curve in this case.

The data sheets provided by manufacturers generally only include a few parameters, such as open-circuit voltage U_{OC0}, short-circuit current I_{SC0}, voltage U_{MPP0} and current I_{MPP0} at the maximum power point with an irradiance of E_{1000} = 1000 W/m² and temperature ϑ_{25} = 25 °C, and temperature coefficients α_U and α_I for voltage and current.

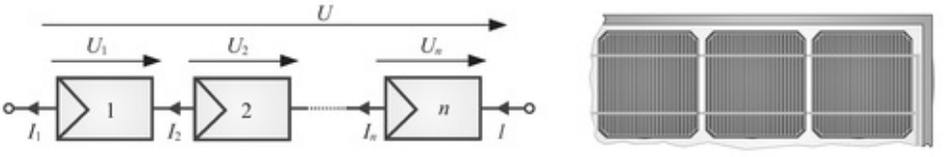

Figure 5.27 Solar cells in a series circuit (left: electrotechnical symbols, current, and voltage; right: view of a section of a module with crystalline cells)

Copyright © 2016. Taylor & Francis Group. All rights reserved.

Quaschning, Volker. Understanding Renewable Energy Systems, Taylor & Francis Group, 2016. ProQuest Ebook Central, http://ebookcentral.proquest.com/lib/byu/detail.action?docID=4470609.
Created from byu on 2021-11-05 15:55:38.

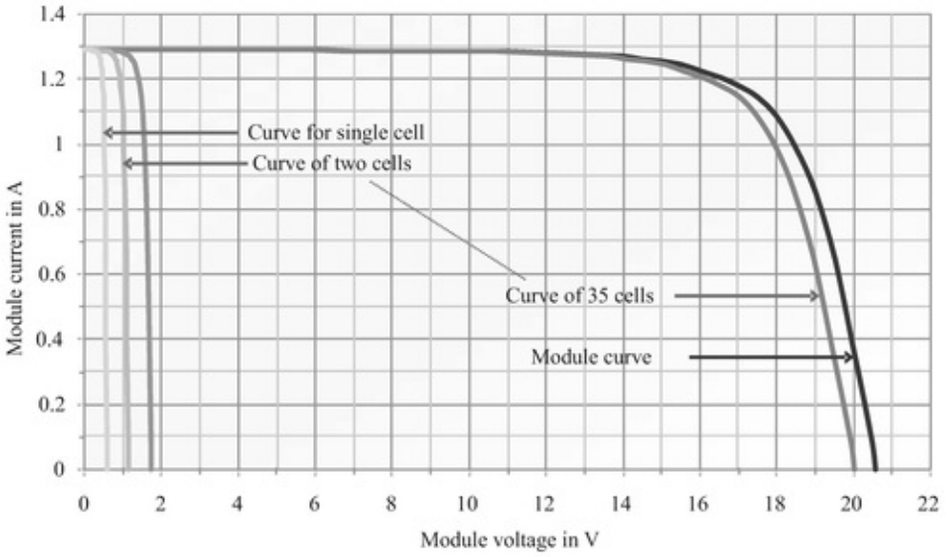

Figure 5.28 A module's characteristic curve based on curves from 36 cells

The formulae

$$U_{OC} = U_{OC0} \cdot \ln(E) / \ln(E_{1000}) \cdot (1 + \alpha_U (\vartheta - \vartheta_{25})) \quad (5.61)$$

$$U_{MPP} = U_{MPP0} \cdot \ln(E) / \ln(E_{1000}) \cdot (1 + \alpha_U (\vartheta - \vartheta_{25})) \quad (5.62)$$

$$I_{MPP} = I_{MPP0} \cdot E / E_{1000} \cdot (1 + \alpha_I (\vartheta - \vartheta_{25})) \quad (5.63)$$

$$I_{SC} = I_{SC0} \cdot E / E_{1000} \cdot (1 + \alpha_I (\vartheta - \vartheta_{25})) \quad (5.64)$$

allow us to roughly determine the module's parameters at different temperatures ϑ and levels of irradiance E. The parameters

$c_1 = I_{SC} \cdot \exp(-c_2 \cdot U_{OC})$ (5.65) and $c_2 = \ln(1 - I_{MPP} / I_{SC}) / (U_{MPP} - U_{OC})$ (5.66)

can also be used to show a rough relation between the module's current I and voltage U:

$I = I_{SC} - c_1 \cdot \exp(c_2 \cdot U)$ (5.67)

For other considerations, see the formulae for rough estimates in [Wag06].

Series circuits under inhomogeneous conditions

In practice, cells do not always operate under identical conditions. Leaves, bird droppings, snow, and other elements – including nearby objects – can shade individual cells. The impact on the module's characteristic curve can be considerable.

If not all of the I—V curves of individual cells are identical, the overall curve is harder to determine. Here, it is assumed that a module with 36 cells in a series circuit has one cell with

Copyright © 2016. Taylor & Francis Group. All rights reserved.

Quaschning, Volker. Understanding Renewable Energy Systems, Taylor & Francis Group, 2016. ProQuest Ebook Central, http://ebookcentral.proquest.com/lib/byu/detail.action?docID=4470609.
Created from byu on 2021-11-05 15:55:38.

75 % less irradiance than the other 35. In this case, the current through all of the cells is identical. The entire characteristic curve can be drawn starting with zero if the current through the cells is preset and the various cell voltages for the cells under full sunlight U_b is determined and added to that of the shaded cell U_a:

$$U = U_a(I) + 35 \cdot U_b(I) \quad (5.68)$$

The characteristic curve can then be easily constructed up to the shaded cell's short-circuit current. This curve, however, only covers a small part of the module's voltage range near the open-circuit voltage. The rest of the curve can only be drawn if the partly shaded cell has greater currents than the cell's short-circuit current. This situation can only occur in the cell's negative voltage range. The shaded cell then consumes power, as described in the equivalent circuit shown in Figure 5.23.

Figure 5.29 shows a point on the module's curve (1). At a given current, the voltage is derived by adding the shaded cell's voltages (1a) to 35 times the voltage of an unshaded cell (1b). If the curve is drawn point for point for various currents, the module's curve then reflects the case of shading, as also shown in the figure.

Shading of the cell clearly reduces the module's output drastically in this example. Although only around 2 % of the module's surface is covered, its maximum output drops by around 70 % from P_1 = 20.3 W to P_2 = 6.3 W. The partly shaded cell consumes power. In this example, the cell's maximum power loss is 12.7 W when the module short-circuits. If a cell is shaded to a different degree, the losses are located elsewhere along the characteristic curve.

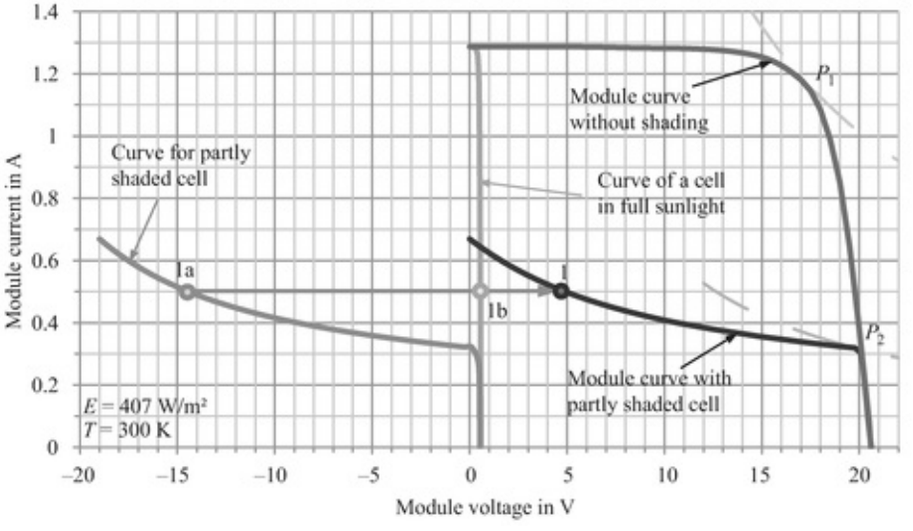

Figure 5.29 A module's characteristic curve with a cell 75 % shaded

In other shading situations and at a higher levels of irradiance, the shaded cell can have a power loss exceeding 30 W. As a result, the cell heats up drastically and can even be destroyed. Individual areas only a few millimetres across – called **hot spots** – heat up and the cell

Copyright © 2016. Taylor & Francis Group. All rights reserved.

Quaschning, Volker. Understanding Renewable Energy Systems, Taylor & Francis Group, 2016. ProQuest Ebook Central, http://ebookcentral.proquest.com/lib/byu/detail.action?docID=4470609.
Created from byu on 2021-11-05 15:55:38.

material literally melts away or at least damages the cell's encapsulation [Qua96a].

Bypass diodes are therefore integrated parallel to the solar cells to prevent individual cells from being destroyed by hot spots. Normally, these diodes are inactive. Power only flows over the diodes when the cells are shaded. The bypass diodes switch on when there is a small negative voltage, say, of around -0.7 V, depending on the type of diode. That threshold is reached when the voltage of the shaded cell is equivalent to the sum of the voltages of all other cells along with the voltage of the bypass diode. Bypass diodes are put in to limit the negative voltage at the solar cells, power losses, and the cell's temperature. Figure 5.30 shows how to bypass diodes that are integrated to serve 18 cells each in a module under normal conditions and with a shaded cell.

Generally, bypass diodes are connected to strings of 18 to 24 cells. According to manufacturers, the main reason for this approach is economics. Diodes can affordably be installed in a module's frame and in the connection socket. However, keep in mind that modern high-performance cells have currents up to and exceeding 8 A, so bypass diodes can get very hot during operation and need to be cooled.

Bypass diodes attached to strings with a relatively large number of cells cannot, however, completely prevent the cells from being damaged. Optimal protection is only provided when each cell has its own bypass diode. **Shade-tolerant modules** have bypass diodes for each cell. They were first serially manufactured by Sharp. When the cells in such modules are exposed to varying levels of irradiance, the losses are far lower [Qua96b]. These diodes can be integrated directly into the semiconductor of the solar cells [Has86]. At present, however, commercial module manufacturers are not pursuing this concept further.

Figure 5.31 shows the I–V curves of bypass diodes across a different number of cells. One cell is 75 % shaded. Clearly, the I–V curve shifts towards greater voltages as the number of cells in a string decreases; in other words, the bypass diode switches on even at low voltages. The power losses and the loads on the individual cell decrease accordingly.

Copyright © 2016. Taylor & Francis Group. All rights reserved.

Quaschning, Volker. Understanding Renewable Energy Systems, Taylor & Francis Group, 2016. ProQuest Ebook Central, http://ebookcentral.proquest.com/lib/byu/detail.action?docID=4470609.
Created from byu on 2021-11-05 15:55:38.

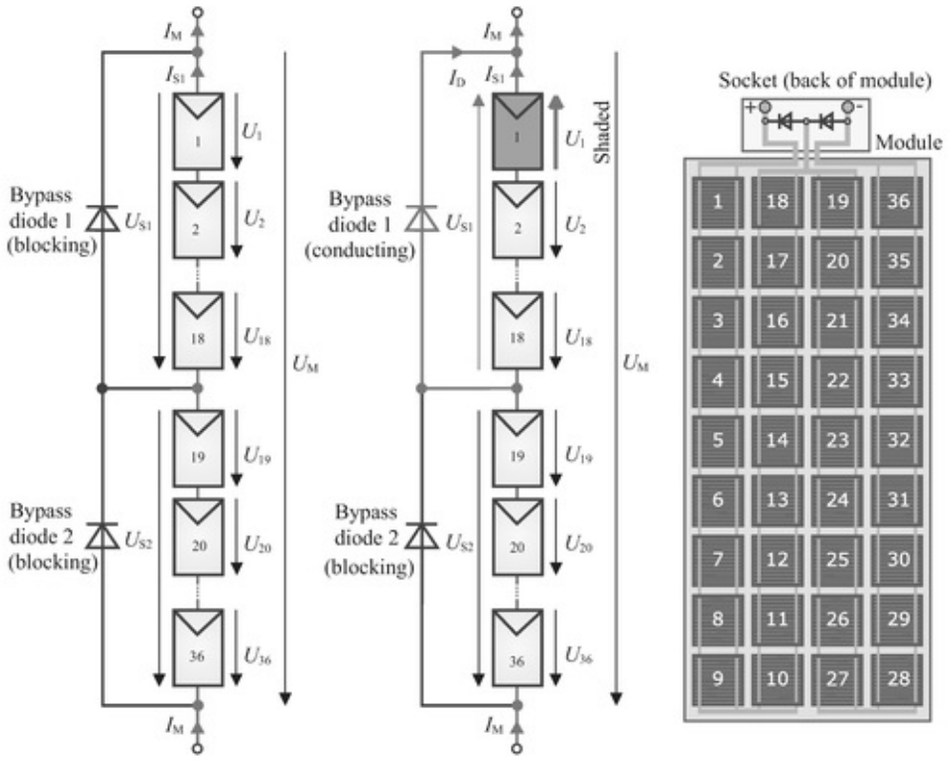

Figure 5.30 Integration of bypass diodes in a solar module with 36 cells. Left: power flow under normal operation; middle: power flow under shading; right: a typical arrangement of cells in diodes in a module

Figures 5.32 and 5.33 show the current-voltage and power-voltage curves for a module with two bypass diodes, each connected to 18 cells. Here, a single cell has different shading. When a single cell is 50% shaded, the module's output is also cut nearly in half. If the shading is greater, the bypass diode keeps the non-shaded half of the module active. In the process, however, the MPP moves to a much lower voltage. In practice, this switch poses a major challenge for downstream equipment, such as the inverter, which is designed to operate at the maximum power point under all operating conditions. Because power losses are generally far greater than the degree of shading with solar modules commonly sold, shading should be avoided to the extent possible during the planning and installation of systems.

Solar cells in parallel circuits

In addition to series circuits, multiple solar cells can also be arranged in parallel circuits. Usually, they are not because currents are then especially great, leading to greater line losses. This option is therefore only briefly dealt with below.

Copyright © 2016. Taylor & Francis Group. All rights reserved.

Quaschning, Volker. Understanding Renewable Energy Systems, Taylor & Francis Group, 2016. ProQuest Ebook Central, http://ebookcentral.proquest.com/lib/byu/detail.action?docID=4470609.
Created from byu on 2021-11-05 15:55:38.

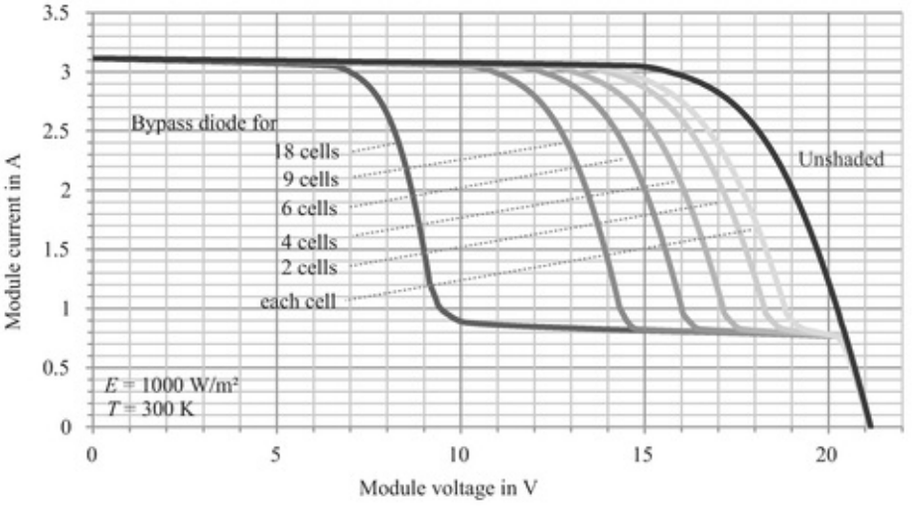

Figure 5.31 A module's characteristic curve with one cell shaded 75 % relative to the number of cells a single bypass diode serves

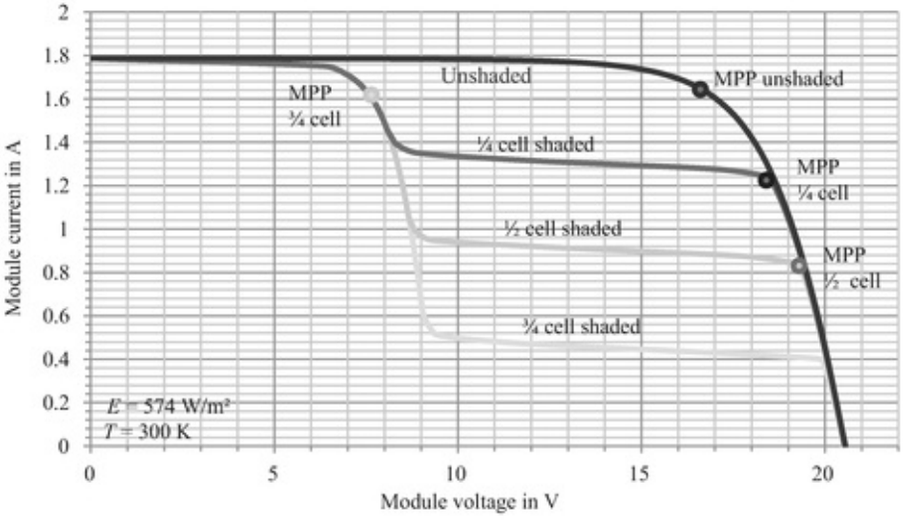

Figure 5.32 I–V curves of a module with 36 cells and two bypass diodes, each covering 18 cells, with one cell shaded differently

When solar cells are in a parallel circuit, all of the cells have the same voltage U. The current of the cells I_i then adds up to produce the total current I.

$$U = U_1 = U_2 = \ldots = U_n \quad (5.69) \qquad I = \sum_{i=1}^{n} I_i \quad (5.70)$$

Copyright © 2016. Taylor & Francis Group. All rights reserved.

Quaschning, Volker. Understanding Renewable Energy Systems, Taylor & Francis Group, 2016. ProQuest Ebook Central, http://ebookcentral.proquest.com/lib/byu/detail.action?docID=4470609.
Created from byu on 2021-11-05 15:55:38.

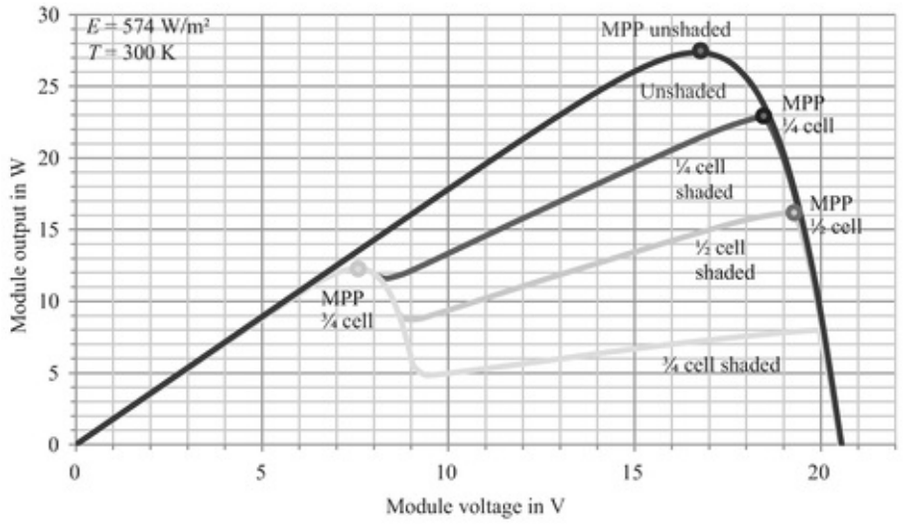

Figure 5.33 P–U curves of a module with 36 cells and two bypass diodes, each covering 18 cells, with one cell shaded differently

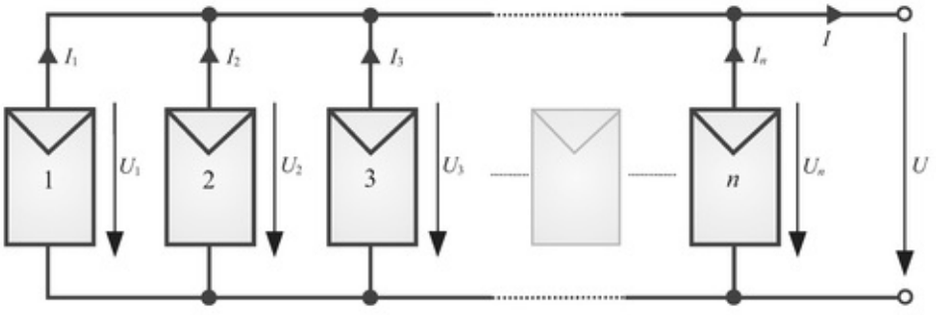

Figure 5.34 *n* solar cells in a parallel circuit

Solar cells in a parallel circuit are much less sensitive to partial shading. The cells are not expected to break then.

In practice, large solar generators have a large number of solar cells in a serial circuit along with several parallel circuits. In such cases, bypass diodes are only needed to protect the cells in series circuits. The series circuits can be protected with **string diodes**. Because the losses are great and little protection is provided, this option is rarely exercised.

Technical data for solar modules

Table 5.10 provides an overview of the various key data for solar modules. The table includes data for modules using different cell technologies. In addition to modules with polycrystalline and monocrystalline solar cells, various thin-film modules consisting of amorphous silicon, CdTe, and CIS are also listed.

Table 5.10 Technical data for selected solar modules

Copyright © 2016. Taylor & Francis Group. All rights reserved.

Quaschning, Volker. Understanding Renewable Energy Systems, Taylor & Francis Group, 2016. ProQuest Ebook Central, http://ebookcentral.proquest.com/lib/byu/detail.action?docID=4470609.
Created from byu on 2021-11-05 15:55:38.

Designation		*X3–140*	*P230/07*	*SW250*	*E20*	*HIT240*	*FS-387*	*Sm-135*
Manufacturer		Inventux	Solon	SolarWorld	Sunpower	Panasonic	First Solar	Avancis
Number of cells		125	60(6 · 10)	60 (6 · 10)	96 (8 · 12)	72 (6 · 12)	154	n/a
Cell type		aSi/μSi	Poly-Si	Mono-Si	Mono-Si	HIT	CdTe	CIS
MPP output P_{MPP}	Wp	140	260	250	333	240	87.5	135
Nominal current I_{MPP}	A	1.08	8.57	8.05	6.09	5.51	1.78	2.84
Nominal voltage U_{MPP}	V	130	30.45	31.1	54.7	43.7	49.2	47.4
Short-circuit current I_{SC}	A	1.32	8.92	8.28	6.46	5.85	1.98	3.14
Open-circuit voltage U_{OC}	V	166	37.8	37.8	65.3	52.4	61.0	61.5
Temperature coefficient α_{ISC}	%/°C	+0.07	+0.04	+0.043	+0.057	+0.03	+0.04	+0.03
Temperature coefficient α_{UOC}	%/°C	–0.3	–/.33	–3.33	–3.27	–7.25	–5.20	–0.28
Temperature coefficient α_{PMPP}	%/°C	–0.25	–5.43	–5.45	–5.38	–8.30	–0.25	–0.39
Module efficiency	%	9.8	15.9	14.9	20.4	19.1	12.2	12.8
Fill factor		0.64	0.77	0.80	0.79	0.78	0.73	0.70
Length	mm	1,100	1,640	1,675	1,559	1,580	1,200	1,587
Width	mm	1,300	1,000	1,001	1,046	798	600	664
Mass	kg	26	23.5	21.2	18.6	15	12	16
Bypass diodes		0	3	3	3	3	0	1

In the past few years, the efficiency of solar modules has increased considerably and now reaches peak values of more than 20 %. At the beginning of the 1990s, the standard was closer to 10 %. The thickness of cells has decreased so that significantly less cell material is needed, which reduces costs.

The HIT cell – a combination of crystalline and amorphous cell material – is especially efficient; Sanyo was the first manufacturer to produce it commercially. Modules from Sunpower are even more efficient, with rear-contact solar cells made of monocrystalline silicon. Because the contacts are no longer on the front, the entire front side is now available as an active surface; there are no contact fingers that lead to losses.

Shade-tolerant crystalline modules with bypass diodes integrated in the cells are no longer widely available. Manufacturers reduce the number of bypass diodes to the absolute minimum. At the time of writing, Unisolar, however, has sold a module made of amorphous silicon with a bypass diode for each cell.

The MPP output and efficiency are each determined under standard test conditions (1,000 W/m², 25 °C, AM1.5g).

Solar generator and load

Resistive load

Above, we only dealt with characteristic curves for solar cells, modules, and generators. In practice, however, solar modules are not the purpose themselves, but rather a means of producing electricity to serve a load.

The simplest kind of load is an **electrical resistance** R (Figure 5.35). A straight line represents resistance, and it can be used to show the relation between current and voltage:

Copyright © 2016. Taylor & Francis Group. All rights reserved.

Quaschning, Volker. Understanding Renewable Energy Systems, Taylor & Francis Group, 2016. ProQuest Ebook Central, http://ebookcentral.proquest.com/lib/byu/detail.action?docID=4470609.
Created from byu on 2021-11-05 15:55:38.

$$I = \frac{1}{R} \cdot U \tag{5.71}$$

If the current I through the resistance is the same as the solar cell's current, the voltage U can be used to determine the common voltage and hence the maximum power point. Generally, numeric calculations are needed again here.

When **graphically determining the MPP**, the resistance line and the solar cell's I–V curve are drawn into the same diagram. The straight line and the curve overlap at the MPP.

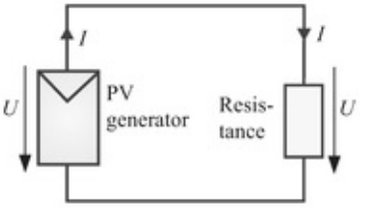

Figure 5.35 Solar generator with resistance

Figure 5.36 shows that the MPP varies greatly depending on the solar module's operating mode. In this example, the module is exposed to an irradiance of 400 W/m² at a temperature of 25 °C near the MPP. Maximum power is output to the resistance here. Under other levels of irradiance and at different temperatures, the module runs at much worse MPPs. Then, the module's actual output is far below its rated output. The voltage and output that reach the resistance vary considerably.

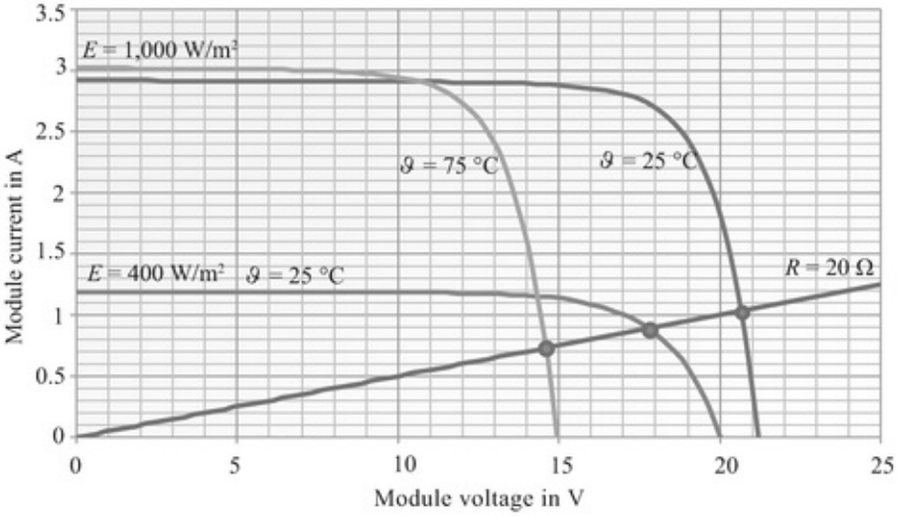

Figure 5.36 A solar module under various operating conditions with electrical resistance

DC-DC converter

Copyright © 2016. Taylor & Francis Group. All rights reserved.

Quaschning, Volker. Understanding Renewable Energy Systems, Taylor & Francis Group, 2016. ProQuest Ebook Central, http://ebookcentral.proquest.com/lib/byu/detail.action?docID=4470609.
Created from byu on 2021-11-05 15:55:38.

The solar generator's output can be greatly improved if a DC–DC converter is installed between the device that consumes power and the solar generator, as shown in Figure 5.37.

The **converter** allows the solar generator to have a different voltage from the appliance. Figure 5.38 shows that constant voltage for the solar generator allows far more power to be produced at greater levels of irradiance than in the example above with a resistance. Power can be increased even further if the solar generator's voltage is adjusted to account for temperature – specifically, if the voltage is increased as temperatures drop.

Good DC–DC converters have efficiencies exceeding 90 %. Only a small part of the power gets lost as heat in the converter. In an ideal converter with an efficiency of 100 %, the input power P_1 and output power P_2 are identical:

$$P_1 = U_1 \cdot I_1 = U_2 \cdot I_2 = P_2 \quad (5.72)$$

Because of the different voltages, however, the currents I_1 and I_2 are different.

Step-down converter

A step-down converter or buck converter, as shown in Figure 5.39, is used when the load is to have a lower voltage than the solar generator at all times.

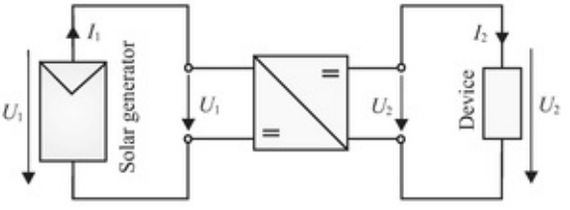

Figure 5.37 Solar generator connected to an appliance via a DC–DC converter

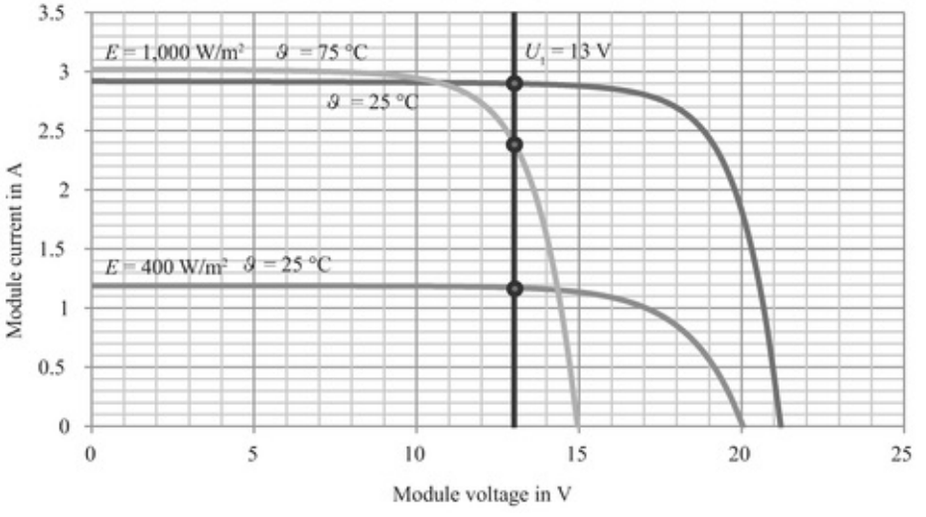

Figure 5.38 A solar module under various operating conditions with a constant voltage load

Copyright © 2016. Taylor & Francis Group. All rights reserved.

Quaschning, Volker. Understanding Renewable Energy Systems, Taylor & Francis Group, 2016. ProQuest Ebook Central, http://ebookcentral.proquest.com/lib/byu/detail.action?docID=4470609.
Created from byu on 2021-11-05 15:55:38.

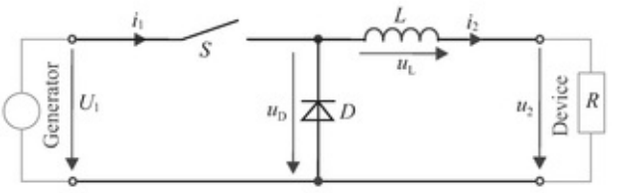

Figure 5.39 A step-down converter with a resistance load

In the following calculations, circuits and diodes are assumed to be ideal elements. The circuit S is closed for the time frame T_E, and the current builds up a magnetic field in which energy is stored because of inductance L. For the voltage u_L of inductance:

$$u_L = L \cdot \frac{\mathrm{d}i_2}{\mathrm{d}t} \tag{5.73}$$

The circuit is then opened for time frame T_A; the inductor's magnetic field weakens, thereby pushing the current through resistance R and diode D.

If we disregard the drop in voltage at the diode in the direction of passage, output voltage u_2 at the appliance is as follows:

$$u_2 = \begin{cases} u_D - u_L = U_1 - u_L & \text{with } u_L > 0 \quad \text{for } 0 \le t \le T_E \\ u_D - u_L \approx -u_L & \text{with } u_L < 0 \quad \text{for } T_E \le t \le T_E + T_A \end{cases} \tag{5.74}$$

After the duration $T_S = T_E + T_A$, the process is repeated. For the average voltage u_D with **duty cycle** $\delta = T_E / T_S$:

$$\overline{u_D} = U_1 \cdot \frac{T_E}{T_S} = U_1 \cdot \delta \tag{5.75}$$

With $I_N = U_1 / R$ and $\tau = L / R$, the following applies for current i_2 with relation to inductance and the device consuming power:

$$i_2(t) = \begin{cases} I_N - (I_N - I_{min}) \cdot \exp(-t/\tau) & \text{for } 0 \le t \le T_E \\ I_{max} \cdot \exp(-(t - T_E)/\tau) & \text{for } T_E \le t \le T_S \end{cases} \tag{5.76}$$

The current i_2 ranges between a maximum

$$I_{max} = I_N - (I_N - I_{min}) \cdot \exp(-T_E/\tau) = I_N \cdot \frac{1 - \exp(-T_E/\tau)}{1 - \exp(-T_S/\tau)} \tag{5.77}$$

Copyright © 2016. Taylor & Francis Group. All rights reserved.

Quaschning, Volker. Understanding Renewable Energy Systems, Taylor & Francis Group, 2016. ProQuest Ebook Central, http://ebookcentral.proquest.com/lib/byu/detail.action?docID=4470609.
Created from byu on 2021-11-05 15:55:38.

and minimum

$$I_{\min} = I_{\max} \cdot \exp(-T_A / \tau) = I_N \cdot \frac{\exp(-T_A / \tau) - \exp(-T_S / \tau)}{1 - \exp(-T_S / \tau)} \tag{5.78}$$

When we then insert $I_{\min}$ and $I_{\max}$, we have the following formula for current [Mic92]:

$$i_2(t) = \begin{cases} I_N + I_N \cdot \dfrac{\exp(-T_A / \tau) - 1}{1 - \exp(-T_S / \tau)} \cdot \exp(-t / \tau) & \text{for } 0 \le t \le T_E \\ I_N \cdot \dfrac{1 - \exp(-T_E / \tau)}{1 - \exp(-T_S / \tau)} \cdot \exp(-(t - T_E) / \tau) & \text{for } T_E \le t \le T_S \end{cases} \tag{5.79}$$

For the average current i_2:

$$\bar{i}_2 = I_N \cdot \frac{T_E}{T_S} = I_N \cdot \delta \tag{5.80}$$

Figure 5.40 shows the current i_2 and voltage u_D. In practice, voltage should be relatively constant at the output. For this reason, capacitors C_1 and C_2 are used, as shown in Figure 5.41. When the circuit is open, capacitor C_1 temporarily stores the solar generator's energy.

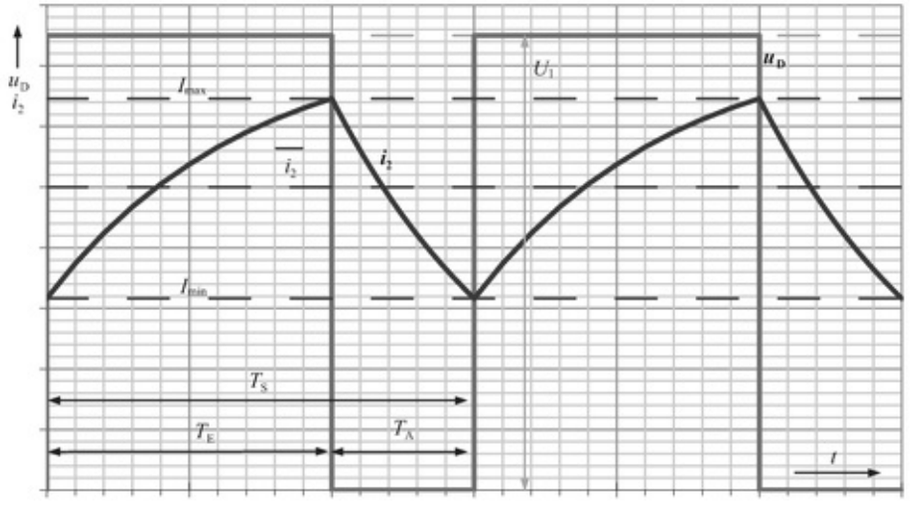

Figure 5.40 The curve for current i_2 and voltage u_D with a step-down converter

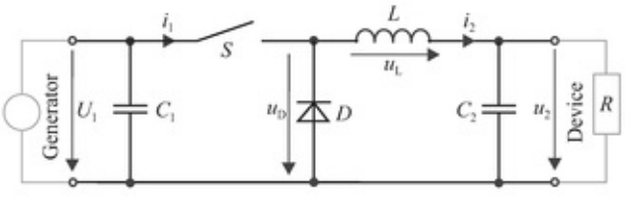

Figure 5.41 Step-down converter with capacitors

Copyright © 2016. Taylor & Francis Group. All rights reserved.

Quaschning, Volker. Understanding Renewable Energy Systems, Taylor & Francis Group, 2016. ProQuest Ebook Central, http://ebookcentral.proquest.com/lib/byu/detail.action?docID=4470609.
Created from byu on 2021-11-05 15:55:38.

For ideal inductance, L the average output voltage

$$U_2 = \overline{u_2} = U_1 \cdot \frac{T_E}{T_S} = U_1 \cdot \delta \tag{5.81}$$

is calculated from the input voltage U_1 and duty cycle δ. For ideal components, the average output voltage

$$I_2 = \overline{i_2} = \overline{i_1} \cdot \frac{T_S}{T_E} = \overline{i_1} \cdot \frac{1}{\delta} \tag{5.82}$$

is calculated based on the average input current and the inverse of the duty cycle. If the average output current I_2 is less than

$$I_{2,\text{limit}} = \frac{T_S}{2 \cdot L} \cdot U_2 \cdot (1 - \frac{U_2}{U_1}) \tag{5.83}$$

the current decreases to zero as a result of inductance during the circuit's lock phase, the diode is blocked, and voltage at inductance falls to zero. Current and voltage thus begin to 'gap'. Proper dimensioning can prevent this problem [Tie02]. If the lower limit current $I_{2,\text{limit}}$ is known, inductance can be calculated thus:

$$L = T_S \cdot \left(1 - \frac{U_2}{U_1}\right) \cdot \frac{U_2}{2 \cdot I_{2,\text{limit}}} \tag{5.84}$$

Clock rates $f = 1 / T$ from 20 kHz to 200 kHz have proven to be a good compromise. The output capacity C_2 is calculated as follows:

$$C_2 = \frac{T_S \cdot I_{2,\text{limit}}}{4 \cdot \Delta U_2} \tag{5.85}$$

from the output voltage's ripple U_2, producing the maximum desired fluctuation ΔU_2.

The circuits S are generally power semiconductors, such as field-effect transistors, bipolar transistors, and thyristors for larger outputs. A number of integrated circuits (ICs) are already available to set the duty cycle for transistors. Circuit breakers are already integrated in a number of ICs for small outputs.

Step-up converters

Copyright © 2016. Taylor & Francis Group. All rights reserved.

Quaschning, Volker. Understanding Renewable Energy Systems, Taylor & Francis Group, 2016. ProQuest Ebook Central, http://ebookcentral.proquest.com/lib/byu/detail.action?docID=4470609.
Created from byu on 2021-11-05 15:55:38.

If the output voltage is to be greater than the input voltage, a step-up or boost converter can be used. A step-up converter is basically the same as a step-down converter with the diode, circuit, and inductance reversed. Figure 5.42 shows a step-up converter.

If circuit S is closed, a magnetic field builds up within inductance L. Voltage $u_L = U_1$ ($u_L > 0$) is produced in the process. If the circuit is open, the voltage at the device consuming power is $u_2 = U_1 - u_L$ ($u_L < 0$), which is greater than the input voltage U_1. Here, no consideration is taken of the voltage decrease at the diode. When the circuit is closed again, capacitor C_2 supports the device's voltage. Diode D prevents the capacitor from being discharged via circuit S. For output voltage U_2, the following applies:

$$U_2 = U_1 \cdot \frac{T_S}{T_A} \tag{5.86}$$

L and C_2 can be dimensioned with $I_{2\text{limit}} = 1/2 \cdot U_1 \cdot (1 - U_1 / U_2) \cdot T_s / L$ via

$$L = U_1 \cdot (1 - \frac{U_1}{U_2}) \cdot \frac{T_S}{2 \cdot I_{2,\text{limit}}} \quad (5.87) \text{ and } \quad C_2 = \frac{T \cdot I_{2,\text{limit}}}{\Delta U_2} \tag{5.88}$$

Additional DC-DC converters

Step-up and step-down converters are not the only options for DC–DC. The **buck-boost converter** shown in Figure 5.43 has an output voltage of

$$U_2 = -U_1 \cdot \frac{T_E}{T_A} \tag{5.89}$$

The single-cycle **flyback converter** shown in Figure 5.44 has a transformer instead of inductance. Its output voltages calculated the same as with the buck-boost converter, but the transformer's ratio also has to be taken into account and it is relative to the relationship between the winding numbers on the two sides of the transformer.

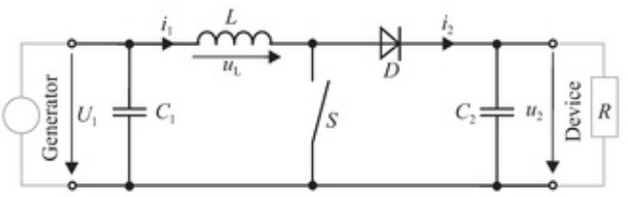

Figure 5.42 How a step-up converter works

Copyright © 2016. Taylor & Francis Group. All rights reserved.

Quaschning, Volker. Understanding Renewable Energy Systems, Taylor & Francis Group, 2016. ProQuest Ebook Central, http://ebookcentral.proquest.com/lib/byu/detail.action?docID=4470609.
Created from byu on 2021-11-05 15:55:38.

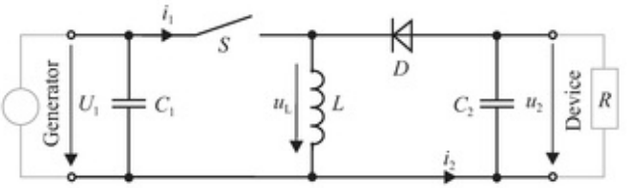

Figure 5.43 A buck-boost converter

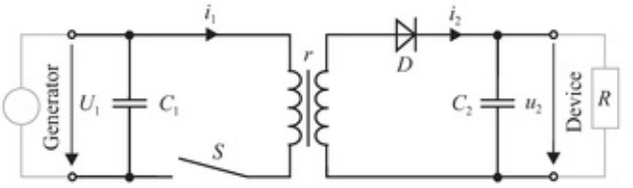

Figure 5.44 How a single-cycle flyback converter works

The following applies for output voltage:

$$U_2 = U_1 \cdot \frac{T_E}{T_A} \cdot \frac{1}{r} \tag{5.90}$$

Push–pull converters are also used for greater outputs, but they require multiple power switches. If capacitors are used instead of inductance, voltage converters can run based on the principle of a charge pump. Examples of circuit converters and control systems for them are given in [Köt96].

MPP trackers

The voltage converters discussed above provide a different voltage level for the solar generator than for the consumption device. If the duty cycle is set to provide a fixed voltage for the solar generator (Figure 5.38), far more energy is produced than would be with power consumption based on resistance, but there would be great losses because of fluctuations in temperature and irradiance. The voltage converter's duty cycle can be changed so that the solar generator's voltage varies.

During normal operation, temperature fluctuations ϑ have the greatest impact on the solar generator's optimal voltage. A temperature sensor can be used to measure the temperature at the solar generator. The temperature coefficients for open-circuit voltage (such as $\alpha_{UOC} = -2.10^{-3}$ /°C . . . -5.10^{-3} /°C for silicon cells) allow the duty cycle

$$\delta = \frac{U_2}{U_1} = \frac{U_2}{U_{MPP}(\vartheta)} = \frac{U_2}{U_{MPP(\vartheta=25\,^\circ C)} \cdot (1 + \alpha_{UOC} \cdot (\vartheta - 25\,^\circ C))} \tag{5.91}$$

Copyright © 2016. Taylor & Francis Group. All rights reserved.

Quaschning, Volker. Understanding Renewable Energy Systems, Taylor & Francis Group, 2016. ProQuest Ebook Central, http://ebookcentral.proquest.com/lib/byu/detail.action?docID=4470609.
Created from byu on 2021-11-05 15:55:38.

to be calculated from a step-down converter's MPP voltage U_{MPP} at a reference temperature and output voltage U_2. If the duty cycle is changed again to take account of fluctuations in irradiance, the solar generator will then generally run at its maximum power point. If the voltage converter ensures that the solar generator runs at its MPP, the converter and its control system is called an MPP tracker.

For MPP controls, there are numerous options, a few of which are explained below:

Sensor-based controls: As explained above, MPP voltage is calculated based on measurements taken by temperature and irradiance sensors.

Setting controls based on a reference cell: The curve / open-circuit voltage U_{OC} and the short-circuit current I_{SC} of a reference cell installed near the solar generator have their performance measured. The solar generator's MPP voltage U_{MPP} can be taken from the measurement values. The MPP current I_{MPP} is calculated from the formula for the simple equivalent circuit:

$$I_{MPP} = I(U_{MPP}) = I_{SC} - I_S \cdot \left(\exp\left(\frac{U_{MPP}}{m \cdot U_T} \right) - 1 \right) \tag{5.92}$$

For maximum output, the derivation of power from voltage is zero:

$$\frac{\mathrm{d}\, P(U_{MPP})}{\mathrm{d}\, U} = \frac{\mathrm{d}(U_{MPP} \cdot I(U_{MPP}))}{\mathrm{d}\, U} = I(U_{MPP}) + U_{MPP} \cdot \frac{\mathrm{d}\, I(U_{MPP})}{\mathrm{d}\, U} = 0 \tag{5.93}$$

If the formula is used for I_{MPP}, the following applies with respect to MPP voltage U_{MPP}:

$$\begin{aligned} U_{MPP} &= m \cdot U_T \cdot \ln\left(\frac{I_{SC} + I_S}{I_S} \right) - m \cdot U_T \cdot \ln\left(1 + \frac{U_{MPP}}{m \cdot U_T} \right) \\ &= U_{OC} - m \cdot U_T \cdot \ln\left(1 + \frac{U_{MPP}}{m \cdot U_T} \right) \end{aligned} \tag{5.94}$$

This formula can be used with rough estimates or numeric methods. The MPP voltage can therefore be determined from the open-circuit voltage. For a more exact calculation, use the two-diode model.

Perturb and observe: The voltage and current are measured at the voltage converter's input or output, and the power value is calculated and saved, as shown in Figure 5.45.

The duty cycle is changed slightly, thereby changing the voltage, and power output is measured again. If the output has increased, the duty cycle is once again changed in the same

Copyright © 2016. Taylor & Francis Group. All rights reserved.

Quaschning, Volker. Understanding Renewable Energy Systems, Taylor & Francis Group, 2016. ProQuest Ebook Central, http://ebookcentral.proquest.com/lib/byu/detail.action?docID=4470609.
Created from byu on 2021-11-05 15:55:38.

direction. If it has worsened, the duty cycle is changed in the opposite direction. At a constant output voltage, the controls simply need to focus on the maximum output current. Power output does not need to be measured.

Incremental conductance: Power and voltage are measured at the generator and multiplied. The derivative dP/dU is created in the process. If it is positive, the generator's voltage must be increased; if it is negative, decreased.

Differential changes: Current and voltage are measured, and their differential changes are determined. The formula

$$\frac{dP}{dU} = \frac{d(U \cdot I)}{dU} = I + U \cdot \frac{dI}{dU} = 0$$

produces

$$I \cdot dU = -U \cdot dI \quad (5.95)$$

meaning that the electronics have to set both of the parameters to the same level.

Curve tracking: Here again, current and voltage are first measured. Depending on the open-circuit voltage $U_A = U_L$, voltage and current are changed as follows alternately:

$$U_B = k \cdot U_A \text{ and } I_c = k \cdot I_B \ (k < 1)$$

Eventually, two points are located to the left and right of the MPP, and the tracker swings between them.

When part of the solar generator is shaded, a lot of MPP trackers have trouble finding the MPP. Wind shading occurs frequently; power losses can therefore be considerable. A good MPP tracker should therefore provide good results not only for normal operation. In such cases, there are several points of maximum power (Figure 5.33), so if a lower generator output is likely to stem from shading, the entire curve needs to be swept in order to find the maximum power point.

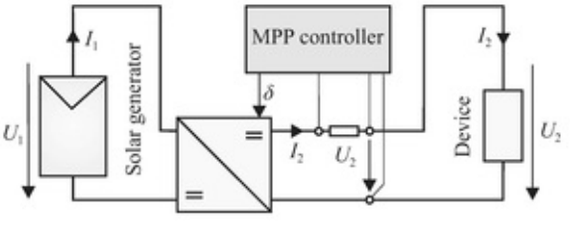

Figure 5.45 How an MPP tracker works

Battery storage

Copyright © 2016. Taylor & Francis Group. All rights reserved.

Quaschning, Volker. Understanding Renewable Energy Systems, Taylor & Francis Group, 2016. ProQuest Ebook Central, http://ebookcentral.proquest.com/lib/byu/detail.action?docID=4470609.
Created from byu on 2021-11-05 15:55:38.

Battery storage types

It is rare for solar generators to be hooked up directly to devices. Generally, more complex systems are used. If there is no grid connection, storage is usually needed. Then energy is available when the sun is not shining, such as at night.

A distinction is made between two types of storage: one to cover a few hours or days during bad weather; the other, to bridge several months, such as to compensate for fluctuations in seasonal irradiation between the summer and the winter. Because long-term storage is generally very complex and expensive, power systems that run all year generally have large PV generators so that enough energy is provided in the winter; alternatively, additional generators are used, such as wind or diesel generators.

For short and midterm storage, batteries have become the standard in terms of cost. Lead batteries are the most widespread because they are the cheapest. Whenever greater energy density is needed to keep the weight down, other battery types are used, such as nickel-metal hydride (NiMH). Over the past few years, very high-performance lithium-ion batteries have become commonplace in high-quality mobile applications, such as cell phones, digital cameras, and laptops. Because they are expensive, however, they are not yet commonly used with solar equipment. Table 5.11 shows some comparative data for a number of battery types.

Lead batteries

Lead batteries are the most common batteries for storing large amounts of energy today. They are the least expensive option. The automotive sector produces large numbers of them as starter batteries. A slightly modified **structure** to produce a longer service life than in the automotive sector is used for lead batteries for solar applications.

Table 5.11 Data for different types of battery

	Lead	*NiCd*	*NiMH*	*NaS*	*Lithium-ion*
Positive electrode	PbO_2	NiOOH	NiOOH	Na (fluid)	Graphite (nC)
Negative electrode	PbO	Cd	Metals	S (fluid)	$LiMn_2O_4$
Electrolyte	$H_2SO_4 + H_2O$	$KOH + H_2O$	$KOH + H_2O$	β-Al_2O_3	Polymer/salt
Energy density in Wh/l	50–110	80–200	100–350	260–390	250–500
Energy density in Wh/kg	25–50	30–70	60–120	120–220	95–200
Cell voltage in V	2	1.2	1.2	2.1	3.6
Charge/discharge cycles	500–1,500	1,500–3,000	ca. 1,000	1,500–3,000	500–10,000
Operating temperature in °C	0–55	–40– +55	–20– +45	270–350	–20– +55
Self-discharge rate in %/month	5–15	20–30	15–50	0[1)]	<5
Wh efficiency in %	70–85	60–70	60–85	70–85	70–90

Note 1) without energy demand to maintain a high operating temperature

In both the automotive and the solar sector, lead batteries have two electrodes. When

Copyright © 2016. Taylor & Francis Group. All rights reserved.

Quaschning, Volker. Understanding Renewable Energy Systems, Taylor & Francis Group, 2016. ProQuest Ebook Central, http://ebookcentral.proquest.com/lib/byu/detail.action?docID=4470609.
Created from byu on 2021-11-05 15:55:38.

charged, the positive electrode is made of PbO_2; the negative, of pure lead (Pb). The two electrodes are separated by a membrane, all of which is within a plastic housing. They are immersed in an electrolyte of diluted sulphuric acid ($H_2\ SO_4$). When nearly fully charged at a temperature of 25 °C, the acid has a density of around 1.24 kg/l. The density changes relative to the temperature and the state of charge and can be measured with a hydrometer or via the battery's voltage. Because a single cell of a lead battery has a nominal voltage of 2 V, 6 cells are usually switched in series to produce an operating voltage of 12 V. The number of cells can be changed accordingly to produce a different voltage level.

The following **chemical reactions** take place in a lead battery, as shown in Figure 5.46.

Negative electrode:

$$\mathrm{Pb} + \mathrm{SO_4^{2-}} \underset{\leftarrow \text{Charge}}{\overset{\text{Discharge}\rightarrow}{\longleftrightarrow}} \mathrm{PbSO_4} + 2\mathrm{e^-} \tag{5.96}$$

Positive electrode:

$$\mathrm{PbO_2} + \mathrm{SO_4^{2-}} + 4\mathrm{H^+} + 2\mathrm{e^-} \underset{\leftarrow \text{Charge}}{\overset{\text{Discharge}\rightarrow}{\longleftrightarrow}} \mathrm{PbSO_4} + 2\mathrm{H_2O} \tag{5.97}$$

Net reaction:

$$\mathrm{PbO_2} + \mathrm{Pb} + 2\mathrm{H_2SO_4} \underset{\leftarrow \text{Charge}}{\overset{\text{Discharge}\rightarrow}{\longleftrightarrow}} 2\mathrm{PbSO_4} + 2\mathrm{H_2O} \tag{5.98}$$

$PbSO_4$ forms during discharging because of the electrolyte, thereby releasing electrons that produce electricity for consumption. When the battery is charged, energy has to be added to it. Pb and PbO_2 are created in the respective electrodes, and more energy has to be added than was taken out. The ratio of the discharge to the charge reflects the charge efficiency. For the charge efficiency, a distinction is made between **Ah efficiency** η_{Ah} and **Wh efficiency** η_{Wh}. Ah efficiency is calculated based on the integrated currents, while Wh efficiency takes account of both current and voltage over the discharge and charge time for the same state of charge, respectively:

$$\eta_{\mathrm{Ah}} = \frac{Q_{\mathrm{out}}}{Q_{\mathrm{in}}} = -\frac{\int_0^{t_{\mathrm{discharge}}} I \cdot \mathrm{d}t}{\int_0^{t_{\mathrm{discharge}}} I \cdot \mathrm{d}t} \tag{5.99}$$

Copyright © 2016. Taylor & Francis Group. All rights reserved.

Quaschning, Volker. Understanding Renewable Energy Systems, Taylor & Francis Group, 2016. ProQuest Ebook Central, http://ebookcentral.proquest.com/lib/byu/detail.action?docID=4470609.
Created from byu on 2021-11-05 15:55:38.

$$\eta_{\mathrm{Wh}} = \frac{Q_{\mathrm{out}} \cdot U_{\mathrm{out}}}{Q_{\mathrm{in}} \cdot U_{\mathrm{in}}} = -\frac{\int_0^{t_{\mathrm{discharge}}} U \cdot I \cdot \mathrm{d}t}{\int_0^{t_{\mathrm{discharge}}} U \cdot I \cdot \mathrm{d}t} \qquad (5.100)$$

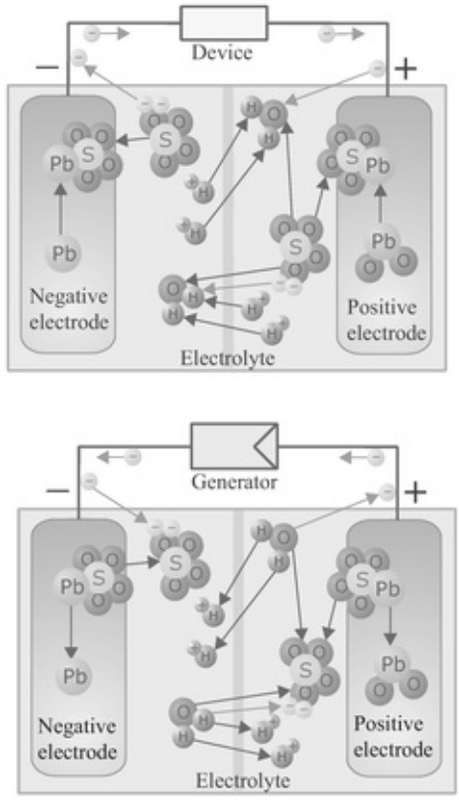

Figure 5.46 Discharging and charging processes within a lead battery

Because voltage is greater during charging than during discharging, Wh efficiency is always lower than Ah efficiency. Depending on the type of battery, the Ah efficiency of a lead battery ranges from 80 to 95 %, with Wh being roughly 10 % lower.

Additional losses that further reduce the overall system's efficiency stem from **self-discharging**. Self-discharge increases along with the temperature; at 25 °C, it is around 0.3 % per day or 10 % per month. Depending on the type of battery, the self-discharge rate can be only half as great.

The **available capacity** of a battery depends on the discharge current, as shown in Figure 5.47. The greater the discharge current, the lower the capacity, and hence the available charge. The discharge voltage is then reached sooner.

Capacity is usually listed along with discharge time when comparing batteries. Here, C_{100} means that this capacity is available when the discharge current is selected so that the battery reaches its end-of-charge voltage in 100 h. If the battery has a capacity of C_{100} = 100 A h, the

Copyright © 2016. Taylor & Francis Group. All rights reserved.

Quaschning, Volker. Understanding Renewable Energy Systems, Taylor & Francis Group, 2016. ProQuest Ebook Central, http://ebookcentral.proquest.com/lib/byu/detail.action?docID=4470609.
Created from byu on 2021-11-05 15:55:38.

discharge current is $I_{100} = C_{100}$ /100 h = 1 A. If the discharge takes 10 h with a current of 8 A, capacity C_{10} drops below 80 % of C_{100}. At a temperature of 0 °C and a 5 h discharge, capacity even drops to around 50 %. The service life – the battery's number of cycles – decreases along with temperature and discharge depth. The recommended discharge depth is generally around 80 %; levels below 50 % (a less than 50 % charge) should be avoided.

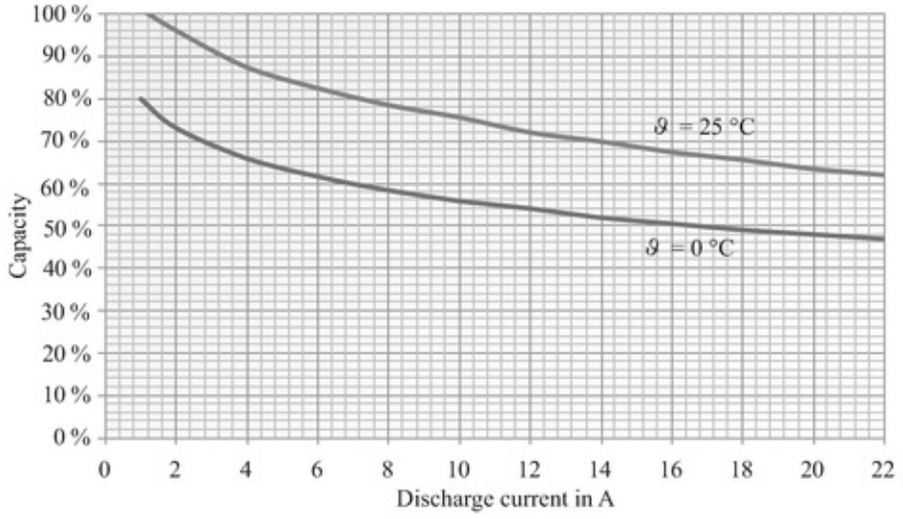

Figure 5.47 A lead battery's available capacity with C_{100} = 100 Ah relative to discharge current and temperature

Table 5.12 shows the open-circuit voltage and acid density for a 12 V battery. Depending on the specific model and purpose, the nominal acid density can vary between 1.22 kg/l and 1.28 kg/l. At low temperatures, a greater acid density has a positive effect on operating properties, while lower acid density reduces the impact of corrosion. The voltage values only apply for open circuits – i.e. a battery that has not been charged or discharged for a long time. If the temperature differs from the nominal temperature, a temperature compensation of – 25 mV/ °C can be included in the calculation. Charging and discharging increases/decreases, respectively, voltage relative to the strength of current far above/ below-circuit voltage. Figure 5.48 shows the voltage curve across the duration of discharge. Starting with a fully charged battery's open-circuit voltage of 12.7 V, voltage quickly drops relative to the charge current. If the initial charge is low, voltage drops more quickly.

Table 5.12 Open-circuit voltage and acid density relative to the state of charge of a 12 V lead battery

State of charge	*100 %*	*75 %*	*50 %*	*25 %*	*0 %*
Voltage in V	12.7	12.4	12.2	12.0	11.9
Acid density in kg/l	1.265	1.225	1.19	1.15	1.12

Copyright © 2016. Taylor & Francis Group. All rights reserved.

Quaschning, Volker. Understanding Renewable Energy Systems, Taylor & Francis Group, 2016. ProQuest Ebook Central, http://ebookcentral.proquest.com/lib/byu/detail.action?docID=4470609.
Created from byu on 2021-11-05 15:55:38.

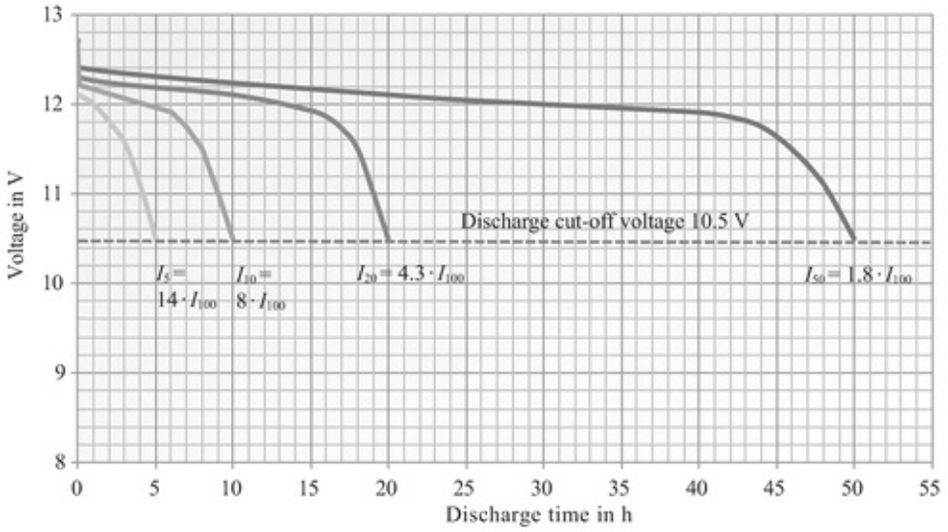

Figure 5.48 Voltage curves relative to discharge time and discharge current

The battery's age also has a minor influence on its voltage. Table 5.13 shows how voltage can be used to determine a battery's state of charge.

The battery should not be excessively charged or discharged. If the battery is completely discharged, lead sulphate crystallizes, making it hard to recharge and reconvert completely. The battery is then permanently damaged. Deep discharges should therefore be avoided at all cost. A residual capacity of around 30 % – equivalent to a battery voltage of around 11.4 V – suffices to prevent this damage. At high discharge currents exceeding I_{10}, a low end-of-charge voltage may be recommendable. When batteries are stored for a long time, self-discharge can also cause damage, so the batteries should be recharged frequently.

When a battery is charged, it begins to 'gas' at a voltage of 14.4 V. In other words, the water in the electrolyte is broken up into hydrogen and oxygen. These gases escape from the battery. The battery therefore has to be refilled with water in regular intervals. If this **gassing** process continues for a long time, it can damage the battery. Charging should therefore be restricted to 13.8 V to 14.4 V. In contrast, charging the battery into the gassing phase occasionally is a good idea in order to mix up the electrolyte.

Table 5.13 What a 12 V battery's voltage tells us about its state of charge

Voltage range	*State of charge*
Greater than 14.4 V	Charging discontinued, battery fully charged
13.5 V-14.1 V	Normal voltage range when charging without consumption load
12.0 V-14.1 V	Normal voltage range when charging with consumption load
11.5 V-12.7 V	Normal voltage during discharging

Copyright © 2016. Taylor & Francis Group. All rights reserved.

Quaschning, Volker. Understanding Renewable Energy Systems, Taylor & Francis Group, 2016. ProQuest Ebook Central, http://ebookcentral.proquest.com/lib/byu/detail.action?docID=4470609.
Created from byu on 2021-11-05 15:55:38.

The battery should be stored in a dry room in which temperatures do not drop too low. The gassing process can create explosive oxyhydrogen, so make sure that rooms in which batteries are stored are always **well ventilated**.

If exact simulations are needed, the battery may need to be described by using an electrical equivalent circuit, which has turned out to be a very difficult task. Today, the best model to represent a battery is still a black bucket with a hole in it, as technicians joke. Nonetheless, various attempts have been made to model batteries, such as by Gretsch [Gre78].

Another type of description is the calculation of state of charge. It only requires consideration of a few properties. If the battery is completely charged, it cannot be charged further. To provide protection against deep discharges, the battery should not be discharged below half of its capacity. During charging and discharging, the charge efficiency must be taken into account along with charge losses from self-discharging. Most simulation programs are based on this principle. Figure 5.49 shows a flowchart of this calculation, which is very easy to implement in a computer program. A battery system can be optimized by varying the photovoltaic output and battery capacity.

Other battery types

As mentioned above, other more expensive systems, such as NiMH and Li-ion, are used along with lead batteries because of their greater energy density, faster charge, and longer service life.

Nickel-cadmium batteries were very widespread for a long time. Compared with lead batteries, they have a slightly greater energy density, a greater number of cycles, and a wider temperature range. However, this battery is increasingly unpopular because cadmium is a dangerous substance. The material used within the battery might enter the environment after the batteries are disposed of. Cadmium builds up in the food chain and is absorbed by the human body, which has a hard time completely eliminating it. At sufficient concentrations, cadmium can damage organs and cause cancer. NiCd batteries are therefore now banned for most applications.

Nickel-metal hydride (NiMH) contain substances that are much less problematic, though small amounts of toxic substances are still added to such batteries in practice. Alloys consisting of nickel, titanium, vanadium, zirconium, and chrome are used. The electrolyte in these batteries and in NiCd batteries is diluted caustic potash. NiMH batteries have other benefits compared with NiCd batteries, such as greater density and the lack of a memory effect. In return, they have a low operating temperature range and a very high self-discharge rate

Copyright © 2016. Taylor & Francis Group. All rights reserved.

Quaschning, Volker. Understanding Renewable Energy Systems, Taylor & Francis Group, 2016. ProQuest Ebook Central, http://ebookcentral.proquest.com/lib/byu/detail.action?docID=4470609.
Created from byu on 2021-11-05 15:55:38.

(around 1 % per day). As with NiCd batteries, the cell voltage is 1.2 V, so NiMH batteries can easily replace NiCd batteries.

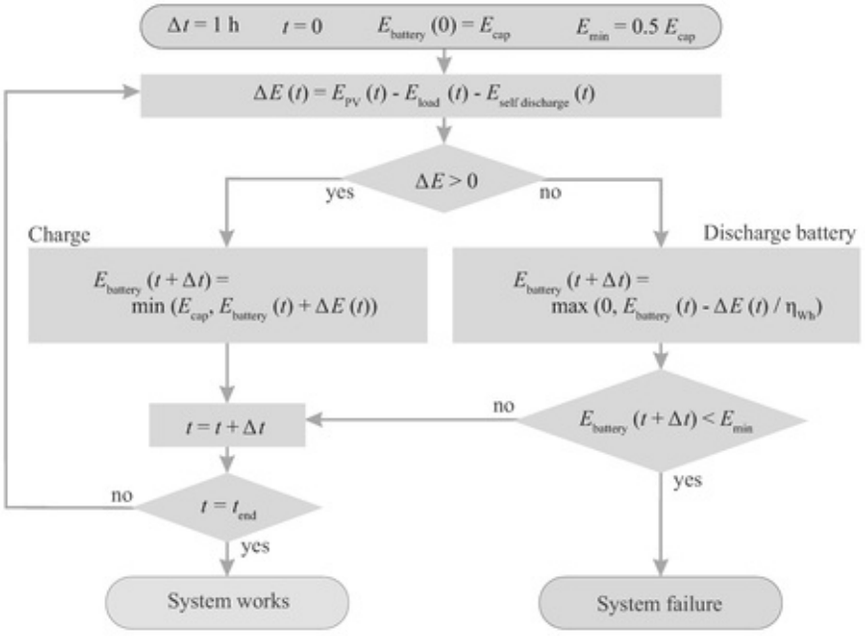

Figure 5.49 Flowchart of the calculation for the state of charge of PV battery systems

A NiMH battery's chemical reactions are as follows:
Negative electrode:

$$MH + OH^- \underset{\leftarrow \text{Charge}}{\overset{\text{Discharge}\rightarrow}{\longleftrightarrow}} M + H_2O + e^- \tag{5.101}$$

Positive electrode:

$$NiOOH + H_2O + e^- \underset{\leftarrow \text{Charge}}{\overset{\text{Discharge}\rightarrow}{\longleftrightarrow}} Ni(OH)_2 + OH^- \tag{5.102}$$

Net reaction:

$$NiOOH + MH \underset{\leftarrow \text{Charge}}{\overset{\text{Discharge}\rightarrow}{\longleftrightarrow}} Ni(OH)_2 + M \tag{5.103}$$

It is much harder to monitor the state of charge with NiCd and NiMH band with lead batteries based on battery voltage because the former are more sensitive to temperature fluctuations, and their voltage even slightly decreases when they are fully charged.

Lithium-ion batteries also have no memory effect and charge quickly. In addition to having great energy density, this battery type also has a low rate of self-discharge. Lower discharge currents are also possible than with batteries that have water-based electrolytes.

Copyright © 2016. Taylor & Francis Group. All rights reserved.

Quaschning, Volker. Understanding Renewable Energy Systems, Taylor & Francis Group, 2016. ProQuest Ebook Central, http://ebookcentral.proquest.com/lib/byu/detail.action?docID=4470609.
Created from byu on 2021-11-05 15:55:38.

The first generation of lithium-ion batteries fell into disrepute because short-circuits and excessive charging caused fires and explosions. Modern cell safety measures now largely rule out such problems. Because of their energy density, lithium-ion batteries are mainly used in mobile applications. New developments in the automotive sector and in stationery PV systems could lead to a boom in the use of these batteries in the next few years. The chemical reactions of a lithium-ion battery – of which there are different versions – are as follows:

Negative electrode:

$$\mathrm{Li}_x\mathrm{C}_n \underset{\leftarrow\text{Charge}}{\overset{\text{Discharge}\rightarrow}{\longleftrightarrow}} n\ \mathrm{C} + x\ \mathrm{Li}^+ + x\ \mathrm{e}^- \tag{5.104}$$

Positive electrode:

$$\mathrm{Li}_{1-x}\mathrm{Mn}_2\mathrm{O}_4 + x\ \mathrm{Li}^+ + x\ \mathrm{e}^- \underset{\leftarrow\text{Charge}}{\overset{\text{Discharge}\rightarrow}{\longleftrightarrow}} \mathrm{LiMn}_2\mathrm{O}_4 \tag{5.105}$$

Net reaction:

$$\mathrm{Li}_{1-x}\mathrm{Mn}_2\mathrm{O}_4 + \mathrm{Li}_x\mathrm{C}_n \underset{\leftarrow\text{Charge}}{\overset{\text{Discharge}\rightarrow}{\longleftrightarrow}} \mathrm{LiMn}_2\mathrm{O}_4 + n\ \mathrm{C} \tag{5.106}$$

In addition to lithium-ion batteries, **sodium-sulphur** (NaS) and **sodium-nickel-chloride** (NaNiCl) batteries are alternatives. NaNiCl batteries are also called **ZEBRA batteries**. A South African developer coined the acronym, which stands for Zeolite Battery Research Africa Project. Both battery types have very great energy density and a very high Ah efficiency.

A sodium-sulphur battery's chemical reactions are as follows:

Negative electrode:

$$2\ \mathrm{Na} \underset{\leftarrow\text{Charge}}{\overset{\text{Discharge}\rightarrow}{\longleftrightarrow}} 2\ \mathrm{Na}^+ + 2\ \mathrm{e}^- \tag{5.107}$$

Positive electrode:

$$x\mathrm{S} + 2\ \mathrm{e}^- \underset{\leftarrow\text{Charge}}{\overset{\text{Discharge}\rightarrow}{\longleftrightarrow}} \mathrm{S}_x^{-2} \tag{5.108}$$

Net reaction:

$$2\ \mathrm{Na} + x\mathrm{S} \underset{\leftarrow\text{Charge}}{\overset{\text{Discharge}\rightarrow}{\longleftrightarrow}} \mathrm{Na}_2\mathrm{S}_x \tag{5.109}$$

NaS batteries have a drawback: an operating temperature of around 300 °C. Lithiumion batteries are thus considered to have a better chance on the market because they do not constantly consume energy for heat.

Copyright © 2016. Taylor & Francis Group. All rights reserved.

Quaschning, Volker. Understanding Renewable Energy Systems, Taylor & Francis Group, 2016. ProQuest Ebook Central, http://ebookcentral.proquest.com/lib/byu/detail.action?docID=4470609.
Created from byu on 2021-11-05 15:55:38.

Battery systems

The simplest battery systems consist of a photovoltaic generator, a battery, and a device that consumes power. Because the photovoltaic generator has relatively small interior resistance, the battery discharges at low levels of irradiance in the evening and overnight via the generator. A **blocking diode** is used between the battery and the photovoltaic generator to prevent such power losses, as shown in Figure 5.50. At the diode, the power losses constantly occur:

$$P_{\text{loss,diode}} = I_{\text{PV}} \cdot U_{\text{D}} \quad (5.110)$$

so diodes with a low forward voltage drop are used, such as Schottky diodes ($U_{\text{D}} \approx 0.55$ V).

Losses also occur in the **feed lines** with cross-section A, specific resistance ρ and lengths l_1 and l_2 leading to and back from the battery:

$$P_{\text{loss,line}} = I_{\text{PV}} \cdot (U_{\text{L1}} + U_{\text{L2}}) = I_{\text{PV}}^2 \cdot (R_{\text{L1}} + R_{\text{L2}}) = I_{\text{PV}}^2 \cdot \frac{\rho}{A} \cdot (l_1 + l_2) \quad (5.111)$$

Copper cables ($\rho_{\text{Cu}} = 0.0175\ \Omega$ mm2/m) with a length of ($l_1 = l_2 = 10$ m) and a cross-section of $A = 1.5$ mm² at a current of $I_{\text{PV}} = 6$ A have significant line losses of $P_{\text{loss, line}} = 8.4$ W. With a 100 W photovoltaic generator, these losses make up almost 12 % of the output power if the diode pass-through losses of 3.3 W are included. To keep these losses down, feed lines should be as short as possible and have large cross-sections. In 12 V systems, the voltage should not drop by more than 3 % or 0.35 V in the lines from the photovoltaic generator to the battery or by more than 7 %, equivalent to 0.85 V, in the lines from the battery to the device consuming power. In the example above, the cables should therefore have a cross-section of 6 mm².

When the lines are longer, losses can be reduced if the system voltage is increased, such as when multiple batteries are in a series circuit, which increases battery voltage U_{Bat}.

The battery at the photovoltaics generator is:

$$U_{\text{pv}} = U_{\text{bat}} + U_{\text{D}} + U_{\text{L1}} + U_{\text{L2}} \quad (5.112)$$

Here, diode voltage U_{D} is nearly constant, while the voltage drops U_{L1} and U_{L2} within the lines proportional to the photovoltaic current I_{PV} . The battery voltage U_{Bat} is relative to the charge current and the state of charge.

Overall, the voltage at the photovoltaics generator slightly increases along with the current – in other words, as irradiation increases – and it varies slightly with the battery's state of charge. When a solar generator is directly connected to a battery, the power point is generally properly set even if irradiation incident on the solar generator changes, as shown in Figure 5.51. For this reason, voltage converters and MPP trackers in combination with battery systems are not often used because the power consumed by the additional electronics may be

Copyright © 2016. Taylor & Francis Group. All rights reserved.

Quaschning, Volker. Understanding Renewable Energy Systems, Taylor & Francis Group, 2016. ProQuest Ebook Central, http://ebookcentral.proquest.com/lib/byu/detail.action?docID=4470609.
Created from byu on 2021-11-05 15:55:38.

higher than the additional energy gains. An MPP tracker may, however, be useful if the solar generator is run under fluctuating irradiation for a long time.

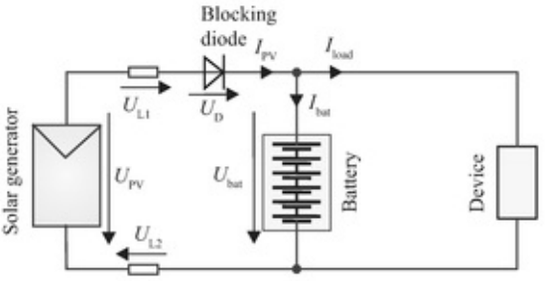

Figure 5.50 A simple photovoltaic system with battery storage

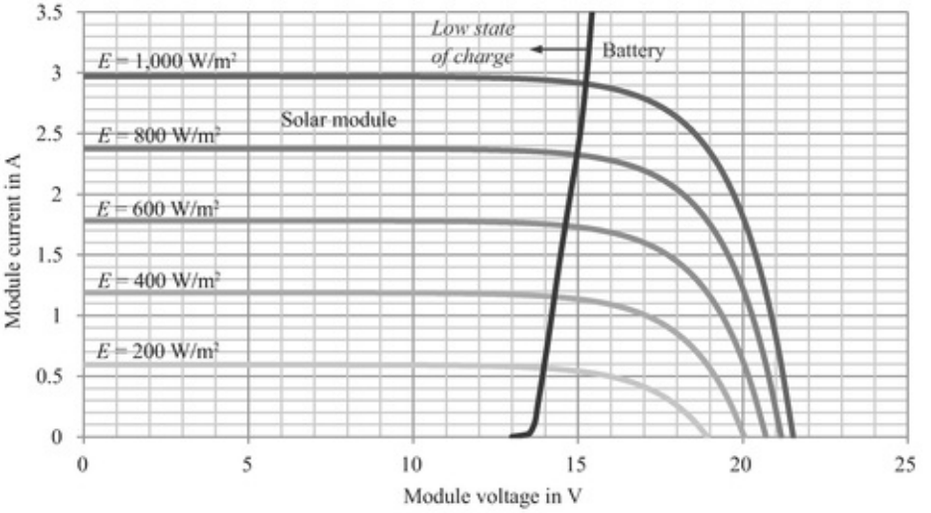

Figure 5.51 A solar generator's power points with a lead battery for storage with a blocking diode and 0.1 Ω line resistance without load

In a simple system in which the photovoltaic generator and power consumers are directly connected to the battery, the battery is not protected from excessive charging or deep discharging. Such systems should therefore only be used when states of charge detrimental to the battery can be prevented. Otherwise, the battery would quickly be damaged and become worthless.

Most battery systems therefore have a **charge controller** (Figure 5.52). With lead batteries, charge controllers generally monitor voltage. Specifically, they measure the battery's voltage U_{Bat}.

If it drops below the lower limit for voltage of deep discharge (around 11.4 V for a 12 V lead battery), switch S_2 separates power consumers from the battery. Once the battery has recovered – that is, once the battery's voltage has reached a minimum level – devices are reconnected. Switch S_1 stops the battery from being charged further if its voltage exceeds its cutofflevel (around 14.4 V for a 12 V lead battery). Here, a distinction is made between **series**

Copyright © 2016. Taylor & Francis Group. All rights reserved.

Quaschning, Volker. Understanding Renewable Energy Systems, Taylor & Francis Group, 2016. ProQuest Ebook Central, http://ebookcentral.proquest.com/lib/byu/detail.action?docID=4470609.
Created from byu on 2021-11-05 15:55:38.

controllers (Figure 5.53) and **shunt controllers** (Figure 5.54).

Power semiconductors and field effect transistors (Power MOSFETS) are used as the switches here. The drawback of serial controllers is that pass-through losses always occur at switch S_1 when the battery is being charged. In contrast, good MOSFETs have a resistance smaller than 0.1 Ω but the losses that field effect transistor BUZ11 entails with a pass-through resistance of 0.04 Ω at 6 A still at up to 1.44 W. If the solar generator's voltage is monitored along with the battery's, no blocking diode is needed as long as the charge controller opens switch S_1 if the solar generator's voltage drops below the battery's.

Shunt controllers are more widely used. When the battery is fully charged, this controller short-circuits the solar generator via switch S_1. The solar generator's voltage drops to the voltage loss at the switch (< 1 V), and the blocking diode prevents current from flowing from the battery via the switch. In normal operation, the short circuit does not pose any problems for the solar generator. If, however, the solar module is shaded unevenly, the load on shaded cells can be tremendous.

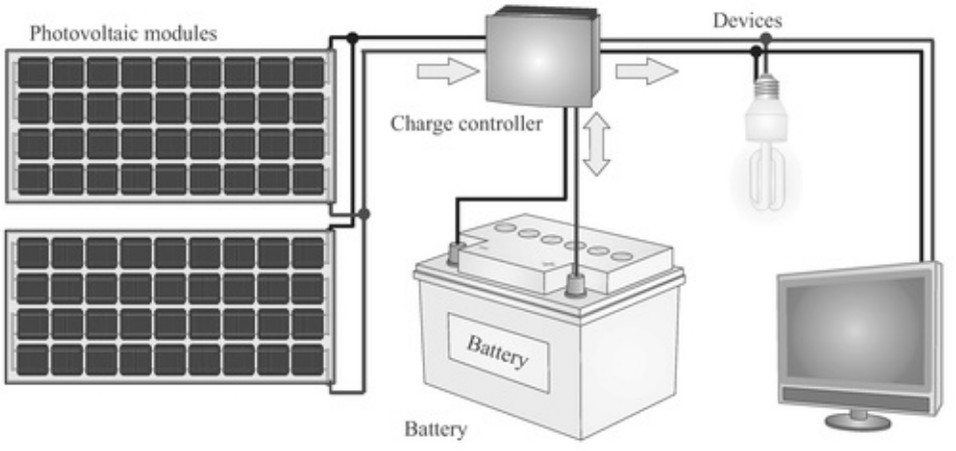

Figure 5.52 A photovoltaic battery system with a charge controller [Qua09]

Individual battery cells are sometimes used to differing extents, especially in large battery systems (such as those used in electric vehicles), so these cells age more quickly. If a cell fails, it detrimentally affects other cells as well. It is therefore a good idea to use battery management systems that not only measure overall battery voltage, but also provide optimal protection for individual cells.

In addition to simple systems consisting only of a photovoltaic generator, battery, charge controller, and consumption device, there are also larger, more complex systems for off-grid power supply, such as to mountain cottages. Usually, the photovoltaic generator is combined here with another source of energy, such as a wind or diesel generator. The combination reduces costs and increases supply security. Such a combination, however, requires a more complex energy management system. Usually, some appliances that consume power will not be available in DC versions. If AC devices are used, an inverter is required (described further

Copyright © 2016. Taylor & Francis Group. All rights reserved.

Quaschning, Volker. Understanding Renewable Energy Systems, Taylor & Francis Group, 2016. ProQuest Ebook Central, http://ebookcentral.proquest.com/lib/byu/detail.action?docID=4470609.
Created from byu on 2021-11-05 15:55:38.

down below).

Other storage options

In addition to electrochemical storage in batteries, there are other ways to store electrical energy. The storage options include:

- capacitors
- superconducting coils
- flywheels
- pumped hydropower
- compressed air
- synthetic gas, methane, and hydrogen.

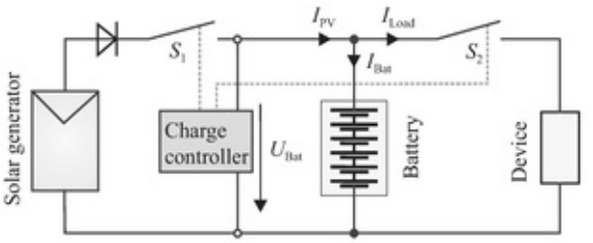

Figure 5.53 A photovoltaic battery system with a serial charge controller

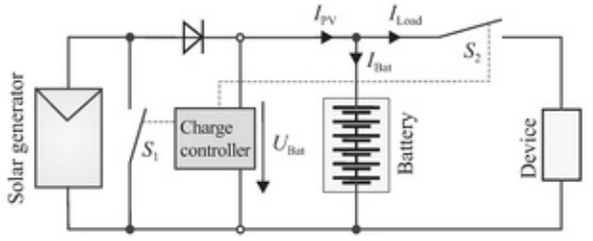

Figure 5.54 Photovoltaic battery system with a shunt controller

For off-grid solar energy systems, these storage options play only a minor role. Pumped hydro storage is discussed in greater detail in the chapter on hydropower; likewise, hydrogen production and storage are dealt with in that chapter.

Inverters

Inverter technology

Copyright © 2016. Taylor & Francis Group. All rights reserved.

Quaschning, Volker. Understanding Renewable Energy Systems, Taylor & Francis Group, 2016. ProQuest Ebook Central, http://ebookcentral.proquest.com/lib/byu/detail.action?docID=4470609.
Created from byu on 2021-11-05 15:55:38.

Up to now, the discussion has assumed that all devices consuming power run on direct current. Power from the grid, however, is alternating current. An off-grid inverter is required to run common appliances connected to an off-grid PV system. If the power from a photovoltaic system is to be exported to the grid, a grid inverter is used. These two types of inverters use similar technology, but there are some decisive differences in terms of design and requirements.

Switchable valves are needed when using power electronics to turn direct-current into alternating current. The following power semiconductor elements can be used for this purpose; depending on the design, the voltages can clearly exceed 1,000 V, or the currents can exceed 1,000 A:

- power MOSFETs (power field effect transistors)
- bipolar power transistors
- IGBTs (insulated gate bipolar transistors)
- thyristors (controllable diodes)
- triacs (dual-direction thyristors)
- GTO thyristors (gate turn-offthyristors).

Below, we take a closer look at only **MOSFETs** (metal-oxide semiconductor field effect transistors). Figure 5.55 shows the circuit of a self-blocking n-channel MOSFET with three connections: G (Gate), S (Source) and D (Drain).

If there is voltage at input G and voltage U_{GS} is greater than threshold voltage U_{th}, the transistor switches. It then becomes conductive between the inputs S and D. If voltage U_{GS} falls below the threshold voltage, the transistor blocks. A body diode is integrated in the field effect transistors between inputs S and D. It facilitates switching because it can derive excess voltage from inductance within the circuit. Because body diodes are usually relatively slow, an additional parallel, fast Schottky diode can be useful.

In an inverter, current periodically has to be transferred from one branch to another. This process is also called **commuting**. To this end, various valves have to be opened or closed. Inverters used to require external controllers with thyristors, but today most inverters have their own controllers with transistors or MOSFETs as switches.

Rectangle and trapezoid inverters are very straightforward and are therefore described below in greater detail first. Because the quality of the output current from these inverters is not very great, pulse-width modulation inverters and resonant inverters described below are more commonly used in photovoltaics.

Rectangle inverter

Copyright © 2016. Taylor & Francis Group. All rights reserved.

Quaschning, Volker. Understanding Renewable Energy Systems, Taylor & Francis Group, 2016. ProQuest Ebook Central, http://ebookcentral.proquest.com/lib/byu/detail.action?docID=4470609.
Created from byu on 2021-11-05 15:55:38.

A **B2 or H bridge** is a very simple way to create an inverter circuit, as shown in Figure 5.56.

It consists of four valves connected to the alternating current grid via a transformer. Below, inverters connected to a fixed grid are discussed further.

At regular intervals, valves one and three are opened, followed by two and four, to produce a roughly rectangular alternating current in the transformer. Valves 1 and 2 can also be replaced with non-controllable diodes so that only half of the components need to be controlled. In this case, the bridge is half-controlled. The valves are switched with a delay around control angle α for the voltage's zero-crossing. Figure 5.52 shows the power curve for a B2 circuit.

The curve looks very different from the desired sine curve. A Fourier analysis – also called a **harmonic analysis** – assesses the power curve. A 2π periodic function $f(\omega t)$ can be broken down into a convergent series in the interval $-\pi \le \omega t \le +\pi$:

$$f(\omega t) = \frac{a_0}{2} + \sum_{n=1}^{\infty} \left(a_n \cdot \cos(n \cdot \omega t) + b_n \cdot \sin(n \cdot \omega t) \right) \tag{5.113}$$

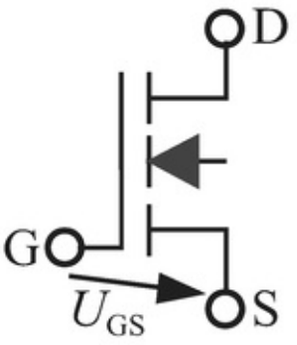

Figure 5.55 Circuit of a self-blocking n-channel MOSFET

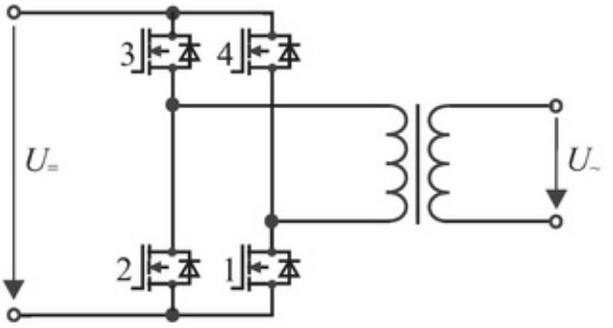

Figure 5.56 H-bridge (B2)

Copyright © 2016. Taylor & Francis Group. All rights reserved.

Quaschning, Volker. Understanding Renewable Energy Systems, Taylor & Francis Group, 2016. ProQuest Ebook Central, http://ebookcentral.proquest.com/lib/byu/detail.action?docID=4470609.
Created from byu on 2021-11-05 15:55:38.

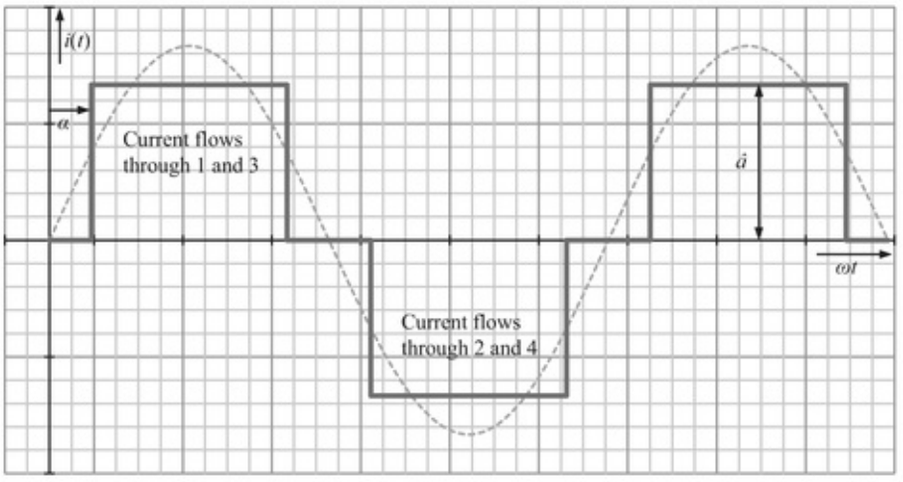

Figure 5.57 An idealized power curve for a semi-controlled B2 bridge

Coefficients a_n and b_n can be determined by means of:

$$a_n = \frac{1}{\pi} \cdot \int_{-\pi}^{\pi} f(\omega t) \cdot \cos(n \cdot \omega t) \, d\omega t \quad (n = 0, 1, 2, \ldots) \tag{5.114}$$

$$b_n = \frac{1}{\pi} \cdot \int_{-\pi}^{\pi} f(\omega t) \cdot \sin(n \cdot \omega t) \, d\omega t \quad (n = 1, 2, \ldots) \tag{5.115}$$

The following harmonic analysis can be performed for the current's rectangular shape with the amplitude $\hat{a}$ and control angle α of the B2 bridge:

$$f(\omega t) = \frac{4 \cdot \hat{a}}{\pi} \cdot \left[\cos\alpha \cdot \sin\omega t + \tfrac{1}{3} \cdot \cos 3\alpha \cdot \sin 3\omega t + \tfrac{1}{5} \cdot \cos 5\alpha \cdot \sin 5\omega t + \cdots \right] \tag{5.116}$$

In addition to the desired sinusoidal fundamental frequency (atomic number 1), there is also the function of oscillations of other periodic durations (atomic number ≥ 2), undesired **harmonics**. Figure 5.58 shows the fundamental frequency and harmonics up to ordinal number 7. If harmonics are added up to ordinal number 7, the rectangle is already visibly mapped, as the thick black curve shows. Additional harmonics would have to be included for a more precise mapping. In practice, an oscilloscope and subsequent computer analysis can be used to perform a harmonic analysis. More complex devices can even determine the share of harmonics independently.

In general, the current can be represented based on the fundamental frequency with amplitude $\hat{i}_1$ and the harmonics with amplitudes $\hat{i}_2$, $\hat{i}_3$ etc.:

$$i(t) = \hat{i}_1 \cdot \sin(\omega t) + \hat{i}_2 \cdot \sin(2 \cdot \omega t) + \hat{i}_3 \cdot \sin(3 \cdot \omega t) + \ldots \tag{5.117}$$

Copyright © 2016. Taylor & Francis Group. All rights reserved.

Quaschning, Volker. Understanding Renewable Energy Systems, Taylor & Francis Group, 2016. ProQuest Ebook Central, http://ebookcentral.proquest.com/lib/byu/detail.action?docID=4470609.
Created from byu on 2021-11-05 15:55:38.

Class A devices with an input current ≤ 16 A can cause harmonic currents in the low-voltage level of the grid, so VDE 0838 part 2 and DIN EN 61000–3–2 specifies maximum values for harmonic currents [DIN05].

In addition to harmonic currents, the inverter can also cause harmonic voltages. VDE 0839 part 2–2 and DIN EN 61000–2–2 specify the admissible harmonic voltages relative to the fundamental frequency's voltage [DIN03]. If multiple harmonics occur simultaneously, the **total harmonic distortion** (THD)

$$D = \sqrt{\sum_{n=2}^{40} \left(\frac{\hat{u}_n}{\hat{u}_1} \right)^2} \tag{5.118}$$

expresses the effect. It is calculated from the voltage amplitudes $\hat{u}_n$ of the harmonics and the fundamental frequency's voltage amplitude $\hat{u}_1$. The maximum admissible total harmonic distortion is $D = 0.8$. In addition to amplitudes, the calculations often use root mean squares.

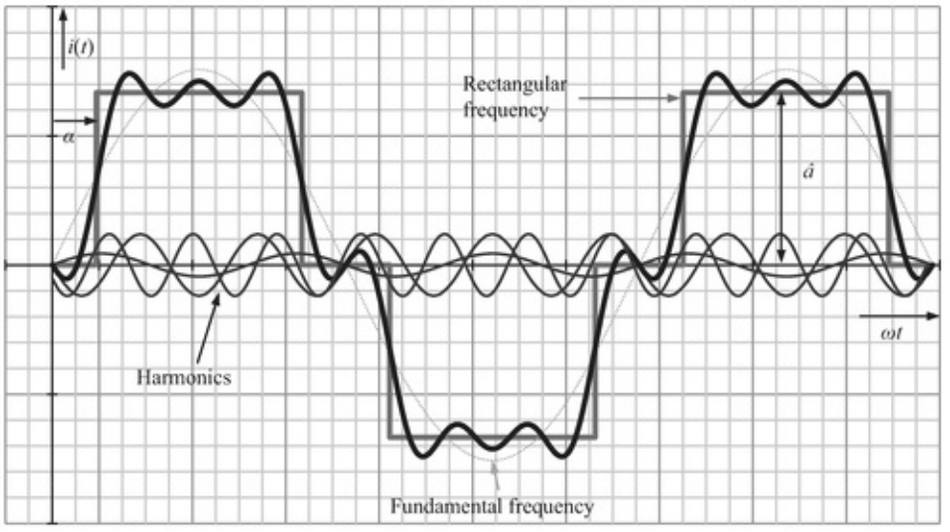

Figure 5.58 Making a rectangular curve out of various sinusoidal waves

Harmonic distortion is another quality factor:

$$k = \sqrt{\frac{\sum_{n=2}^{\infty} U_n^2}{\sum_{n=1}^{\infty} U_n^2}} \tag{5.119}$$

It is derived from the ratio of the root mean squares for harmonics to the root mean squares for fundamental frequencies and harmonics. The harmonic distortion of good inverters is below 3 %. If the harmonics are too great, filters must be used to reduce them.

Copyright © 2016. Taylor & Francis Group. All rights reserved.

Quaschning, Volker. Understanding Renewable Energy Systems, Taylor & Francis Group, 2016. ProQuest Ebook Central, http://ebookcentral.proquest.com/lib/byu/detail.action?docID=4470609.
Created from byu on 2021-11-05 15:55:38.

Often, transformers are integrated in inverters. Transformers separate the inverter from the grid and can adjust voltage between the inverter's and the grid's voltage. However, transformers always lead to losses and can be dispensed with in principle. But then, greater safety measures must be taken because the grid and the solar generator are no longer galvanically isolated.

The B2 bridge only supplies alternating current into only one phase conductor. On the grid, which has three phases, the result is asymmetries. Therefore, lines larger than 4.6 kVA have to have three-phase current in the three-phase conductors in Germany. Chapter 6 (wind power) discusses the basic properties of three-phase power in greater detail. Figure 5.59 shows the six-pulse bridge **(B6 bridge)** used in the inverter circuit to generate three-phase power. In this circuit, the valves are opened cyclically so that alternating current and voltage is produced in three phases shifted by a third each.

In addition to B2 and B6 bridges, others such as M2 and M3 midpoint circuits and other bridge circuits are used. These options work the same, however, as those described above.

Modern inverter topologies

In inverters that use **pulse width modulation (PWM)** one of the aforementioned circuits – such as B2 and B6 – is used. Here, the valves are not only opened and closed once every half-wave, but several times to produce pulses of different widths, as shown in Figure 5.60. After filtering, the fundamental wave is sinusoidal. The quality of a sine wave is much better than that of rectangular waves from inverters; specifically, there are fewer undesirable harmonics. For this reason, most inverters now used have PWM.

To produce especially high inverter efficiencies, other circuit concepts are used in addition to the bridges described above. Single-phase inverters sometimes have an **H5 or HERIC circuit** (Highly Efficient and Reliable Inverter Concept). They are based on the concept of H bridges. Other transistors ensure that choke current can be drawn offduring switching in the freewheeling phase, which reduces switching losses.

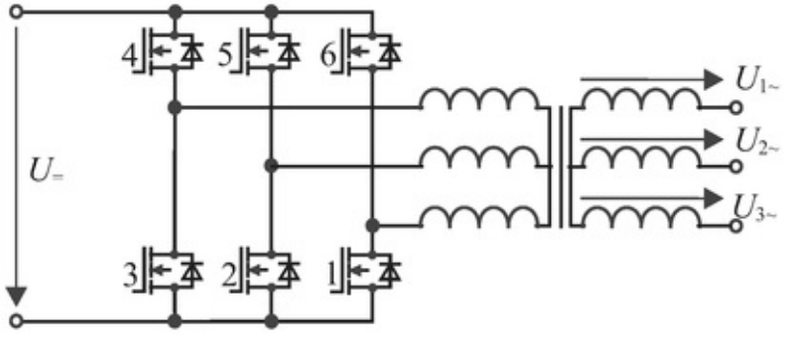

Figure 5.59 Six pulse bridge (B6)

Copyright © 2016. Taylor & Francis Group. All rights reserved.

Quaschning, Volker. Understanding Renewable Energy Systems, Taylor & Francis Group, 2016. ProQuest Ebook Central, http://ebookcentral.proquest.com/lib/byu/detail.action?docID=4470609.
Created from byu on 2021-11-05 15:55:38.

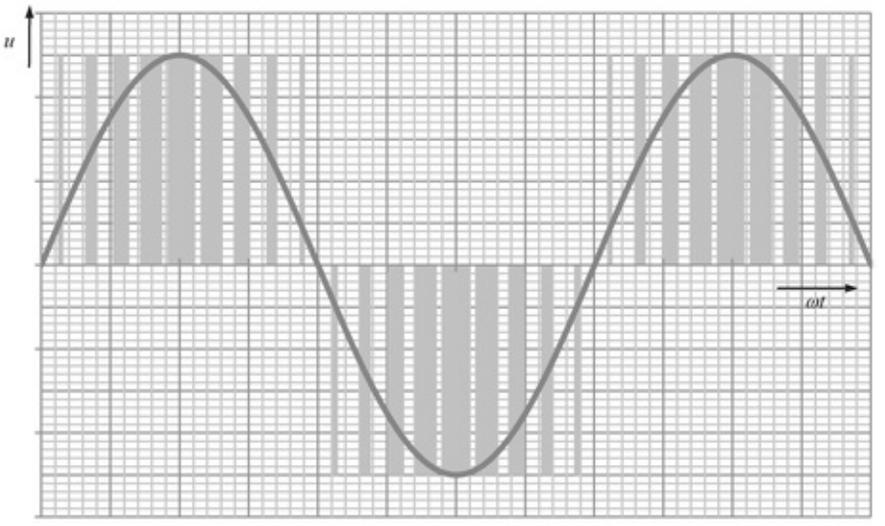

Figure 5.60 A curve from pulse width modulation

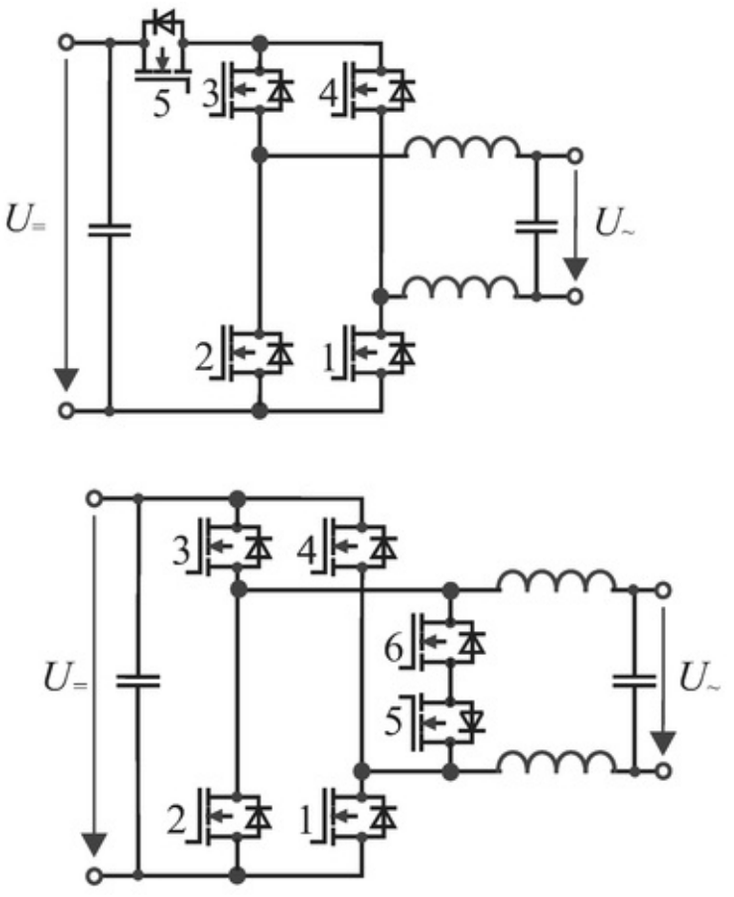

Figure 5.61 Highly efficient inverter circuits. Left: H5 topology, right: HERIC topology

Inverters for photovoltaics

An inverter's functions and tasks

Copyright © 2016. Taylor & Francis Group. All rights reserved.

Quaschning, Volker. Understanding Renewable Energy Systems, Taylor & Francis Group, 2016. ProQuest Ebook Central, http://ebookcentral.proquest.com/lib/byu/detail.action?docID=4470609.
Created from byu on 2021-11-05 15:55:38.

Photovoltaic inverters perform far more tasks than merely converting direct into alternating current, as Figure 5.62 shows. The grid always determines the output voltage. The inverter has to adjust the DC voltage for the photovoltaic generator so that it always runs at its MPP. Good inverters have very high MPP tracking speeds. The **MPP tracking efficiency** can exceed 99 % considerably even under changing irradiance conditions. In other words, the losses due to deviations from the actual MPP are smaller than 1 %. A step-up converter between the photovoltaic generator and the bridge adjusts DC voltage. The bridge in a pulse width modulation inverter can also adjust DC voltage, however. The step-up converter is not needed then, and leaving it out improves the inverter's efficiency. Then, however, the solar generator's voltage needs to be high. The minimum MPP voltage for a single-phase inverter without a transformer is then around 350 V.

A **transformer** can adjust the alternating current voltage and provide galvanic isolation between the grid and the photovoltaic generator. Inverters without transformers are now commonly used in photovoltaics. By doing without a transformer, losses are reduced, thereby enabling especially great inverter efficiencies. To ensure safety, however, residual current has to be monitored universally and the grid connection reliably if there is a flaw. Before using an inverter that has no transformer, make sure that the photovoltaic modules you are using have been approved by the manufacturer for this combination. Certain moduels undergo potential-induced degradation (PID) when used with inverters that have no transformer. TCO corrosion in particular destroys the front contacts of thin-film modules and can destroy them in the process. Grounding one of the module's poles – generally the minus pole – considerably reduces the risk of degradation.

Inverters for off-grid applications differ fundamentally from those designed for grid connections. Off the grid, inverters often have a battery charge controller integrated in them. In return, grid-connected inverters have to fulfil specific criteria and perform certain tasks in line with grid quality, while such requirements are less strict for off-grid inverters. VDE-AR-N 4105 [VDE11] specifies these rules for low-voltage grid connections in Germany. The rules include maximum values for voltage changes and harmonic currents.

Comprehensive grid and equipment protection must perform the following functions and disconnect the photovoltaic system from the grid reliably:

- protection against voltage drops, $U < 184$ V
- protection against voltage increases, $U > 253$ V
- protection against frequency drops, $f < 47.5$ Hz
- protection against frequency increases, f>51.5 Hz
- detection of grid connection loss (unplanned micro-grid).

The system can only be switched on again when the grid voltage lies within 195.5 and 253

Copyright © 2016. Taylor & Francis Group. All rights reserved.

Quaschning, Volker. Understanding Renewable Energy Systems, Taylor & Francis Group, 2016. ProQuest Ebook Central, http://ebookcentral.proquest.com/lib/byu/detail.action?docID=4470609.
Created from byu on 2021-11-05 15:55:38.

V, with the grid frequency being between 47.5 and 50.05 Hz. At a grid frequency above 50.2 Hz, the power output has to be reduced linearly relative to frequency down to 48 % at 51.5 Hz.

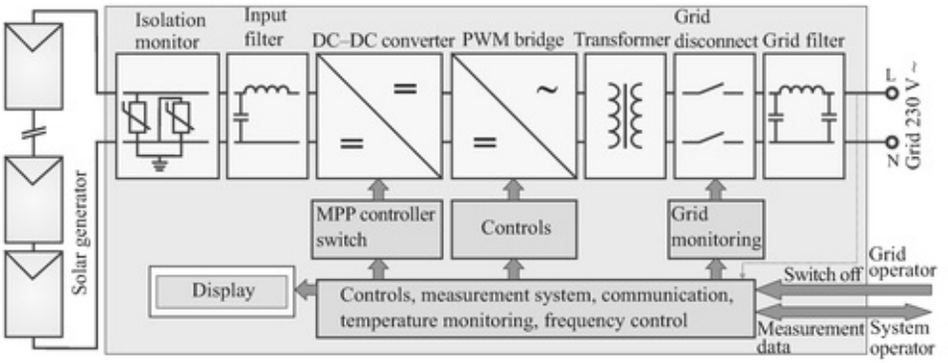

Figure 5.62 The components in a photovoltaic inverter

The unbalanced load must not exceed 4.6 kVA. Three unconnected, single-phase inverters distributed across three different phases could then produce a maximum AC power of 13.8 kVA. If the output needs to be greater, either three-phase inverters need to be used, or single-phase inverters need to be connected, though the unbalanced load still must not be allowed to exceed 4.6 kVA.

Starting at 3.68 kVA, the inverter also has to be able to provide reactive power as defined by the grid operator. Then, more photovoltaic systems can be integrated on the grid at a single connection point.

Inverter efficiencies

Inverters used in photovoltaics rarely work in nominal operation at nominal output P_N. Because the level of irradiance changes, the inverter runs at partial load over long periods of time. It is therefore important for the inverter to be efficient even when running at low output. The inverter should not be over-dimensioned. To take a simple example, if a 1 kW inverter is connected to a 500 W photovoltaic system, the inverter will only run at a maximum of 50 % of its nominal output. Greater losses can be expected if the inverter runs constantly at partial load. The inverter itself should consume as little power as possible. Shutting it off at night is one way to reduce its power consumption.

One way of comparing inverters is in terms of their European efficiency:

$$\eta_{Euro} = 0.03 \cdot \eta_{5\%} + 0.06 \cdot \eta_{10\%} + 0.13 \cdot \eta_{20\%} + 0.1 \cdot \eta_{30\%} + 0.48 \cdot \eta_{50\%} + 0.2 \cdot \eta_{100\%} \quad (5.120)$$

It represents the average weighted efficiency. Account is taken of the inverter's response at partial loads that commonly occur under average irradiation levels in Western Europe.

Copyright © 2016. Taylor & Francis Group. All rights reserved.

Quaschning, Volker. Understanding Renewable Energy Systems, Taylor & Francis Group, 2016. ProQuest Ebook Central, http://ebookcentral.proquest.com/lib/byu/detail.action?docID=4470609.
Created from byu on 2021-11-05 15:55:38.

Figure 5.63 shows the **efficiency curve** relative to input power. Modern inverters reach maximum efficiencies of up to 98 %. Even under partial loads, efficiencies are still high, and they only collapse under extreme partial loads. The figure also shows the energy output for this particular DC system output relative to the overall yield for Berlin. The share of very high outputs is small because such levels only occur a few hours per year. The middle range makes up the biggest share, which is why efficiency at 50% partial load has such a heavy weighting in European efficiency. The calculations described here are based on hourly averages of irradiance. If more realistic, shorter intervals are used for irradiance, the energy shares shift towards greater outputs.

In other parts of the world, however, levels of irradiation are very different, so the energy shares look a lot different. Figure 5.64 shows the shares of energy relative to hourly DC system output, but this time for Los Angeles, not Berlin. Clearly, greater system output is more frequent. The California Energy Commission (CEC) has also defined an average efficiency with a much greater weighting of high power outputs than is used in the calculation of European efficiency. **CEC efficiency** is defined as follows:

$$\eta_{\mathrm{CEC}} = \frac{1}{3}\sum_{i=1}^{3}\left(\begin{matrix}0.04\cdot\eta_{10\%} + 0.05\cdot\eta_{20\%} + 0.12\cdot\eta_{30\%} \\ +0.21\cdot\eta_{50\%} + 0.53\cdot\eta_{75\%} + 0.05\cdot\eta_{100\%}\end{matrix}\right)_{U_i} \tag{5.121}$$

In addition to operation under partial load, the inverter's input voltage influences its efficiency. Figure 5.64 shows the efficiency curve for two different voltages. CEC efficiency also takes account of these factors by determining the average efficiencies for three different DC voltages (U_1 = $U_{\mathrm{MPP,min}}$, U_2 = $U_{\mathrm{MPP,nom}}$, and U_3 = $U_{\mathrm{MPP,max}}$) at the lower end of the inverter's MPP range, under nominal voltage, and at the top end of the range.

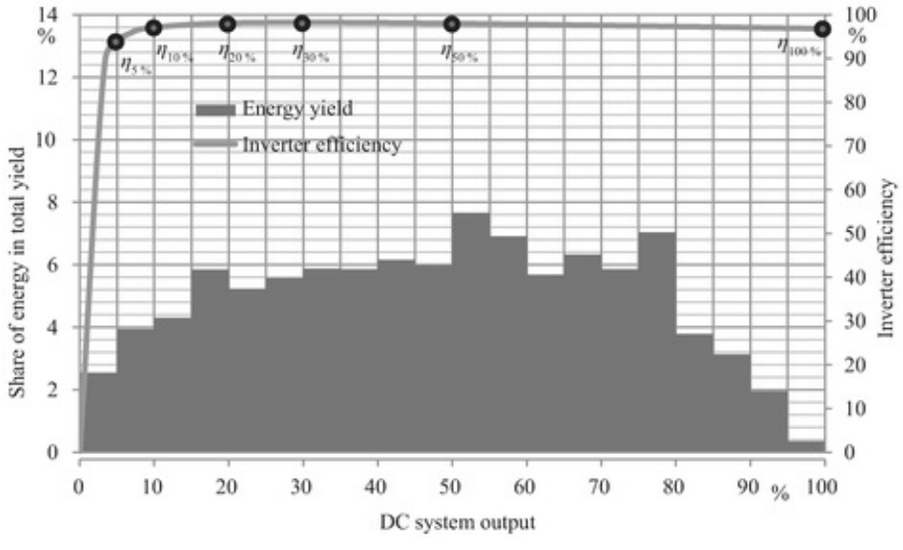

Figure 5.63 Inverter efficiency relative to DC system output and typical energy shares for the average hourly system output in overall yield for Berlin

Copyright © 2016. Taylor & Francis Group. All rights reserved.

Quaschning, Volker. Understanding Renewable Energy Systems, Taylor & Francis Group, 2016. ProQuest Ebook Central, http://ebookcentral.proquest.com/lib/byu/detail.action?docID=4470609.
Created from byu on 2021-11-05 15:55:38.

Table 5.14 shows the **technical data** for a number of inverters. The inverters shown cover the entire output range from module inverters up to central megawatt inverters.

Modern inverters have very high efficiencies. The maximum efficiency can be 98 % at 6 kVA. The use of new silicon-carbide (SiC) semiconductor transistors might even increase efficiency to 99 %.

System concepts

There are three basic concepts for grid-connected inverters in photovoltaic systems:

- central inverters
- string inverters
- module inverters (micro-inverters).

Figure 5.65 shows solar modules connected to a central inverter. Here, modules are switched in series until the desired DC voltage is attained. For greater outputs, multiple strings of the same size are connected in parallel. The string diodes shown in the graphic often do not need to be used because they provide little protection; leaving them out can be a good idea because they always cause pass-through losses.

The **master–slave principle** is increasingly applied to improve performance under partial load. Here, multiple inverters are interconnected to produce one big inverter. Figure 5.66

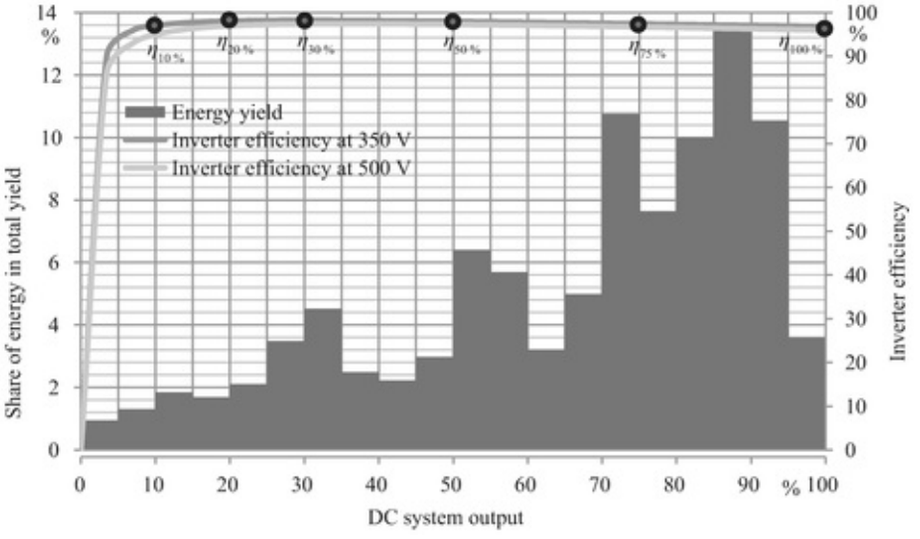

Figure 5.64 Inverter efficiency relative to DC system output at two different DC voltages and typical energy shares for the average hourly system output in overall yield for Los Angeles

Table 5.14 Selected technical data for a number of photovoltaic inverters

Copyright © 2016. Taylor & Francis Group. All rights reserved.

Quaschning, Volker. Understanding Renewable Energy Systems, Taylor & Francis Group, 2016. ProQuest Ebook Central, http://ebookcentral.proquest.com/lib/byu/detail.action?docID=4470609.
Created from byu on 2021-11-05 15:55:38.

Device		*Enecsys SMI-D360*	*Sunways NT2500*	*SMA 6000TL*	*REFUSOL 15 K*	*SINVERT PVS2400*
Topology		Enecsys	HERIC	H5	UtraEta	PVS
Phases		1	1	1, connectable	3	3
Nominal output AC	kVA	0.34	2.5	6.0	15.0	2,400
Max. AC power	kVA	0.34	2.5	6.0	16.5	2,400
Max. DC power	kW	0.38	2.65	6.2	17.5	2,452
Max. DC voltage	V	54	900	700	900	1,000
MPP range DC	V	30–42	340–750	333–500	460–800	570–750
Max. DC current	A	13.4	7.5	19	36	4416
Power exported starting at	W	n/a	4	10	20	n/a
Overnight consumption	W	<0.03	<0.1	0.25	<0.2	n/a
Harmonic distortion, AC current	%	<5	<3	<4	<2.5	n/a
Max. efficiency	%	95.4	97.8	98.0	>98.0	98.7
European efficiency	%	93.5	97.4	97.7	97.7	98.6
Mass	kg	1.8	26	31	38	8520

shows the principle of a central inverter consisting of three units. Initially, only one inverter outputs power. At a third of overall output, it is running at maximum capacity. When the generator's output increases, additional units are switched on one by one.

Under partial shading and when individual modules have lower output, the central inverter concept is particularly unproductive because the losses are above average in such cases. If partial shading is expected or if individual parts of the photovoltaic system have a different orientation, it makes sense to separate strings or use smaller units or individual string inverters. Another benefit is that the length of the direct current lines needed is also shorter.

Micro-inverters are the optimal solution for partial shading. They allow a different voltage to be set for each module. Cabling is also much more straightforward because no direct current lines are needed at all. Another benefit is that the photovoltaic system is easy to expand. The lower inverter efficiency and higher cost largely outweigh these benefits, however, so that micro-inverters have not become the standard. Figure 5.67 shows the two options.

Direct consumption of photovoltaics

The following sections discuss first a simple off-grid combination of a photovoltaic generator and a battery and, second, a simple grid-connected system. These two options have dominated photovoltaics up to now. But the trend is towards more complex systems optimized for the direct consumption of solar power.

In numerous regions, the cost of solar power is now lower than the retail electricity rate. Germany reached this level of 'grid parity' in 2012. Straightforward grid-connected systems will remain attractive as long as Germany has its current feed-in tariffs. It is also clear that

Copyright © 2016. Taylor & Francis Group. All rights reserved.

Quaschning, Volker. Understanding Renewable Energy Systems, Taylor & Francis Group, 2016. ProQuest Ebook Central, http://ebookcentral.proquest.com/lib/byu/detail.action?docID=4470609.
Created from byu on 2021-11-05 15:55:38.

photovoltaic systems will have to make do without high feed-in tariffs in the future.

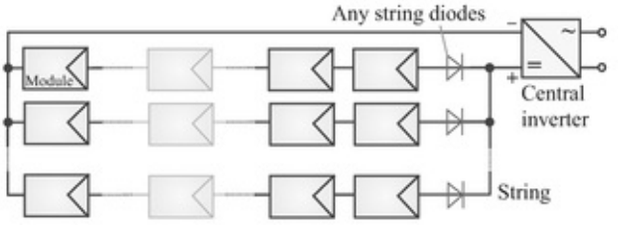

Figure 5.65 A photovoltaic system consisting of multiple strings connected to a central inverter

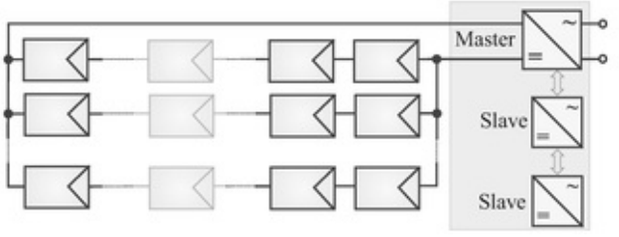

Figure 5.66 Central master–slave inverter for photovoltaic system

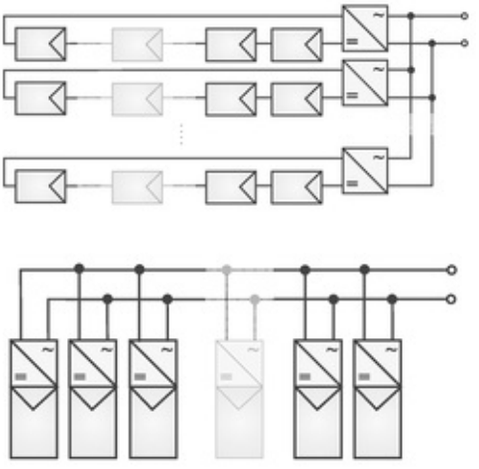

Figure 5.67 Photovoltaic generator with string inverters (left) and micro-inverters (right)

If the owner of the photovoltaic system consumes most of its power directly, photovoltaic systems still pay for themselves. But this option generally only works with extremely small systems. The larger the system, the greater the amount of solar power that cannot be consumed immediately. There is always the option of exporting excess power to the grid. But as the share of solar power on the grid increases, the potential revenue decreases. In a few years, peak solar power production can be expected to begin exceeding total power demand in Germany on the grid. When there is a lot of sunshine, solar power sold to the grid will be relatively worthless.

In the future, systems that can store excess solar power for later use without having to be exported to the grid or use it to create heat will increasingly become important. At present, it

Copyright © 2016. Taylor & Francis Group. All rights reserved.

Quaschning, Volker. Understanding Renewable Energy Systems, Taylor & Francis Group, 2016. ProQuest Ebook Central, http://ebookcentral.proquest.com/lib/byu/detail.action?docID=4470609.
Created from byu on 2021-11-05 15:55:38.

seems that batteries will be the main type of storage for grid-connected systems. A control system sends the excess power to the battery. Power is only exported to the grid when the battery is full; the system also shuts down the solar energy system in extreme cases. If the solar output cannot meet demand, power can be taken from the battery to cover the gap. When the battery is empty, power can be taken from the grid. The system can also react to the grid's demand with smart charging management; then, excess power would be exported to the grid when the grid needs it the most. If devices are properly timed, the share of solar power consumed directly can be increased further, thereby optimizing affordability. In principle, the battery could then also be used to stabilize the grid.

Theoretically, such a system could work as a micro-grid during a power outage, thereby increasing individual supply security. This option would require, however, an inverter capable of creating a micro-grid. A disconnect also has to separate the system from the grid so that a micro-grid can be produced. Figures 5.68 and 5.69 show **grid-connected photovoltaic systems with battery storage**.

Battery storage can in principle be connected either to the AC or DC lines. If it is connected to AC lines, the battery storage can be integrated to an already completed photovoltaic system. In this case, however, a second inverter is needed for the battery, which leads to additional costs and power losses. If the storage is connected to DC lines, only one inverter is needed for both the battery and the photovoltaic system.

Instead of battery storage, hydrogen storage can also be integrated in grid-connected photovoltaic systems. Batteries generally are only designed for short-term storage, while hydrogen storage can be seasonal. Hydrogen can be produced during the summer from excess power to provide energy during the winter. When properly dimensioned, the components in such a system can provide complete **independence** from the grid. Photovoltaic systems with hydrogen storage have, however, much greater losses during charging and discharging that battery systems do. Furthermore, hydrogen storage is still very expensive, so such systems are still only used in very small numbers.

Copyright © 2016. Taylor & Francis Group. All rights reserved.

Quaschning, Volker. Understanding Renewable Energy Systems, Taylor & Francis Group, 2016. ProQuest Ebook Central, http://ebookcentral.proquest.com/lib/byu/detail.action?docID=4470609.
Created from byu on 2021-11-05 15:55:38.

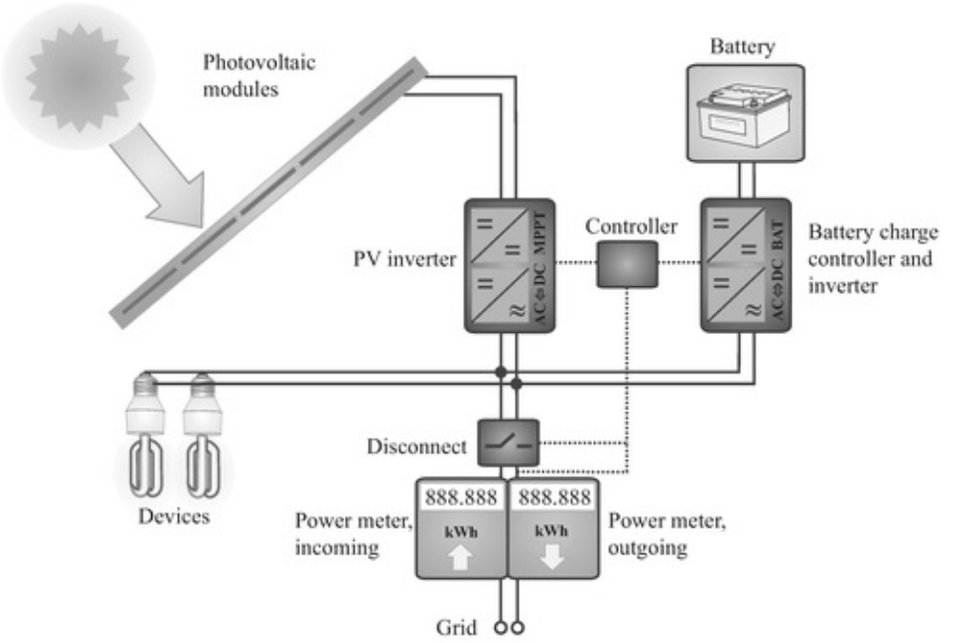

Figure 5.68 Grid-connected photovoltaic system with AC-coupled battery storage

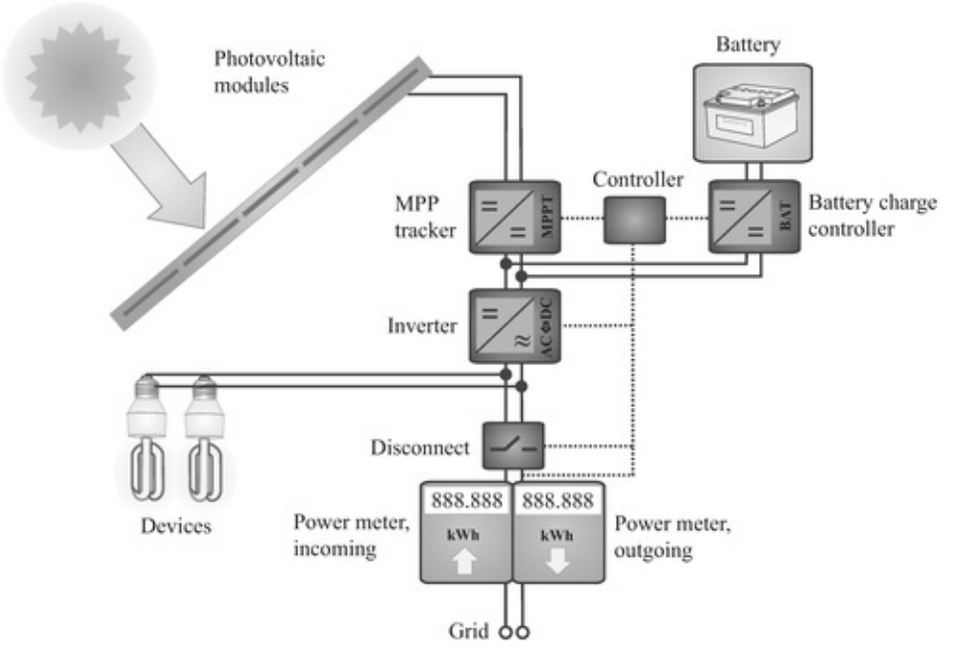

Figure 5.69 Grid-connected photovoltaic system with DC-coupled battery storage

Another way of increasing direct consumption is thermal storage. A simple cartridge heater uses excess solar power to store heat. This approach even saves money if the offset fuel costs are higher than the possible revenue from the sale of the solar power. If the heat storage unit is full or if there is not enough solar power to cover power consumption, power can be purchased from the grid. If a heat pump is already in place or planned, it can directly replace the cartridge heater. Heat pumps generally do not pay for themselves as additions to existing heating systems if the heat pump is merely to serve as an efficient way of using excess solar

Copyright © 2016. Taylor & Francis Group. All rights reserved.

Quaschning, Volker. Understanding Renewable Energy Systems, Taylor & Francis Group, 2016. ProQuest Ebook Central, http://ebookcentral.proquest.com/lib/byu/detail.action?docID=4470609.
Created from byu on 2021-11-05 15:55:38.

power.

Demand for cooling will grow in the future. Because cooling loads closely correlate to levels of irradiance, inexpensive vapour-compression refrigerators are a good way of exploiting excess solar power. Figure 5.71 depicts such a system, which can be combined with battery storage if need be.

Another way of storing excess solar power is the methanation of hydrogen so that this synthetic hydrogen can be exported to natural gas networks. Chapter 10 discusses this option in detail.

Planning and design

Off-grid systems

The planning and design of photovoltaic systems is very different if the goal is to be connected to the grid or off the grid. This section only discusses the simple combination of photovoltaics and batteries for off-grid power supply. Hybrid systems with other power generators, such as wind generators, can generally only be properly dimensioned with the aid of simulation programs.

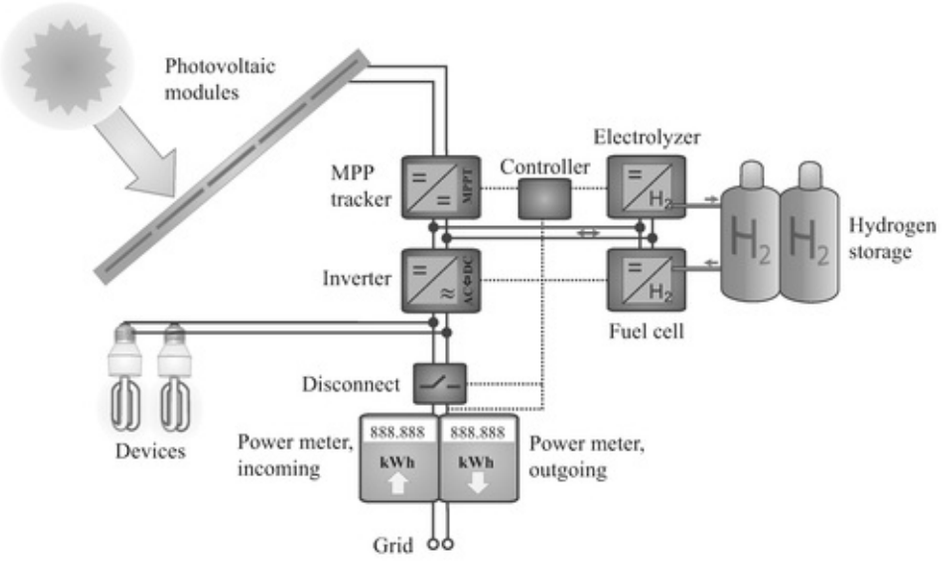

Figure 5.70 Grid-connected photovoltaic system with hydrogen storage

Copyright © 2016. Taylor & Francis Group. All rights reserved.

Quaschning, Volker. Understanding Renewable Energy Systems, Taylor & Francis Group, 2016. ProQuest Ebook Central, http://ebookcentral.proquest.com/lib/byu/detail.action?docID=4470609.
Created from byu on 2021-11-05 15:55:38.

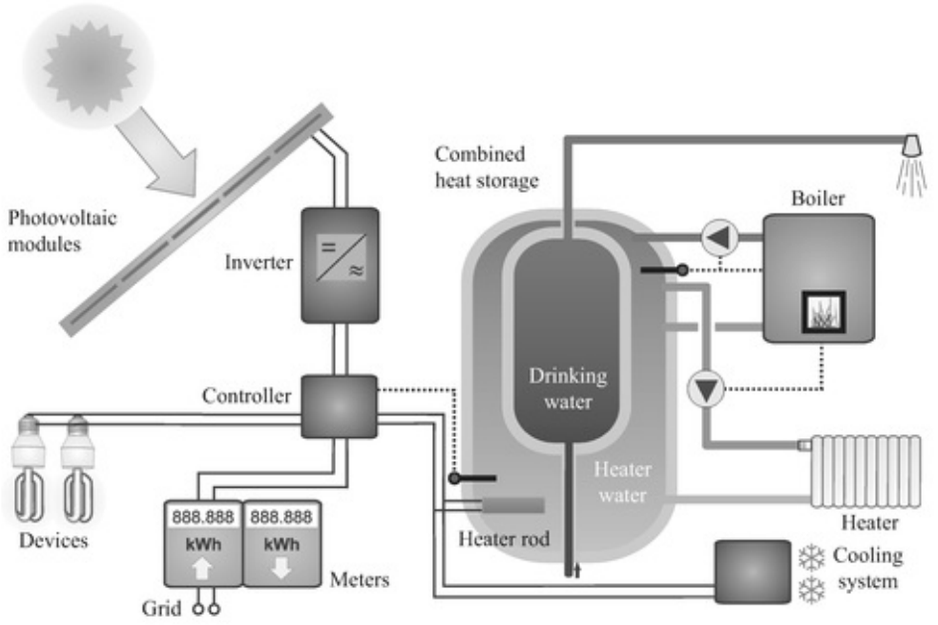

Figure 5.71 A grid-connected photovoltaic system with thermal storage of excess power

Off-grid systems should generally only have enough storage to cover a few days in order to keep costs down. While seasonal storage from the summer for the winter is technically possible, it is expensive in countries like Germany, where the differences over the year are great.

An off-grid photovoltaic system should therefore be designed for the worst month of the year, which is typically December in Germany. Here, the orientation should have a much greater angle than would be common for grid-connected systems. A 60 to 70° angle facing the south would optimally capture the sun in December. Because supply security is not a problem in the summer, the losses from this suboptimal orientation would be acceptable then.

Figure 5.72 shows the daily and monthly averages for irradiation in Berlin on a horizontal plane and on a surface tilted 60° towards the south. The 60° angle provides far greater yield, especially on days with greater daily averages for irradiation. On cloudy days, the yield even drops slightly from this orientation. Table 5.15 shows the monthly and yearly sums for various locations and orientations. In the winter, irradiation in Cairo can be up to six times greater than in Berlin. Photovoltaic off-grid systems can then be accordingly smaller and less expensive.

The photovoltaic generator now needs to be dimensioned so that it can cover monthly power demand with the monthly supply of solar energy. The battery ensures that supply is smooth. Figure 5.72 shows that only a few days need to be bridged.

Table 5.15 Monthly and annual sum of solar irradiation $H_{G,gen,M}$ / $H_{G,gen,a}$ in kWh/m² for various locations and orientations

Copyright © 2016. Taylor & Francis Group. All rights reserved.

Quaschning, Volker. Understanding Renewable Energy Systems, Taylor & Francis Group, 2016. ProQuest Ebook Central, http://ebookcentral.proquest.com/lib/byu/detail.action?docID=4470609.
Created from byu on 2021-11-05 15:55:38.

Location	*Berlin*		*Freiburg*		*Madrid*		*Cairo*
Orientation	30° South	60° South	30° South	60° South	30° South	60° South	30° South
January	28	31	44	51	95	108	157
February	49	52	61	64	105	111	163
March	87	86	103	102	169	164	200
April	117	106	131	117	171	149	204
May	159	136	156	133	148	122	214
June	151	127	162	133	206	162	214
July	161	135	175	145	223	175	221
August	153	135	162	141	213	180	220
September	108	104	128	120	179	165	210
October	68	70	87	91	134	135	201
November	37	42	52	59	95	104	160
December	21	25	38	45	81	92	146
Year	1,139	1,042	1,296	1,198	1,819	1,667	2,310

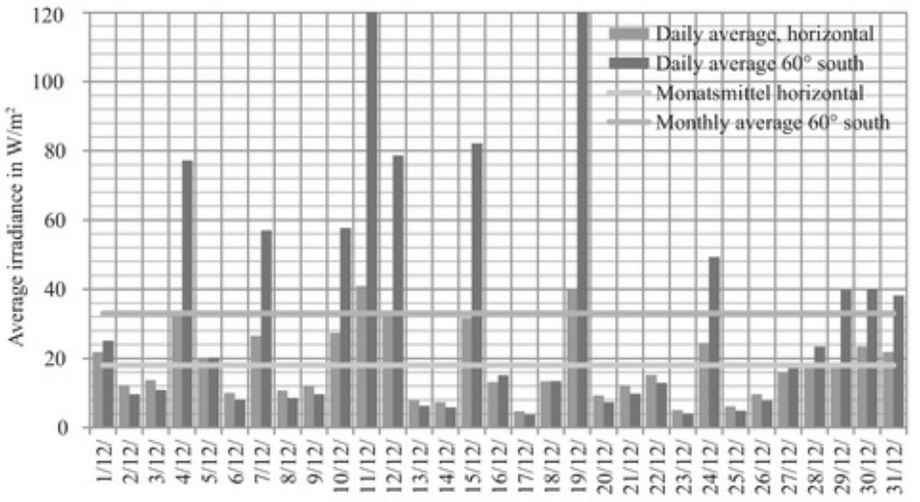

Figure 5.72 Daily and monthly average levels of irradiance on a horizontal plane and a surface facing 60° to the south in December in Berlin

The required MPP output P_{MPP} from the solar modules can be roughly estimated from the irradiation $H_{G,gen,M}$ in the worst month in kWh/m² on the slanted module plane, power demand $E_{demand,M}$ in that month, a safety bonus f_S of at least 50 % and performance ratio PR:

$$P_{MPP} = \frac{(1+f_s)\cdot E_{demand,M}}{PR} \cdot \frac{1\,\frac{kW}{m^2}}{H_{G,gen,M}} \qquad (5.122)$$

The performance ratio PR describes typical system losses from dirt on the modules, shading, partial load, heat losses, and losses from lines and the battery. The values are generally around 0.7 for unshaded off-grid systems.

A lead battery should be dimensioned so that it is only discharged to 50 % under normal conditions and can completely meet demand for a certain number of days. For safe operation in the winter, around 4 to 5 reserve days d_R are needed in Germany, while only 2 to 3 would be required in countries with greater levels of irradiation. The battery voltage U_{bat} (such as 12

Copyright © 2016. Taylor & Francis Group. All rights reserved.

Quaschning, Volker. Understanding Renewable Energy Systems, Taylor & Francis Group, 2016. ProQuest Ebook Central, http://ebookcentral.proquest.com/lib/byu/detail.action?docID=4470609.
Created from byu on 2021-11-05 15:55:38.

V) is used to calculate the required battery capacity:

$$C = \frac{2 \cdot E_{\text{demand,M}}}{U_{\text{bat}}} \cdot \frac{d_{\text{R}}}{31} \tag{5.123}$$

For example, a photovoltaic system is to power an 11 watt light bulb for three hours a day even in the winter in a garden cottage. The monthly power demand is then $E_{\text{demand,M}} = 31 \cdot 11\ \text{W} \cdot 3\ \text{h} = 1{,}023\ \text{Wh}$. With a safety bonus of 50 % = 0.5 and a performance ratio of 0.7, the required MPP output of a module facing the south at a 60° angle in Berlin would be:

$$P_{\text{MPP}} = \frac{(1+0.5) \cdot 1023\ \text{Wh}}{0.7} \cdot \frac{1\ \frac{\text{kW}}{\text{m}^2}}{25\ \frac{\text{kWh}}{\text{m}^2}} = 87.7\ \text{W}$$

With four reserve days and a battery voltage of 12 V, the battery capacity would be:

$$C = \frac{2 \cdot 1023\ \text{Wh}}{12\ \text{V}} \cdot \frac{4}{31} = 22\ \text{Ah}$$

Grid-connected systems

While battery systems are almost always designed to meet the demand load, this load hardly plays a role when designing grid-connected systems. Usually, it is assumed that the grid will be able to cover all loads. The focus is therefore usually on the available space and budget.

For the area available A_{PV} for the installation of a photovoltaic generator, the capacity that can be installed is relative to module efficiency η_{PV} (cf. Table 5.6):

$$P_{\text{PV}} = \eta_{\text{PV}} \cdot A_{\text{PV}} \cdot 1000\ \frac{\text{W}}{\text{m}^2} \tag{5.124}$$

For instance, a roof area of 50 m² and an efficiency of 14 % for crystalline silicon solar modules add up to an output of 7 kW_p.

To prevent frequent operation under partial loads, the inverter's nominal capacity should be the same as the total capacity of the solar modules if the system is optimally oriented and unshaded or if the system is in a location with a lot of irradiation. Otherwise, it might make sense to have the inverter's output 10 to 30 % smaller. Inverter manufacturers generally provide design recommendations.

Once you have chosen an inverter, you have to decide what the optimal number of modules is for the desired photovoltaic module type. Here, various boundary conditions need to be

Copyright © 2016. Taylor & Francis Group. All rights reserved.

Quaschning, Volker. Understanding Renewable Energy Systems, Taylor & Francis Group, 2016. ProQuest Ebook Central, http://ebookcentral.proquest.com/lib/byu/detail.action?docID=4470609.
Created from byu on 2021-11-05 15:55:38.

kept in mind. First, photovoltaic generator must not exceed the inverter's maximum DC voltage $U_{max,inverter}$ lest the inverter be damaged. The maximum possible voltage is the sum of the open-circuit voltages U_L of all of the photovoltaic modules connected in series under great irradiance and at low module temperatures. In the German climate, irradiance is generally assumed to be 1,000 W/m²; and the module's temperature, −10 °C. Use the formulae in the section 'Solar cells in series circuit' earlier in this chapter to convert STC data from a photovoltaic module's datasheet.

The maximum number n_{max} of photovoltaic modules that can be connected in series is then:

$$n_{max} = \frac{U_{max,inverter}}{U_{OC}(1000\ \frac{W}{m^2}, -10\ °C)} \tag{5.125}$$

Next, make sure that the photovoltaic generator's MPP never leaves the inverter's MPP range under any operating condition. Maximum MPP voltage occurs at high irradiance at low temperatures; minimum MPP voltage, at low irradiance. Figure 5.73 shows different voltage ranges.

Finally, the number of parallel module strings needs to be determined from the admissible current and output.

If a photovoltaic generator is planned and its output and surface area have been defined, the next step is generally a yield forecast. The ideal energy yield E_{ideal} of a photovoltaic system is calculated from the photovoltaic surface area A_{PV}, the photovoltaic efficiency η_{pv}, and solar irradiation $H_{G,gen}$ incident on the modules:

$$E_{ideal} = A_{PV} \cdot \eta_{PV} \cdot H_{G,gen} = \frac{P_{PV} \cdot H_{G,gen}}{1000\ \frac{W}{m^2}} \tag{5.126}$$

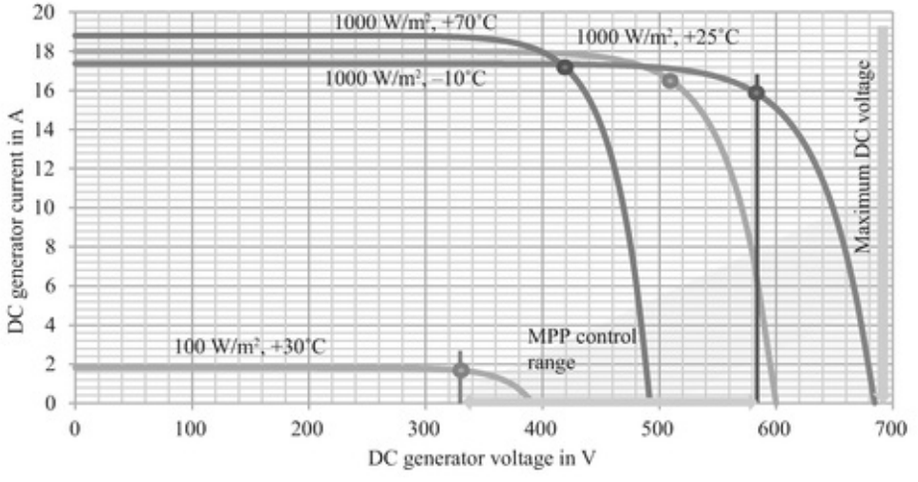

Figure 5.73 Voltage ranges for a photovoltaic generator and an inverter

Copyright © 2016. Taylor & Francis Group. All rights reserved.

Quaschning, Volker. Understanding Renewable Energy Systems, Taylor & Francis Group, 2016. ProQuest Ebook Central, http://ebookcentral.proquest.com/lib/byu/detail.action?docID=4470609.
Created from byu on 2021-11-05 15:55:38.

If the module efficiency η_{PV} is 10 % and irradiation $H_{G,gen}$ is 1,100 kWh/(m² a) on a 50 m² area facing 30° to the south, the photovoltaic system can have 5 kW_p, enough to produce an annual ideal energy yield of 5,500 kWh/a.

In reality, a photovoltaic system's energy yield is much lower because the following effects cause power losses in practice:

- lower efficiency from hotter modules
- lower efficiency under partial load
- lower actual output than indicated on data sheets
- mismatch losses when modules and cells of different output are connected
- reflection losses from sunlight incident at an angle
- efficiency changes from different spectral compositions
- losses from dirt and snow
- losses from shading
- line and diode losses
- the MPP tracker's tracking flaws
- the inverter's voltage conversion losses and own power consumption
- module and inverter failure.

The **performance ratio** *PR* describes the ratio between actual and ideal energy yield:

$$E_{real} = PR \cdot E_{ideal} \quad (5.127)$$

The average system has a performance ratio of 0.75 %. This value can be used as an average when designing a new system. Very good systems have values exceeding 0.8. The performance ratio of inefficient systems can drop below 0.6. In such cases, inverter failures and long-term shading play a crucial role.

The change in annual irradiation has a relatively small impact on the performance ratio. The PR value therefore is a good way of assessing the quality of completed photovoltaic systems. The real yield E_{real} comes from the photovoltaic system's meter. To determine the ideal yield E_{ideal}, either the annual irradiation on the photovoltaic generator must be measured or horizontal measurements close to the photovoltaic system have to be converted to the plane of the modules.

If the 5 kW_p photovoltaic system from the example above produces a real annual yield of 4,500 kWh/a, the performance ratio is 81.1 %. The system thus produces nearly optimal operating results.

In addition to the performance ratio *PR*, the specific yield Y_F provides additional information on the system. It is calculated from the ratio of the real yield E_{real} to the photovoltaic nominal output P_{PV}:

Copyright © 2016. Taylor & Francis Group. All rights reserved.

Quaschning, Volker. Understanding Renewable Energy Systems, Taylor & Francis Group, 2016. ProQuest Ebook Central, http://ebookcentral.proquest.com/lib/byu/detail.action?docID=4470609.
Created from byu on 2021-11-05 15:55:38.

$$Y_F = \frac{E_{real}}{P_{PV}} \tag{5.128}$$

Specific yield depends considerably upon location but can be used to compare similar systems within a location. It is similar to the full load hours given for other technologies. For the example above, the specific yield is:

$$Y_F = \frac{4500 \ \frac{kWh}{a}}{5 \ kW_p} = 900 \ \frac{\frac{kWh}{a}}{kW_p} = 900 \ \frac{h}{a}$$

If the same system were installed in northern Africa at an irradiation of 2,200 kWh/(m² a), the yield could be 9,000 kWh/a, but the performance ratio would remain unchanged at 81.8 %. In contrast, the specific yield would increase to 1,800 h/a.

The designs and yield calculations provided here only allow for rough estimates. For a more detailed calculation, use professional design and simulation software.

Direct-consumption systems

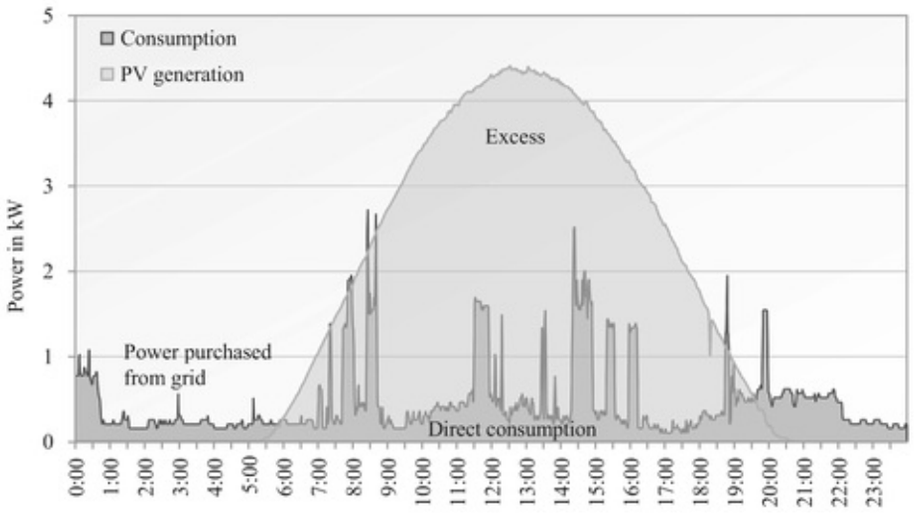

Figure 5.74 Typical load for a single-family home in Germany on a sunny spring weekend with a resolution of one minute compared with production from a 5 kW photovoltaic system

Up to now, countries like Germany, Spain, and Italy have mainly installed grid-connected photovoltaic systems, but systems tailored to direct consumption will dominate the market there soon. This option is financially attractive when the cost of solar power from the system is below the retail rate, a situation called **grid parity**. German households reached grid parity in 2012 (see Chapter 11). Other countries are soon to follow. Direct-consumption systems will

Copyright © 2016. Taylor & Francis Group. All rights reserved.

Quaschning, Volker. Understanding Renewable Energy Systems, Taylor & Francis Group, 2016. ProQuest Ebook Central, http://ebookcentral.proquest.com/lib/byu/detail.action?docID=4470609.
Created from byu on 2021-11-05 15:55:38.

then be attractive without any compensation for power sold to the grid – provided that the solar power generated is largely consumed without producing excesses. Towards that end, immediate complete consumption of all solar power generated is practically impossible without additional storage because demand in households fluctuates greatly (Figure 5.74).

The **self-consumption rate** e can be determined from the PV system's power produced $\overline{P}_{PV}$ over a certain interval of time Δt and the power $\overline{P}_{feed\text{-}in}$ generally for a year.

$$e = \frac{\sum \overline{P}_{PV} \cdot \Delta t - \sum \overline{P}_{feed\text{-}in} \cdot \Delta t}{\sum \overline{P}_{PV} \cdot \Delta t} = \frac{\sum \min\left(\overline{P}_{PV}; \overline{P}_{consumption}\right) \cdot \Delta t}{\sum \overline{P}_{PV} \cdot \Delta t} = \frac{\sum \overline{P}_{self\text{-}consumption} \cdot \Delta t}{\sum \overline{P}_{PV} \cdot \Delta t} \tag{5.129}$$

If the time interval Δt is too large, peak generation could be flattened, thereby making the share directly consumed seem larger than it is. For the most exact calculation of the share of power consumed directly, the time interval should not be longer than 15 minutes, though an interval of one minute is preferable. The larger the photovoltaic system, the lower the possible self-consumption rate.

Without storage, high shares of directly consumed solar power are only possible with relatively small photovoltaic systems, as Figure 5.75 shows. In a typical five-person household in Germany, a 90 % rate is only possible with a 1 kW system. Then, only 10 % of the power generated would not be directly consumed within the household immediately. Such a system would pay for itself without any compensation for power exported to the grid as soon as solar power from the system costs 10 % less than the retail power rate. As the PV system gets bigger or the household and its consumption smaller, the difference between the retail rate and the cost of solar power must be larger.

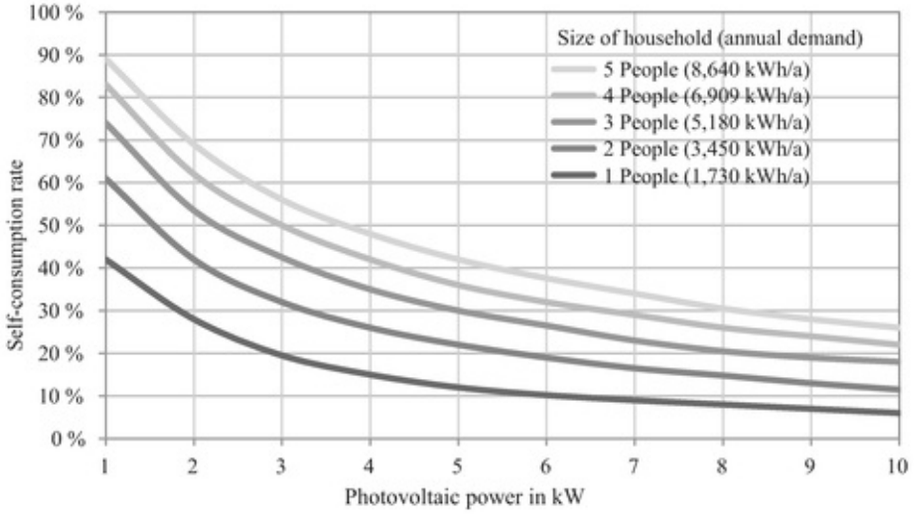

Copyright © 2016. Taylor & Francis Group. All rights reserved.

Quaschning, Volker. Understanding Renewable Energy Systems, Taylor & Francis Group, 2016. ProQuest Ebook Central, http://ebookcentral.proquest.com/lib/byu/detail.action?docID=4470609.
Created from byu on 2021-11-05 15:55:38.

Figure 5.75 Typical annual average self-consumption rate in a German single-family home relative to the size of the PV system and household (Data: [Wen12])

The self-consumption rate is often greater for industrial and commercial consumers, whose power consumption is more regular. Standard load profiles for various types of businesses can be used to estimate the potential self-consumption rate.

In Germany, the following **standard load profiles** are used by distribution grid operators with a 15-minute resolution:

- G0: General commercial
- G1: Commercial, workdays 8 am to 6 pm
- G2: Commercial with great or primary consumption in the evening
- G3: Commercial, around-the-clock
- G4: Stores/hairdressers
- G5: Bakeries
- G6: Weekend operation
- L0: Farms
- L1: Farms with dairy production or other ancillary facilities
- L2: Other special farms
- H0: Households

Figure 5.76 shows solar power generation on a sunny spring workday compared with the power demand at a typical commercial enterprise with a G0 standard load profile. If the photovoltaic system is properly designed, the self-consumption rate can be very high because the generation curve for solar power will remain completely within the area of demand on cloudy days.

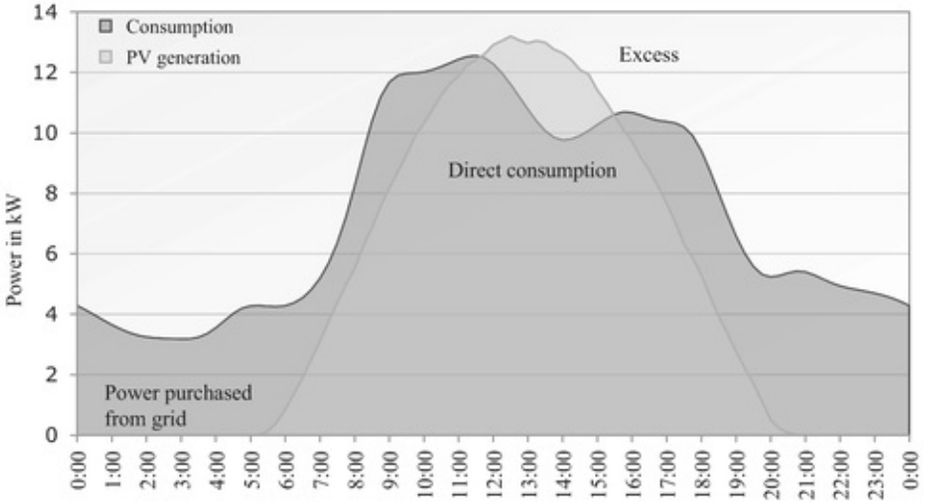

Figure 5.76 A typical load curve for a commercial enterprise (standard load profile G0) with an annual power consumption of

Copyright © 2016. Taylor & Francis Group. All rights reserved.

Quaschning, Volker. Understanding Renewable Energy Systems, Taylor & Francis Group, 2016. ProQuest Ebook Central, http://ebookcentral.proquest.com/lib/byu/detail.action?docID=4470609.
Created from byu on 2021-11-05 15:55:38.

60,000 kWh on a spring workday with a 15-minute resolution compared with power generated by a 15 kW photovoltaic system in Germany

It is, however, also possible for a photovoltaic system to pay for itself even at low self-consumption rates. Here, you simply have to decide how the excess solar power is to be used, and there are various options. In general, the option that pays the most will be chosen.

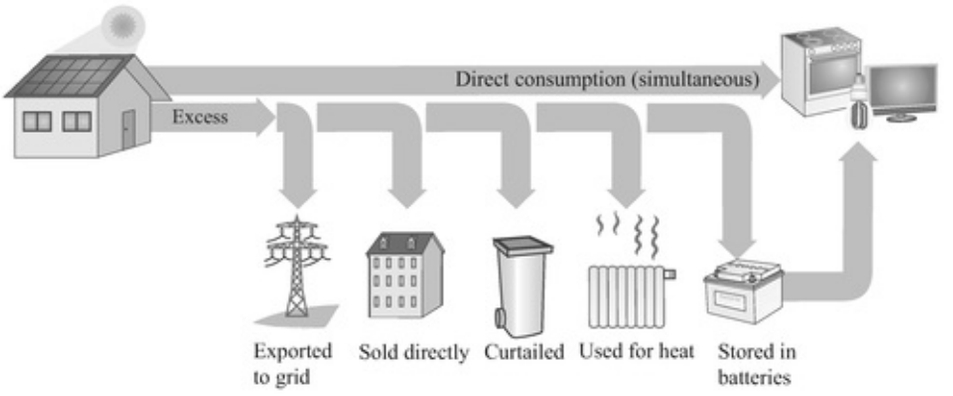

Figure 5.77 Ways of using excess power from a solar energy system not consumed directly

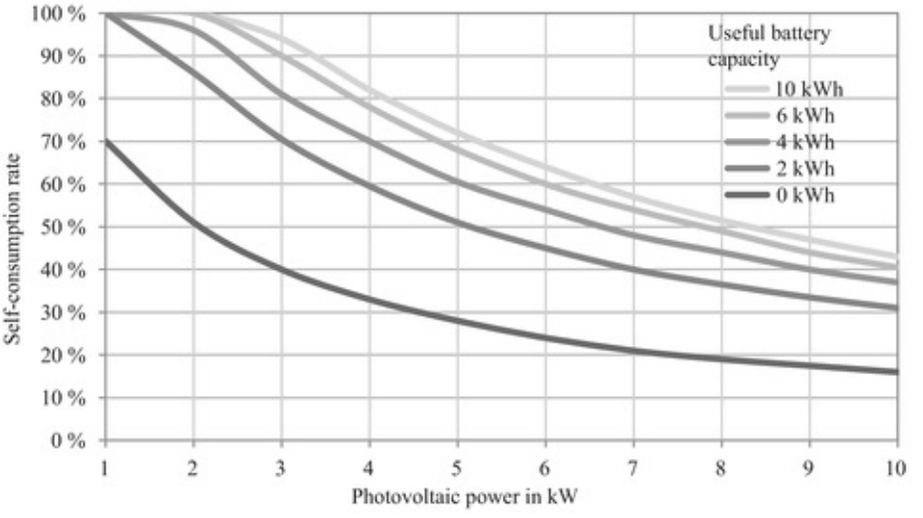

Figure 5.78 Typical annual averages of the self-consumption rate relative to photovoltaic capacity and battery storage capacity in a German single-family household with an annual consumption of 4,700 kWh (Data: [Wen12])

As long as there is attractive payment for power sold to the grid, such as German feed-in tariffs, grid exports of excess power makes sense. In numerous countries, the conditions are either worse than in Germany, or power cannot be sold to the grid at all. Production of power from the photovoltaic system may then need to be curtailed. There is no technical obstacle here; the MPP tracker simply needs to move voltage into an unfavourable range so that power production is reduced to the desired level. But before a photovoltaic system is curtailed and

Copyright © 2016. Taylor & Francis Group. All rights reserved.

Quaschning, Volker. Understanding Renewable Energy Systems, Taylor & Francis Group, 2016. ProQuest Ebook Central, http://ebookcentral.proquest.com/lib/byu/detail.action?docID=4470609.
Created from byu on 2021-11-05 15:55:38.

solar power production artificially reduced, other buyers can be looked for (Figure 5.77).

Owners of small photovoltaic systems will soon be able to serve as power providers by selling their excess electricity to their own customers or resellers at low prices. In the midterm, the revenue will probably not be great because the amount of excess solar power will be relatively low. Then, technical solutions that increase the self-consumption rate will become more important. Battery systems can temporarily store a lot of the excess and make it available at times of low irradiation or overnight, thereby increasing the share of direct consumption noticeably. Typical households will need a battery storage capacity of 4 to 6 kWh for this purpose (Figure 5.78).

Another way of increasing direct consumption is to use excess solar power to generate heat (Figure 5.71). If a photovoltaic system with a battery that has a useful storage capacity of 5 kWh is combined with an 800-litre storage tank for drinking water, a 4 to 5 kW photovoltaic system can reach 90 to 100 % direct consumption. In this case, some 30 % of the solar energy would be used to generate heat.

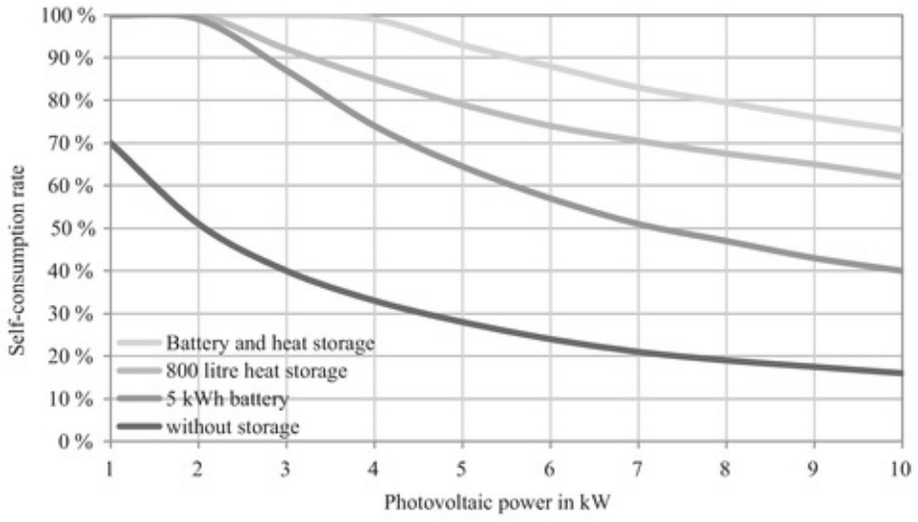

Figure 5.79 Typical annual averages of the self-consumption rate for different self-consumption systems relative to photovoltaic and battery storage capacity in a German single-family household with an annual consumption of 4,700 kWh (Data: [Qua12])

The share can vary considerably depending on consumption and system configuration. Estimating the self-consumption rate is even more complex for industrial and commercial firms. A detailed design is only possible if you use a simulation program based on good consumption profiles. The resolution of the simulation should be by the minute if possible or at least in increments of 15 minutes in line with standard load profiles in order to represent the simultaneity of power generation and consumption. Even without simulations, the values from this chapter can at least be used as starting points for system design.

Copyright © 2016. Taylor & Francis Group. All rights reserved.

Quaschning, Volker. Understanding Renewable Energy Systems, Taylor & Francis Group, 2016. ProQuest Ebook Central, http://ebookcentral.proquest.com/lib/byu/detail.action?docID=4470609.
Created from byu on 2021-11-05 15:55:38.

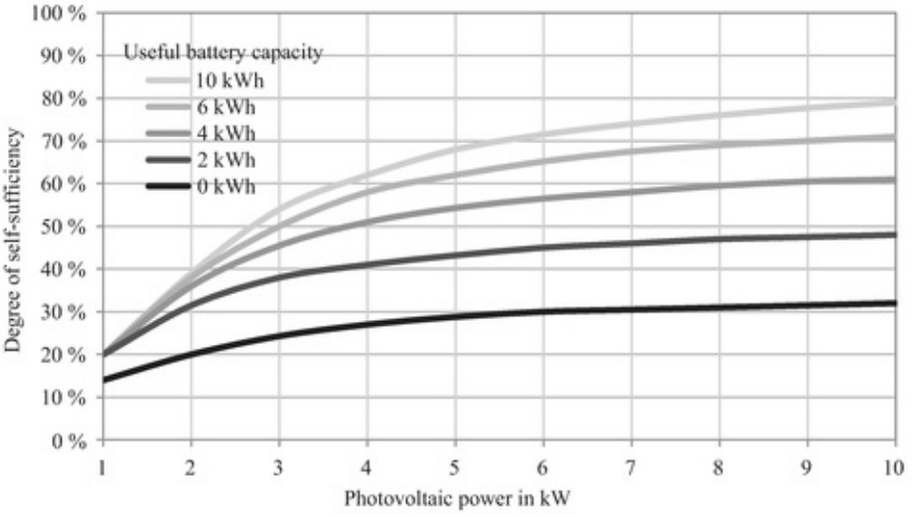

Figure 5.80 Typical annual averages of the degree of self sufficiency relative to photovoltaic capacity and battery storage capacity in a German single-family household with an annual consumption of 4,700 kWh (Data: [Wen12])

A lot of consumers increasingly want to consume the largest possible share of their own solar power in order to become less dependent on the grid. Here, one speaks of the degree of self-sufficiency. It is largely equivalent to the solar coverage rate for solar thermal systems.

The **degree of self-sufficiency** a is calculated by adding up the total consumption $\overline{P}_{\text{consumption}}$ and amount of power purchased from the grid $\overline{P}_{\text{grid-supply}}$ over a given timeframe Δt:

$$a = \frac{\sum \overline{P}_{\text{consumption}} \cdot \Delta t - \sum \overline{P}_{\text{grid-supply}} \cdot \Delta t}{\sum \overline{P}_{\text{consumption}} \cdot \Delta t} \tag{5.130}$$

$$= \frac{\sum \min\left(\overline{P}_{\text{PV}}; \overline{P}_{\text{consumption}}\right) \cdot \Delta t}{\sum \overline{P}_{\text{consumption}} \cdot \Delta t}$$

$$= \frac{\sum \overline{P}_{\text{self-consumption}} \cdot \Delta t}{\sum \overline{P}_{\text{consumption}} \cdot \Delta t}$$

At a 100 % degree of self-sufficiency, no power is purchased from the grid; the photovoltaic system directly covers all power consumption. In practice, however, complete autonomy in a country like Germany is difficult to attain. Even with a 10 kW photovoltaic system, a typical single-family household will only obtain a roughly 35 % degree of self-sufficiency without battery storage. With battery storage of an affordable size, that level can, however, be increased to up to 80 % (Figure 5.80).

Copyright © 2016. Taylor & Francis Group. All rights reserved.

Quaschning, Volker. Understanding Renewable Energy Systems, Taylor & Francis Group, 2016. ProQuest Ebook Central, http://ebookcentral.proquest.com/lib/byu/detail.action?docID=4470609.
Created from byu on 2021-11-05 15:55:38.